Fall 2016

Efficient time-dependent system reliability analysis

Zhifu Zhu

Recommended Citation

EFFICIENT TIME-DEPENDENT SYSTEM RELIABILITY ANALYSIS

by

ZHIFU ZHU

A DISSERTATION

Presented to the Faculty of the Graduate School of the

MISSOURI UNIVERSITY OF SCIENCE AND TECHNOLOGY

In Partial Fulfillment of the Requirements for the Degree

DOCTOR OF PHILOSOPHY

in

MECHANICAL ENGINEERING

2016

Approved

Dr. Xiaoping Du, Advisor

Dr. K. Chandrashekhara

Dr. Lokeswarappa Dharani

Dr. Serhat Hosder

Dr. Xuerong Meggie Wen

PUBLICATION DISSERTATION OPTION

This dissertation consists of the following four articles that have been published or submitted for publication as follows:

Pages 6-35 have been published in the proceedings of the ASME 2015 International Design Engineering Technical Conferences and Computers & Information in Engineering Conference (IDETC/CIE 2015), August 2-5, Boston, Massachusetts.

Pages 36-82 have been published in ASME Journal of Mechanical Design.

Pages 83-117 have been published in the proceedings of the ASME 2016 International Design Engineering Technical Conferences and Computers & Information in Engineering Conference (IDETC/CIE 2016), August 21-24, Charlotte, North Carolina, and have been submitted to Structural and Multidisciplinary Optimization.

Pages 118-152 have been submitted to Reliability Engineering & System Engineering.

This dissertation has been prepared in the style utilized by the Missouri University of Science and Technology.

ABSTRACT

Engineering systems are usually subjected to time-variant loads and operate under time-dependent uncertainty; system performances are therefore time-dependent. Accurate and efficient estimate of system reliability is crucial for decision makings on system design, lifetime cost estimate, maintenance strategy, etc. Although significant progresses have been made in time-independent reliability analysis for components and systems, time-dependent system reliability methodologies are still limited. This dissertation is motivated by the need of accurate and effective reliability prediction for engineering systems under time-dependent uncertainty. Based on the classic First and Second Order Reliability Method (FORM and SORM), a system reliability method is developed for multidisciplinary systems involving stationary stochastic processes. A dependent Kriging method is also developed for general components. This method accounts for dependent responses from surrogate models and is therefore more accurate than existing Kriging Monte Carlo simulation methods that neglect the dependence between responses. The extension of the dependent Kriging method to systems is also a contribution of this dissertation. To overcome the difficulty of obtaining extreme value distributions and get rid of global optimization with a double-loop procedure, a Kriging surrogate modeling method is also proposed. This method provides a new perspective of surrogate modeling for time-dependent systems and is applicable to general systems having random variables, time, and stochastic processes. The proposed methods are evaluated through a wide range of engineering systems, including a compound cylinders system, a liquid hydrogen fuel tank, function generator mechanisms, slider-crank mechanisms, and a Daniels system.

ACKNOWLEDGEMENTS

TABLE OF CONTENTS

LIST OF ILLUSTRATIONS

LIST OF TABLES

PAPER IV

1. INTRODUCTION

1.1 BACKGROUND

Engineering systems are exposed to uncertainties in design, manufacturing and operation. Uncertainties are classified into time-independent uncertainties and time-dependent uncertainties. Time-independent uncertainties do not change with time, such as manufacturing variations in dimensions and variations in material properties. These uncertainties are modeled as random variables. Time-dependent uncertainties vary with time. Examples include the stochastic wind loading and river flow loading [1]; these uncertainties are modeled as stochastic processes. When a system response is a function of time and/or stochastic processes, the system performance is time-dependent. Therefore, time-dependent reliability analysis methodologies are required for the prediction of the system reliability.

In the past decades, many methods have been developed to improve the accuracy and efficiency of time-dependent component and time-independent system reliability methods. For example, based on the Rice's formula [2, 3] and independent upcrossing assumption, various upcrossing rate methods [1, 4, 5] were proposed. Upcrossing rate methods are effective for some problems, but for problems with highly nonlinear performance functions or strongly dependent upcrossings, or both, their accuracy is poor. With the improvement of computer technologies, more and more engineers resort to sampling methods for reliability estimate. Various surrogate modeling methods [6, 7], importance sampling methods [8, 9], and surrogate-based importance sampling methods [10, 11] have been proposed. Among the surrogate models used for reliability analysis,

the Kriging model [12, 13] has been extensively studied since the model provides not only a prediction on an untried point, but also the uncertainty of the prediction.

Compared to significant progresses made in time-dependent component and time-independent system reliability analysis, methods for time-dependent systems are limited [14]. Besides upcrossing rate methods, extreme values methods are widely used. But obtaining an accurate extreme value distribution is difficult, especially when stochastic processes are involved over a long time period. This dissertation was motivated by the lack of effective reliability methods that could handle general time-dependent systems with good accuracy and efficiency. The outcomes of this work make the reliability estimate for general engineering systems having time-dependent performances possible and affordable.

1.2 RESEARCH OBJECTIVE

The objective of this dissertation is to develop accurate and efficient reliability methodologies for components and systems with time-dependent uncertainty. To achieve this objective, three research tasks are performed.

Research task 1 focuses on reliability analysis for multidisciplinary systems. This research task is for multidisciplinary systems involving only stationary stochastic processes and performance functions that are implicit with respect to time [15]. Since the involvement of stochastic processes, the system performance varies randomly over time. And as the subsystems within a multidisciplinary system are coupled, the output of one subsystem is the input of other subsystems, and vice versa. This makes estimating the system reliability much more complicated than the time-independent system analysis. The proposed method uses the equations of linking variables as constraints in the Most

Probable Point (MPP) search. This not only guarantees the consistency of the multidisciplinary system but also ensures high efficiency. This research task results in Paper 1 [15].

Research task 2 concentrates on improving the accuracy of time-independent component reliability analysis, on which time-dependent system analysis are based in research task 3. The major approach used is the Kriging method. Current Kriging methods do not consider correlations between Kriging predictions, and only the sign of the predictions are used to estimate reliability; they are therefore called independent Kriging methods [16, 17]. A dependent Kriging method, together with a new learning function and a new way of calculating reliability, is developed [18] to improve the accuracy of independent Kriging methods. This is achieved by accounting for the correlations and making good use of information provided by Kriging predictions and Kriging variances. This research task produces Paper 2 [18].

Research task 3 develops two new methods for system reliability analysis. The first method is the extension of research task 2 from components to systems. The outcome is a dependent Kriging method for system reliability [19]. The purpose of the other method is to remove extreme value distributions and global optimization from existing double-loop procedures of time-dependent system reliability [20]. As distributions of the extreme values are difficult to obtain and global optimization is time-consuming, accuracy and efficiency of time-dependent systems should be improved. This method aims at providing a new way of building surrogate models for general time-dependent systems. This research task produces Papers 3 [19] and 4 [21].

The outcomes of above research tasks are expected to enable engineers to understand how uncertainty affects the performance of engineering systems and how to predict system reliability efficiently with good accuracy. Potential areas that will benefit include reliability engineering, uncertainty based design, and maintenance.

1.3 ORGANIZATION OF DISSERTATION

As discussed in Section 1.2, the three research tasks in this study have produced four papers, which constitute this dissertation.

The first paper is entitled "Reliability Analysis for Multidisciplinary Systems Involving Stationary Stochastic Processes." A reliability analysis method based on the First and Second Order Reliability Methods (FORM and SORM) is developed. The method modifies FORM and SORM so that the Multidisciplinary Analysis (MDA) is incorporated. Then Monte Carlo simulation is used to estimate reliability without calling the original performance functions. The proposed method is successfully applied to estimate the reliability of a compound cylinder system over 10 years. And the results show that proposed method has much better accuracy than the upcrossing rate method.

The second paper, entitled "Reliability Analysis with Monte Carlo Simulation and Dependent Kriging Predictions", improves the accuracy of Kriging methods. The current independent Kriging methods are based on two assumptions: 1) Predictions from a Kriging model are independent. But since the predictions are different realizations of the same Gaussian process and likely dependent, the independent assumption may adversely affect the effectiveness of the surrogate modeling process. 2) If accurate surrogate models can be obtained, the reliability analysis results based on these surrogate models will also be accurate. Although this assumption is valid, it emphasizes the accuracy of surrogate

models, instead of the accuracy of reliability analysis itself. To overcome the above drawbacks, the proposed dependent Kriging method accounts for the dependency between Kriging predictions. A new learning function is developed, and the new way of calculating reliability uses all the information provided by a Kriging model. Five examples from literature, including a nonlinear oscillator, a cantilever tube, a roof truss structure, and a slider-crank mechanism are used to test the new method.

The third paper "A System Reliability Method with Dependent Kriging Predictions" derives all the equations and procedures needed to extend dependent Kriging method to systems. In a system, some components have larger contributions to system reliability than other components. To save computational efforts on components or training points whose contributions to system reliability are insignificant, the composite criterion approach [22, 23] is employed. Three examples from literature show that the new method outperforms independent system Kriging method in accuracy, efficiency, and robustness.

The fourth paper is entitled "A Kriging Method for Time-Dependent System Reliability Analysis." The objective of this method is to overcome the drawbacks of using extreme values with a double-loop procedure and time-consuming global optimization by the current methods. It develops a new surrogate modeling method that is applicable to general time-dependent systems that have random variables, time, and stochastic processes in performance functions. By removing global optimization and building surrogate models for performance functions directly, the proposed method is in general more efficient than extreme value methods. Four examples, covering systems with and without stochastic processes, and systems with series and parallel configurations, are used to test the new method.

PAPER

I. RELIABILITY ANALYSIS FOR MULTIDISCIPLINARY SYSTEMS INVOLVING STATIONARY STOCHASTIC PROCESSES

Zhifu Zhu, Zhen Hu, Xiaoping Du

Department of Mechanical and Aerospace Engineering

Missouri University of Science and Technology

ABSTRACT

The response of a component in a multidisciplinary system is affected by not only the discipline to which it belongs, but also by other disciplines of the system. If any components are subject to time-dependent uncertainties, responses of all the components and the system are also time dependent. Thus, time-dependent multidisciplinary reliability analysis is required. To extend the current time-dependent reliability analysis for a single component, this work develops a time-dependent multidisciplinary reliability method for components in a multidisciplinary system under stationary stochastic processes. The method modifies the First and Second Order Reliability Methods (FORM and SORM) so that the Multidisciplinary Analysis (MDA) is incorporated while approximating the limit-state function of the component under consideration. Then Monte Carlo simulation is used to calculate the reliability without calling the original limit-state function. Two examples are used to demonstrate and evaluate the proposed method.

1. INTRODUCTION

Engineering systems are more and more sophisticated, and they commonly involve multiple interacting disciplines, for example, systems with coupled fluid and structure disciplines [1] and aircraft wing design with coupled aerodynamic and structure disciplines [2]. Multidisciplinary systems are commonly found in aerospace [3] and marine applications [4, 5]; automobile engineering [6]; and renewable energy field [7, 8]. Due to the highly coupled disciplines or subsystems, the reliability analysis of a multidisciplinary system is much more difficult than that of a single disciplinary system [9].

Many studies have been devoted to reliability analysis and reliability-based design for multidisciplinary systems [2, 9-14] where only random variables are involved. Padmanabhan and Batill [15, 16] develop a reliability-based design optimization method for multidisciplinary systems using the concurrent subspace optimization framework and the collaborative reliability analysis method. Du and Guo [14] propose a sequential optimization and reliability assessment (SORA) method for multidisciplinary systems design. Sues et al. [17] apply the response surface method to the reliability analysis of multidisciplinary systems. Koch et al. [18] propose a multi-stage parallel implementation strategy for the probabilistic design optimization of multidisciplinary problems.

The aforementioned methods are only appliable for time independent reliability that does not change over time. The reasons are that limit-state functions are not time-dependent and that the input variables are time-independent random variables. When some of the input random variables are time-dependent (stochastic processes), the responses of the multidisciplinary system become time variant. Time-dependent problems

are commonly encountered. For example, a ship is subjected to stochastic wave loading [19] that varies over time, and a wind turbine is subjected to wind loading in the form of time series (a special type of stochastic processes) [20].

For multidisciplinary systems with stochstic processes, which vary randomly over time, the resposnses of the system are aslo time-dependnet stochstic processes. As a result, the reliability is defined in a period of time, during which the system is supposed to operate. This kind of reliability is called the time-dependent reliability. It usully decreases with time. Time-dependent reliability methods should then be employed. Many methods have been developed for time-dependent reliability, and they incldue the upcrossing rate methods [8, 21, 22], the extreme value methods [23, 24], the envelop method [25], the composite limit state method [26-28], and several sampling-based approaches [29-33]. These methods, however, are only for components or single disciplinary systems. They may not be applicable for multidisciplinary systems.

Time-dependent uncertainty in the form of stochastic processes widely exists in multidisciplinary systems. For example, the wave loadings on offshore structures are stochastic processes [34]; transmission towers are under stochastic process citations [35]; hydrokinetic turbine blade under time-variant river flow loading [36]; and off-road vehicles subjecting to stochastic road excitations [37]. But it is a challenging task to develop time-dependent reliability methodologies for general multidisciplinary systems. This work deals with only a special case where the input stochastic processes are stationary. Loosely speaking, a stationary process is a process whose statistical properties does not change over time, and the process at any two different time instances, however, are generally dependent. For example, random excitations are usually modeled as

stationary stochastic processes. Although stochastic loadings are usually modeled as non-stationary loadings, for a short term, the loadings can be assumed to be stationary. For this special case, we assume that time t does not appear explicitly in all the functions of the responses.

The objective of this work is to develop a reliability method for the aforementioned special case. Although only stationary stochastic processes are involved, due to the dependence between responses at any pairs of time instants, the time-dependent reliability generally decreases over time although the distribution of the process remains the same at any time instant. This makes the time-dependent reliability analysis more complicated than its time-independent counterpart.

The major approach is the extension of the time-invariant reliability methods, including the First and Second Order Reliability Methods (FORM and SORM), into multidisciplinary systems with stationary stochastic processes and random variables. After the responses are approximated by FORM and SORM, we use Monte Carlo simulation (MCS) to estimate the reliability. The reasons of using MCS are twofold. The first is that no analytical solutions exist even after the use of FORM or SORM and that it is convenient to use MCS; the second is that MCS will not call the original limit-state function, and the computational cost is therefore not a concern.

In Section 2, we provide an overview about Multidisciplinary System Analysis (MDA) and time-dependent reliability analysis. We then discuss the reliability analysis for multidisciplinary systems with stationary stochastic processes and random variables in Section 3, followed by two examples in Section 4. Conclusions are made in Section 5.

2. BACKGROUND

In this section, we provide the background information about multidisciplinary systems and time-dependent reliability.

2.1 MULTIDISCIPLINARY SYSTEMS WITH STOCHASTIC PROCESSES

Figure 2.1 shows a multidisciplinary system with three disciplines or subsystems. The input to the system includes both random variables and stochastic processes.
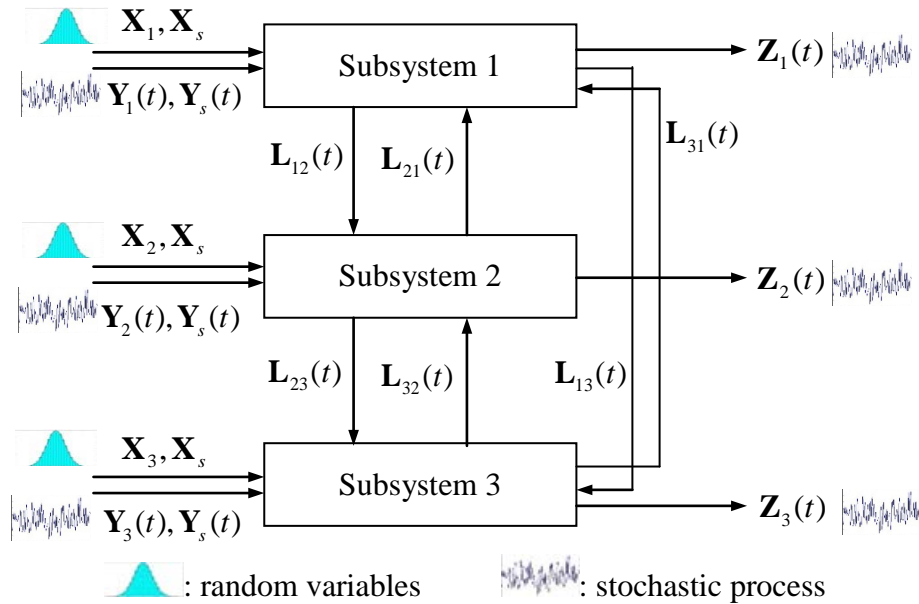
Figure 2.1 Multidisciplinary system with random variables and stochastic processes

The notations in Figure 2.1 are given as follows:

$\mathbf{X}_s$: shared input random variables for all disciplines,

$\mathbf{X}_i$: local input random variables of subsystem i ,

$\mathbf{Y}_s(t)$: shared stochastic processes for all disciplines,

$\mathbf{Y}_i(t)$: local input stochastic processes of subsystem i ,

$\mathbf{L}_{ij}(t)$: linking (coupling) variables from subsystem i to subsystem j,

$\mathbf{Z}_i(t)$: output of subsystem i.

As indicated in Figure 2.1, output variables (or responses) $\mathbf{Z}_i(t)$ and coupling variables $\mathbf{L}_{ij}(t)$ are all time-dependent due to the involvement of stochastic processes in the input variables and the coupling between subsystems. The output of one subsystem is often the input of other subsystems and vice versa. Since the subsystems are coupled with each other, for a single system analysis, we need to solve for all the linking variables $\mathbf{L}_{ij}(t)$ and then calculate the responses. This process is called a multidisciplinary analysis (MDA).

Let linking variables from the i-th subsystem be given by

$$\mathbf{L}_{i\bullet}(t) = \{\mathbf{L}_{ij}(t)\}_{j=1,2,\cdots,n;j\neq i} = \mathbf{g}_{\mathbf{L}_{i\bullet}}(\mathbf{X}_s,\mathbf{X}_i,\mathbf{Y}_s(t),\mathbf{Y}_i(t),\mathbf{L}_{\bullet i}(t)) \qquad (1)$$

in which n is the number of subsystems, $\mathbf{L}_{i\bullet}(t)$ is the vector of linking variables, which are output variables from subsystem i, $\mathbf{L}_{\bullet i}(t)$ is the vector of linking variables, which are input variables to subsystem i from other subsystems, and $\mathbf{g}_{\mathbf{L}_{i\bullet}}(\bullet)$ is a vector of the functions that map the input variables into $\mathbf{L}_{i\bullet}(t)$. In this work, we assume that time t does not appear explicitly in all the functions.

The system consistency is guaranteed by the above system of simultaneous equations over the interfaces between coupled subsystems. Expanding Eq. (1) over the whole system in Figure 2.1 yields

$$\begin{cases} \mathbf{L}_{12}(t) = \mathbf{g}_{\mathbf{L}_{12}}(\mathbf{X}_s, \mathbf{X}_1, \mathbf{Y}_s(t), \mathbf{Y}_1(t), \mathbf{L}_{\bullet 1}(t)) \\ \mathbf{L}_{13}(t) = \mathbf{g}_{\mathbf{L}_{13}}(\mathbf{X}_s, \mathbf{X}_1, \mathbf{Y}_s(t), \mathbf{Y}_1(t), \mathbf{L}_{\bullet 1}(t)) \\ \mathbf{L}_{21}(t) = \mathbf{g}_{\mathbf{L}_{21}}(\mathbf{X}_s, \mathbf{X}_2, \mathbf{Y}_s(t), \mathbf{Y}_2(t), \mathbf{L}_{\bullet 2}(t)) \\ \mathbf{L}_{23}(t) = \mathbf{g}_{\mathbf{L}_{23}}(\mathbf{X}_s, \mathbf{X}_2, \mathbf{Y}_s(t), \mathbf{Y}_2(t), \mathbf{L}_{\bullet 2}(t)) \\ \mathbf{L}_{31}(t) = \mathbf{g}_{\mathbf{L}_{31}}(\mathbf{X}_s, \mathbf{X}_3, \mathbf{Y}_s(t), \mathbf{Y}_3(t), \mathbf{L}_{\bullet 3}(t)) \\ \mathbf{L}_{32}(t) = \mathbf{g}_{\mathbf{L}_{32}}(\mathbf{X}_s, \mathbf{X}_3, \mathbf{Y}_s(t), \mathbf{Y}_3(t), \mathbf{L}_{\bullet 3}(t)) \end{cases} \tag{2}$$

and solving the above equations needs to call disciplinary analyses or repeat the evaluations of $\mathbf{g}_{\mathbf{L}_{i\bullet}}(\bullet)$, if the functions are nonlinear.

After the linking variables are obtained, responses from any disciplines can be easily solved. For example, for subsystem i, a general response $Z_i(t)$ can be computed by

$$Z_i(t) = g_{Zi}(\mathbf{X}_s, \mathbf{X}_i, \mathbf{Y}_s(t), \mathbf{Y}_i(t), \mathbf{L}_{\bullet i}(t)) \tag{3}$$

2.2 TIME-DEPENDENT RELIABILITY

For the response in Eq. (3), the time-dependent reliability over the period of time $[t_0, t_s]$ is defined by

$$R(t_0, t_s) = \Pr\{Z_i(t) = g_{Zi}(\mathbf{X}_s, \mathbf{X}_i, \mathbf{Y}_s(t), \mathbf{Y}_i(t), \mathbf{L}_{\bullet i}(t)) < e, \forall t \in [t_0, t_s]\} \tag{4}$$

where $\Pr\{\cdot\}$ stands for the probability, and e is the limit state. If there exists a time instant t such that $Z_i(t) > e$, a failure occurs. The time-dependent probability of failure is

$$p_f(t_0, t_s) = \Pr\{Z_i(t) = g_{Zi}(\mathbf{X}_s, \mathbf{X}_i, \mathbf{Y}_s(t), \mathbf{Y}_i(t), \mathbf{L}_{\bullet i}(t)) > e, \exists t \in [t_0, t_s]\} \tag{5}$$

where $\exists$ means "there exists".

Many methods have been proposed to calculate the time-dependent reliability [8, 21-30]. One of the dominating methods is the upcrossing rate method based on Rice's formula [38]. Herein, we briefly review the upcrossing rate method. More details are

available in [39]. The time-dependent probability of failure is estimated using the upcrossing rate by

$$p_f(t_0, t_s) = 1 - R(t_0) \exp\left\{-\int_{t_0}^{t_s} v^+(t)dt\right\}$$

(6)

where $R(t_0)$ is the reliability at the initial time instant t_0, and $v^+(t)$ is the upcrossing rate at t. $v^+(t)$ is given by

$$v^+(t) = \lim_{\Delta t \to 0} \frac{\Pr\{Z_i(t) < e \cap Z_i(t + \Delta t) > e\}}{\Delta t}$$

(7)

in which $\cap$ stands for intersection.

Directly evaluating $v^+(t)$ is difficult as there is no close- form expression available for the joint probability of general problems. One way is using the Rice's formula [38], which approximates the upcrossing rate as follows:

$$v^+(t) = \omega(t)\phi(\beta(t))\Psi(\dot{\beta}(t)/\omega(t))$$

(8)

where $\omega(t)$, $\beta(t)$, and $\dot{\beta}(t)$ are parameters computed from the First Order Reliability Method (FORM), $\phi(\bullet)$ is the probability density function (PDF) of a standard normal variable, and $\Psi(x) = \phi(x) - x\Phi(-x)$, where $\Phi(\cdot)$ is the cumulative distribution function (CDF) of a standard normal variable. Details can be found in [39].

The upcrossing rate method is accurate when the probability of failure is low or the limit state is high. When the threshold is low, the Poisson assumption, based on which Rice's formula is derived, may not hold. The upcrossing rate method may produce large errors.

In the following section, we discuss how to approximate the time-dependent probability of failure for multidisciplinary systems based on FORM and SORM.

3. MULTIDISCIPLINARY RELIABILITY ANALYSIS

The method is based on FORM and SORM, whose details can be found in [39-41]. The methods approximate response functions at the Most Probable Point (MPP) with a first order and second order, respectively. For time independent problems, only random variables exist, an analytical solution to the reliability is available if FORM is used, and an analytical solution is also available if SORM is used after some transformation. For the current problem with stationary stochastic processes, no analytical solution exists. The major reason is that the failures at all the time instants in the period of time under consideration are dependent. MCS is therefore used, it is noted that MCS will not call MDA.

Different from FORM and SORM for component reliability analysis, the reliability analysis herein needs to call MDA repeatedly in the process of researching for the MPP. A decoupling approach is used for the MDA as shown in the next section.

3.1 OVERVIEW

The overall procedure of the proposed method is given in Figure 3.1. Detailed implementing procedures are discussed in Subsections 3.2 and 3.3. There are five steps.

- Step 1: Initialization: transform random variables and stochastic processes into standard normal variables at a specific time instant.

- Step 2: Decoupling and the MPP search: perform the MPP search by decoupling the multidisciplinary subsystems and considering the consistency of the system.

- Step 3: Approximation: approximate the limit-state function using the first or second order Taylor series expansion at the MPP.

- Step 4: Sampling: perform sampling using MCS.

- Step 5: Reliability analysis: evaluate reliability or probability of failure based on the samples generated in Step 4.
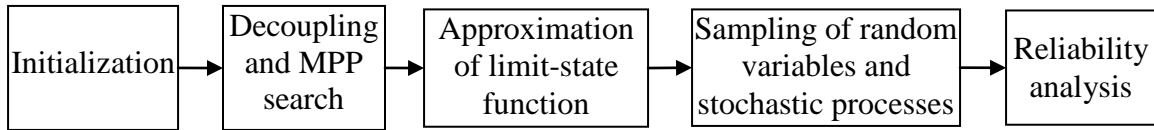
Figure 3.1 Procedure of reliability analysis of multidisciplinary systems

3.2 APPROXIMATION USING FORM AND SORM

The task is to calculate the time-dependent probability of failure associated with a response of a specific discipline or subsystem. Let a general response from the *i*-th discipline or the *i*-th subsystem be $Z_i(t) = g_{Zi}(\mathbf{X}_s, \mathbf{X}_i, \mathbf{Y}_s(t), \mathbf{Y}_i(t), \mathbf{L}_{\bullet i}(t))$. As indicated in Figure 3.1, we at first build an approximate model for $Z_i(t) = g_{Zi}(\mathbf{X}_s, \mathbf{X}_i, \mathbf{Y}_s(t), \mathbf{Y}_i(t), \mathbf{L}_{\bullet i}(t))$ and then perform the reliability analysis based on the approximate model using MCS. In this work, we approximate the limit-state function by the first and second order Taylor series expansions. To minimize the accuracy loss, we use the MPP as the expansion point. Since only stationary stochastic processes are involved, their distributions at all the time instants are the same, and only one MPP search is needed.

3.2.1 MPP Search. During the MPP search process, MDA is called repeatedly to solve for linking variables. This will therefore require a double-loop process. As suggested in [14], the two loops can be combined by treating the system consistency equations in Eq. (1) as constraints in the MPP search. By extending the MPP search

model for problems with only random variables to the multidisciplinary problem, the MPP model is given by [14]

$$\begin{cases} \min_{(\mathbf{u},\mathbf{L})} \|\mathbf{u}\| \\ s.t. \\ \hat{g}_{Z_i}(\mathbf{u}_i,\mathbf{L}_{\cdot i}) > 0 \\ \mathbf{L}_{j\cdot}(t) = \hat{g}_{\mathbf{L}_j}(\mathbf{u}_j,\mathbf{L}_{\cdot j}), \ j=1,2,\ldots,n \end{cases} \tag{9}$$

where $\mathbf{u} = [\mathbf{u}_{\mathbf{X}_S}, \mathbf{u}_{\mathbf{X}_i}, \mathbf{u}_{\mathbf{Y}_S}, \mathbf{u}_{\mathbf{Y}_i}]_{i=1,2,\ldots,n}$, $\mathbf{u}_i = [\mathbf{u}_{\mathbf{X}_S}, \mathbf{u}_{\mathbf{X}_i}, \mathbf{u}_{\mathbf{Y}_S}, \mathbf{u}_{\mathbf{Y}_i}]$, $\mathbf{L} = [\mathbf{L}_{ij}]_{i,j=1,2,\cdots,n, \ i \neq j}$, and n is the number of subsystems. $\hat{g}_{Z_i}(\cdot)$ is the same function as $g_{Z_i}(\cdot)$ given in the beginning of this section, but $\hat{g}_{Z_i}(\cdot)$ is a function of transformed variables $\mathbf{u}$.

Solving the above MPP search only needs a single optimization loop and is therefore more efficient than the double-loop procedure where the MDA loop is embedded in the MPP search. Then the response function $Z_i(t) = g_{Zi}(\bullet)$ is approximated at the MPP.

3.2.2 Approximation Of The Limit-State Function. When FORM is employed, the limit-state function is approximated as

$$\hat{g}_{Z_i}(\mathbf{U}) \approx \hat{g}_{Z_i}(\mathbf{u}_i^*) + \nabla \hat{g}_{Z_i}(\mathbf{u}_i^*)(\mathbf{U}_i - \mathbf{u}_i^*)^T \tag{10}$$

which can be transformed to

$$\Pr\{Z_i(t) > e\} = \Pr\{H(t) > \beta\} \tag{11}$$

where $Z_i(t)$ is the output of the i-th subsystem, and

$$H(t) = \boldsymbol{\alpha}(t)\mathbf{U}(t) \tag{12}$$

And

$$\boldsymbol{\alpha}(t) = \nabla \mathbf{g}(\mathbf{U}^*(t),t) / \|\nabla \mathbf{g}(\mathbf{U}^*(t),t)\| \tag{13}$$

When SORM is employed, we have

$$\hat{g}_{Z_i}(\mathbf{U}) \approx \hat{g}_{Z_i}(\mathbf{u}_i^*) + \nabla \hat{g}_{Z_i}(\mathbf{u}_i^*)(\mathbf{U}_i - \mathbf{u}_i^*)^T$$
$$+ \frac{1}{2}(\mathbf{U}_i - \mathbf{u}_i^*)\nabla^2 \hat{g}_{Z_i}(\mathbf{u}_i^*)(\mathbf{U}_i - \mathbf{u}_i^*)^T \qquad (14)$$

where $\mathbf{u}_i^* = [\mathbf{u}_{\mathbf{X}_S}^*, \mathbf{u}_{\mathbf{X}_i}^*, \mathbf{u}_{\mathbf{Y}_S}^*, \mathbf{u}_{\mathbf{Y}_i}^*]$, $\nabla \hat{g}_{Z_i}(\mathbf{u}_i^*)$ is the first partial derivatives of $\hat{g}_{Z_i}(\mathbf{U})$ at $\mathbf{u}_i^*$,

and $\nabla^2 \hat{g}_{Z_i}$ is the Hessian matrix, which is a symmetric square matrix of second partial

derivatives of $\hat{g}_{Z_i}(\mathbf{U})$.

With the forward difference method, $\nabla \hat{g}_{Z_i}(\mathbf{u}_i^*)$ is given by

$$\left.\frac{\partial \hat{g}_{Z_i}}{\partial U_i}\right|_{\mathbf{u}_i^*} \approx \frac{\hat{g}_{Z_i}(\mathbf{u}_i^* + \Delta \mathbf{u}) - \hat{g}_{Z_i}(\mathbf{u}_i^*)}{\Delta u} \qquad (15)$$

where the i-th element of $\Delta \mathbf{u}$ is Δu, the other elements of $\Delta \mathbf{u}$ are all zero, and Δu is a

small step size.

The second derivative $\left.\dfrac{\partial^2 \hat{g}_{Z_i}}{\partial U_j \partial U_k}\right|_{\mathbf{u}_i^*}$ is given by

$$\left.\frac{\partial^2 \hat{g}_{Z_i}}{\partial U_j \partial U_k}\right|_{\mathbf{u}_i^*} \approx \frac{\hat{g}_{Z_i}(\mathbf{u}_i^{*,++}) - \hat{g}_{Z_i}(\mathbf{u}_i^{*,j+}) - \hat{g}_{Z_i}(\mathbf{u}_i^{*,k+}) + \hat{g}_{Z_i}(\mathbf{u}_i^*)}{\Delta u_j \Delta u_k} z_i^{max}(j)$$
$$= \max_{k=1,\cdots,m} \{\hat{g}_{Z_i}(\tilde{\mathbf{u}}_j, t_k)\} \text{ where } j = 1, 2, \ldots, N \qquad (16)$$

where $\mathbf{u}_i^{*,++} = \mathbf{u}_i^* + \Delta \mathbf{u}^{++}$, in which the j-th and k-th elements of $\Delta \mathbf{u}^{++}$ are Δu_j and Δu_k,

respectively, and the other elements of $\Delta \mathbf{u}^{++}$ are all zero; $\mathbf{u}_i^{*,j+} = \mathbf{u}_i^* + \Delta \mathbf{u}_i^{j+}$, in which the

j-th element of $\Delta \mathbf{u}_i^{j+}$ is Δu_j, and the other elements of $\Delta \mathbf{u}_i^{j+}$ are all zero; and

$\mathbf{u}_i^{*,k+} = \mathbf{u}_i^* + \Delta \mathbf{u}_i^{k+}$, in which the k-th element of $\Delta \mathbf{u}_i^{k+}$ is Δu_k, and the other elements of

$\Delta \mathbf{u}_i^{k+}$ are all zero.

$\hat{g}_{Z_i}(\mathbf{u}_i^{*,++})$ is computed as follows：

$$\hat{g}_{Z_i}(\mathbf{u}_i^{*,++}) = \hat{g}_{Z_i}(\mathbf{U}_i, \mathbf{L}_{\bullet i}(t))\Big|_{\mathbf{U}_i=\mathbf{u}_i^*+\Delta\mathbf{u}^{++}} \tag{17}$$

in which $\mathbf{L}_{\bullet i}(t)\Big|_{\mathbf{U}=\mathbf{u}_i^*+\Delta\mathbf{u}^{++}}$ is computed from the following equations

$$\begin{cases} \mathbf{L}_{1i}(t) = \hat{\mathbf{g}}_{\mathbf{L}_{1i}}(\mathbf{U}_i, \mathbf{L}_{\bullet 1}(t))\Big|_{\mathbf{U}_i=\mathbf{u}_i^*+\Delta\mathbf{u}^{++}} \\ \quad\vdots \qquad\qquad\qquad \vdots \\ \mathbf{L}_{(i-1)i}(t) = \hat{\mathbf{g}}_{\mathbf{L}_{(i-1)i}}(\mathbf{U}_i, \mathbf{L}_{\bullet(i-1)}(t))\Big|_{\mathbf{U}_i=\mathbf{u}_i^*+\Delta\mathbf{u}^{++}} \\ \mathbf{L}_{(i+1)i}(t) = \hat{\mathbf{g}}_{\mathbf{L}_{(i+1)i}}(\mathbf{U}_i, \mathbf{L}_{\bullet(i+1)}(t))\Big|_{\mathbf{U}_i=\mathbf{u}_i^*+\Delta\mathbf{u}^{++}} \\ \quad\vdots \qquad\qquad\qquad \vdots \\ \mathbf{L}_{ni}(t) = \hat{\mathbf{g}}_{\mathbf{L}_{ni}}(\mathbf{U}_i, \mathbf{L}_{\bullet n}(t))\Big|_{\mathbf{U}_i=\mathbf{u}_i^*+\Delta\mathbf{u}^{++}} \end{cases} \tag{18}$$

3.3 MCS ON APPROXIMATED LIMIT-STATE FUNCTION

After the limit-state function is approximated into a linear or quadratic form, it is still hard to find the time-dependent probability of failure analytically or even numerically. Let us look at the simpler case with a linearized limit-state function. The linear function is now a stationary Gaussian process. It is well known that the time-dependent probability of failure is equal to the probability that the extreme (maximum) value of the stationary Gaussian response is greater than the limit state. The distribution of the extreme value, however, can be hardly found because an analytical solution does not exist. We therefore resort to Monte Carlo simulation (MCS). After the approximation, we use MCS based on the approximated limit-state function. Note that MCS will not call the limit-state function or MDA any more. There are two sampling tasks – one is sampling of random variables and the other is sampling of stochastic processes.

Since all the random variables follow standard normal distributions as shown in Eqs. (10) and (14), their samples can be easily generated. All the stochastic processes are

standard Gaussian processes. To generate their samples, we first divide time interval

$[t_0, t_s]$ into m time points $(t_i)_{i=1,2,\cdots,m} = (t_1 = t_0, t_2, \ldots, t_m, t_m = t_s)$. The samples of standard

Gaussian stochastic process $U(t)$ are then generated by the Expansion Optimal Linear

Estimation (EOLE) method [42].

$$U(t) = \sum_{i=1}^{p} \frac{V_i}{\sqrt{\eta_i}} \varphi_i^T \rho_U(t, t_i) \tag{19}$$

where V_i ($i = 1, 2, \cdots, p \leq m$) are independent standard normal random variables, and η_i

and φ_i^T are the eigenvalues and eigenvectors of the matrix Σ, respectively. Σ is given

by

$$\Sigma = \begin{pmatrix} \rho_U(t_1, t_1) & \rho_U(t_1, t_2) & \cdots & \rho_U(t_1, t_m) \\ \rho_U(t_2, t_1) & \rho_U(t_2, t_2) & \cdots & \rho_U(t_2, t_m) \\ \vdots & \vdots & \ddots & \vdots \\ \rho_U(t_m, t_1) & \rho_U(t_m, t_2) & \cdots & \rho_U(t_m, t_m) \end{pmatrix}_{m \times m} \tag{20}$$

where $\rho_U(t_1, t_2)$ is the autocorrelation function of $U(t)$. More details about the sampling

generation method can be found in [42].

Let the N samples be $\tilde{\mathbf{u}}_j$ ($j = 1, 2, \ldots, N$), the samples of response Z_i are then

available as shown below.

$$[\mathbf{z}_i(1); \mathbf{z}_i(2); \ldots; \mathbf{z}_i(\mathbf{m})] = \begin{bmatrix} \widehat{g}_{Z_i}(\tilde{\mathbf{u}}_1, t_1) & \cdots & \widehat{g}_{Z_i}(\tilde{\mathbf{u}}_1, t_m) \\ \vdots & \ddots & \vdots \\ \widehat{g}_{Z_i}(\tilde{\mathbf{u}}_N, t_1) & \cdots & \widehat{g}_{Z_i}(\tilde{\mathbf{u}}_N, t_m) \end{bmatrix} \tag{21}$$

Note that the original limit-state function is not called, and $\widehat{g}_{Z_i}(\bullet)$ in the above

equation is replaced by the approximate limit-state function at the MPP.

With the samples in Eq. (21), we now find the samples of the maximum response as follows:

$$z_i^{\max}(j) = \max_{k=1,\cdots,m} \{\widehat{g}_{Z_i}(\tilde{\mathbf{u}}_j, t_k)\} \text{ where } j = 1, 2, \ldots, N \tag{22}$$

Then the time-dependent probability of failure is estimated by

$$p_f(t_0, t_s) = \frac{N_f}{N} \tag{23}$$

where

$$N_f = \sum_{j=1}^{N} I_j \tag{24}$$

in which, the indicator function is defined by

$$I_j = \begin{cases} 1, \text{if } z_i^{\max}(j) \geq e \\ 0, \text{otherwise} \end{cases} \tag{25}$$

4. EXAMPLES

Two examples are used to demonstrate the proposed method. The first one is a mathematical problem representing a simple multidisciplinary system and is used for a clear demonstration. The second one is an engineering problem. The two problems are solved using the following four methods:

- Proposed method based on FORM (FORM-MCS)

- Proposed method based on SORM (SORM-MCS)

- Upcrossing rate method (Upcrossing)

- Direct Monte Carlo Simulation (MCS) that calls the original limit-state functions

The reason we use the above methods is to evaluate the accuracy and efficiency of the proposed method.

4.1 MATHEMATICAL EXAMPLE

Figure 4.1 shows the structure of a multidisciplinary system. There are two subsystems. For subsystem 1,

$$
\begin{aligned}
L_{12}(t) &= X_1^2 + X_2 + Y_1(t) - 0.2L_{21}(t) \\
Z_1(t) &= X_2^2 + Y_1(t) + L_{12}(t) + L_{21}^2(t)
\end{aligned}
\tag{26}
$$

For subsystem 2,

$$
\begin{aligned}
L_{21}(t) &= \sqrt{L_{12}(t)} + X_1 + Y_1(t) \\
Z_2(t) &= X_1^2 + Y_1(t) + L_{21}(t) + e^{-L_{12}(t)}
\end{aligned}
\tag{27}
$$

where X_1 and X_2 are random variables, and $Y_1(t)$ is a stationary Gaussian process.

The information of above random variables and Gaussian process is given in Table 4.1. The autocorrelation coefficient function of $Y_1(t)$ is given by

$$\rho_{Y_1}(t_1, t_2) = \exp\left\{-\left[(t_2 - t_1)/\lambda\right]^2\right\} \tag{28}$$

where $\lambda = 0.9$, which is a correlation length.
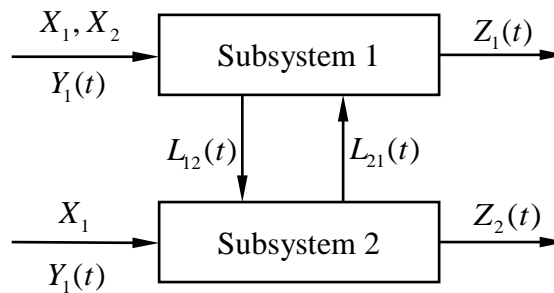
Figure 4.1 Mathematical example

The following time-dependent probability of failure needs to be evaluated:

$$p_f(t_0, t_s) = \Pr\left\{Z_1(t) > e_1, t \in [t_0, t_s]\right\} \tag{29}$$

where $e_1 = 22$ is the limit state of output $Z_1(t)$, and $[t_0, t_s] = [0, 10]$.

Table 4.1 Inputs of mathematical example

Variable	Mean	Standard deviation	Distribution	Autocorrelation
x_1	1	0.1	Normal	N/A
x_2	1	0.1	Normal	N/A
$Y_1(t)$	1	0.1	Gaussian Process	Eq. (28)

For MCS, the time interval $[0,10]$ was divided into 200 time instants and 10^6 samples were generated at each time instant. We use the number of MDA calls to measure the efficiency and the following percentage error to measure the accuracy:

$$\varepsilon = \frac{\left| p_f(t_0, t_s) - p_f^{MCS}(t_0, t_s) \right|}{p_f^{MCS}(t_0, t_s)} \times 100\% \tag{30}$$

where $p_f^{MCS}(t_0, t_s)$ and $p_f(t_0, t_s)$ are the probabilities of failure obtained from MCS and a non-MCS method, respectively.

The results for time intervals $[0,1], [0,2], \cdots, [0,10]$ are plotted in Figure 4.2, and the results for one time interval $[0,10]$ are given in Table 4.2.
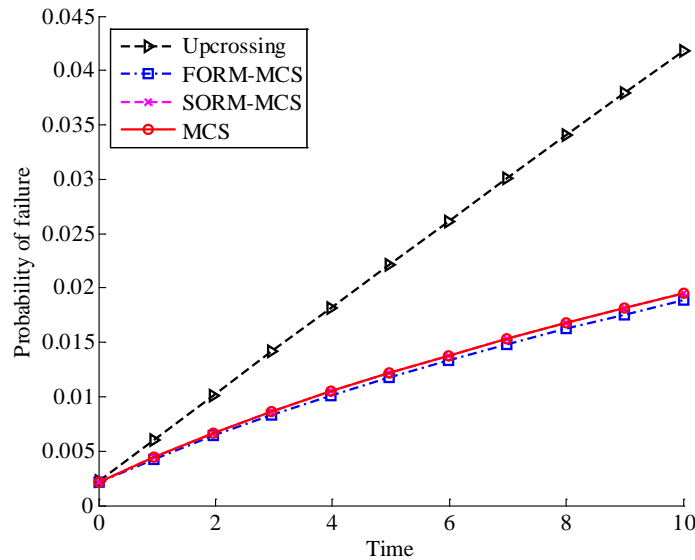
Figure 4.2 Probabilities of failure on different time intervals

The results show the good accuracy and efficiency of the proposed method. The SORM-MCS method produced the results almost identical to those from MCS and is more accurate due to the use of the second order Taylor series expansion. Its efficiency, however, is lower than that of FORM-MCS. Both FORM-MCS and SORM-MCS are much more accurate than the traditional upcrossing rate method.

Table 4.2 Results comparison of mathematical example

Method	p_f	Error (%)	MDA calls
Upcrossing	0.041853	114.42	54
FORM-MCS	0.018857	3.39	54
SORM-MCS	0.019517	0.01	90
MCS	0.019519	N/A	2×10^8

The proposed method with FORM has the same efficiency as the upcrossing method. Both methods require one MPP search, after which no additional MDA calls.

4.2 COMPOUND CYLINDER PROBLEM

An engineering example [14, 43] is used as our second example. The compound cylinder system is treated as a multidisciplinary system, and its inner and outer cylinders are considered as Subsystems 1 and 2, respectively. Its structure is shown in Figures 4.3 and 4.4.

In Figure 4.3, a is the inner radius of the inner cylinder, b is the external radius of the inner cylinder but also the inner radius of the outer cylinder, and c is the external

radius of the outer cylinder. $p_0(t)$ is the internal pressure, which is a stationary Gaussian stochastic process, and its autocorrelation coefficient function is

$$\rho_{p_0}(t_1, t_2) = \exp\left\{-\left[(t_2 - t_1)/\lambda\right]^2\right\} \tag{31}$$

where $\lambda = 0.9$ years is the correlation length of $p_0(t)$.

The inputs and outputs of subsystems are given below.
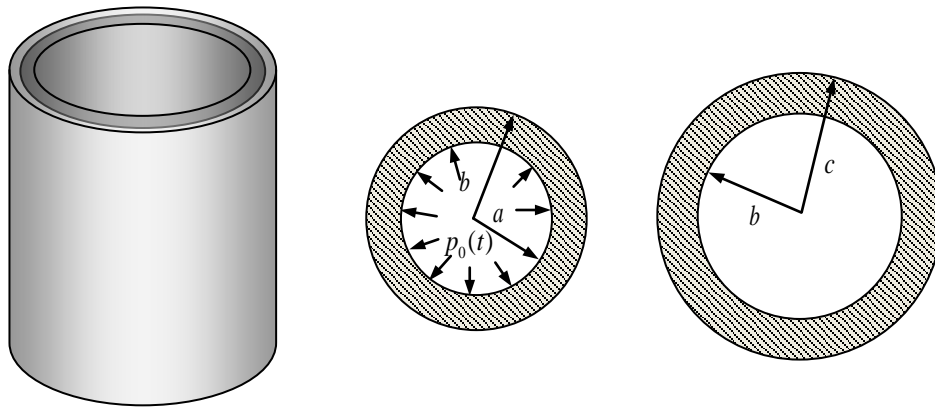
Compound cylinder system   Subsystem 1: Inner cylinder   Subsystem 2: outer cylinder

Figure 4.3 The compound cylinders
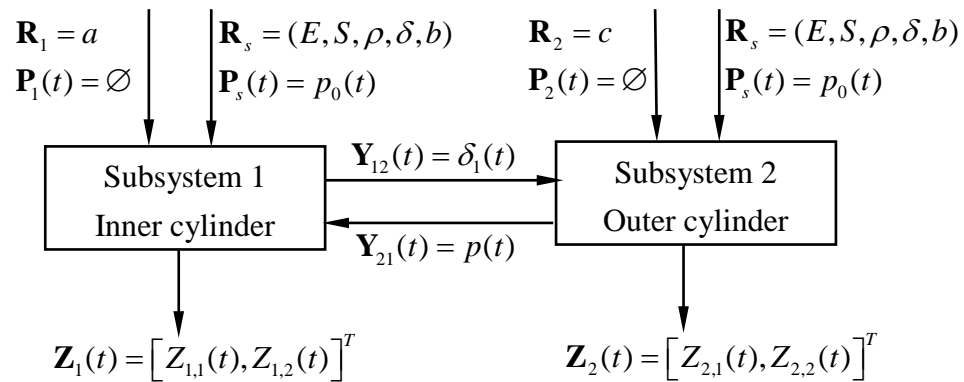
Figure 4.4 System structure of the compound cylinders

For Subsystem 1:

Inputs: $\mathbf{X}_1 = a, \mathbf{Y}_1(t) = \varnothing, \mathbf{X}_s = (E, S, \rho, \delta, b)^T, \ \mathbf{Y}_s(t) = p_0(t), \mathbf{L}_{.1}(t) = L_{21}(t)$

where $L_{21}(t) = p(t), \delta = \delta_1(t) + \delta_2(t)$ and

$$p(t) = \frac{E\delta_2(t)}{b} \bigg/ \left(\frac{b^2 + c^2}{c^2 - b^2} + \rho \right) \tag{32}$$

Outputs: $\mathbf{Z}_1(t) = \left[Z_{1,1}(t), Z_{1,2}(t) \right]^T, \ \mathbf{L}_{1.} = L_{12}(t) = \delta_1(t)$

$$\delta_1(t) = \frac{p(t)b}{E} \left(\frac{b^2 + a^2}{b^2 - a^2} - \rho \right) \tag{33}$$

$$Z_{1,1}(t) = \sigma_a(t) - S \tag{34}$$

$$Z_{1,2}(t) = \sigma_b^{in}(t) - S \tag{35}$$

$$\sigma_a(t) = \frac{-2p(t)b^2}{b^2 - a^2} + \frac{(a^2 + c^2)p_0(t)}{c^2 - a^2} \tag{36}$$

$$\sigma_b^{in}(t) = \frac{-p(t)(b^2 + a^2)}{b^2 - a^2} + \frac{a^2(b^2 + c^2)p_0(t)}{(c^2 - a^2)b^2} \tag{37}$$

where E is the young's modulus, S is the allowable stress, δ is the total allowable shrinkage of the two cylinders at the interface, ρ is the Poisson's ratio, and these are random variables.

$p(t)$ is the contact stress at the interface, $\sigma_a(t)$ and $\sigma_b^{in}(t)$ are the tangential stresses of the inner cylinder at the internal radius a and the external radius b, respectively, and and $\delta_2(t)$ are the radial deformation of the inner and outer cylinder at radius b, respectively.

Table 4.3 Inputs of compound cylinder problem

Input	μ	σ	Distribution	Autocorrelation
E (psi)	3×10^7	3×10^6	Normal	N/A
S (psi)	4×10^4	4×10^3	Normal	N/A
ρ (psi)	0.3	0.03	Normal	N/A
δ (in.)	0.004	0.0004	Normal	N/A
a (in.)	7.5	0.4	Normal	N/A
b (in.)	10	0.6	Normal	N/A
c (in.)	15	0.8	Normal	N/A
$p_0(t)$ (psi)	20×10^3	2×10^3	Gaussian Process	Eq. (31)

Table 4.4 Results comparison of compound cylinder problem

Method	p_f	Error (%)	MDA calls
Upcrossing	0.092251	46.99	596
FORM-MCS	0.058273	7.15	596
SORM-MCS	0.064065	2.08	1215
MCS	0.06276	N/A	2×10^8

For Subsystem 2:

Inputs: $\mathbf{X}_2 = c$, $\mathbf{Y}_2(t) = \varnothing$, $\mathbf{X}_s = (E, S, \rho, \delta, b)^T$, $\mathbf{Y}_s(t) = p_0(t)$, $\mathbf{L}_{\cdot 2}(t) = L_{12}(t) = \delta_1(t)$

Outputs: $\mathbf{Z}_2(t) = \left[Z_{2,1}(t), Z_{2,2}(t) \right]^T$, $\mathbf{L}_{2\cdot}(t) = L_{21}(t)$, $L_{21}(t) = p(t)$

$$p(t) = \frac{E\delta_2(t)}{b} \Big/ \left(\frac{b^2 + c^2}{c^2 - b^2} + \rho \right) \tag{38}$$

$$Z_{2,1}(t) = \sigma_b^{out}(t) - S \tag{39}$$

$$Z_{2,2}(t) = \sigma_c(t) - S \tag{40}$$

$$\sigma_b^{out}(t) = \frac{p(t)(b^2 + c^2)}{c^2 - b^2} + \frac{a^2(b^2 + c^2)p_0(t)}{(c^2 - a^2)b^2} \tag{41}$$

$$\sigma_c(t) = \frac{2b^2 p(t)}{c^2 - b^2} + \frac{2a^2 p_0(t)}{c^2 - a^2} \tag{42}$$

where $\sigma_b^{out}(t)$ and $\sigma_c(t)$ are the tangential stress of the outer cylinder at the internal radius b and the external radius c, respectively.

The following time-dependent probability of failure needs to be estimated:

$$p_f(t_0, t_s) = \Pr\left\{ Z_{1,1}(t) = \sigma_a(t) - S > 0 \right\} \tag{43}$$

where $Z_{1,1}(t)$ is the first response of Subsystem 1.

The random variables and stochastic process are given in Table 4.3.

The results shown in Figure 4.5 and Table 4.4 indicate that the proposed method also has good accuracy and efficiency for this engineering example. The same conclusions can be drawn as those from the last example.
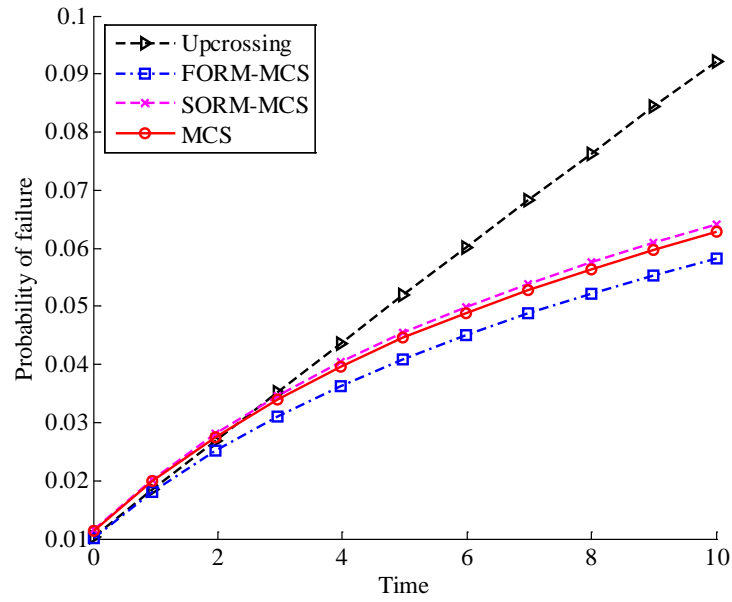
Figure 4.5 Probabilities of failure of $Z_{1,1}(t)$ over different time intervals

5. CONCLUSIONS

In this work, we developed a reliability analysis method based on FORM and SORM for time-dependent multidisciplinary systems with stationary stochastic processes. To deal with the challenge of strong coupling between multiple subsystems, we use the equations of linking variables as constraints in the MPP search. This not only guarantees the consistency of the multidisciplinary system but also ensures high efficiency. Since the MPP has the highest probability density, approximating limit-state functions at their MPPs minimizes the accuracy loss. After the approximation, MCS is used to estimate the time-dependent probability of failure. Two examples showed the accuracy and efficiency of the present method.

The proposed method is limited to multidisciplinary systems involving stationary stochastic processes and with response functions that are not explicit functions of time. Its efficiency could be improved if advanced MDA techniques can be used. This will be our future work.

ACKNOWLEDGEMENTS

REFERENCES

[1] Lund, E., Møller, H., and Jakobsen, L. A., 2003, "Shape Design Optimization of Stationary Fluid-Structure Interaction Problems with Large Displacements and Turbulence," Structural and Multidisciplinary Optimization, 25(5-6), pp. 383-392.

[2] Guo, J., and Du, X., 2010, "Reliability Analysis for Multidisciplinary Systems with Random and Interval Variables," AIAA Journal, 48(1), pp. 82-91.

[3] Maute, K., and Allen, M., 2004, "Conceptual Design of Aeroelastic Structures by Topology Optimization," Structural and Multidisciplinary Optimization, 27(1-2), pp. 27-42.

[4] Peri, D., and Campana, E. F., 2003, "Multidisciplinary Design Optimization of a Naval Surface Combatant," Journal of Ship Research, 47(1), pp. 1-12.

[5] Hart, C. G., and Vlahopoulos, N., 2010, "An Integrated Multidisciplinary Particle Swarm Optimization Approach to Conceptual Ship Design," Structural and Multidisciplinary Optimization, 41(3), pp. 481-494.

[6] Kodiyalam, S., Yang, R., Gu, L., and Tho, C.-H., 2004, "Multidisciplinary Design Optimization of a Vehicle System in a Scalable, High Performance Computing Environment," Structural and Multidisciplinary Optimization, 26(3-4), pp. 256-263.

[7] Grujicic, M., Arakere, G., Pandurangan, B., Sellappan, V., Vallejo, A., and Ozen, M., 2010, "Multidisciplinary Design Optimization for Glass-Fiber Epoxy-Matrix Composite 5 Mw Horizontal-Axis Wind-Turbine Blades," Journal of materials engineering and performance, 19(8), pp. 1116-1127.

[8] Hu, Z., and Du, X., 2012, "Reliability Analysis for Hydrokinetic Turbine Blades," Renewable Energy, 48, pp. 251-262.

[9] Tao, Y. R., Han, X., Duan, S. Y., and Jiang, C., 2013, "Reliability Analysis for Multidisciplinary Systems with the Mixture of Epistemic and Aleatory Uncertainties," International Journal for Numerical Methods in Engineering.

[10] Agarwal, H., and Renaud, J. E., 2004, "Reliability Based Design Optimization Using Response Surfaces in Application to Multidisciplinary Systems," Engineering Optimization, 36(3), pp. 291-311.

[11] Ahn, J., and Kwon, J. H., 2004, "Sequential Approach to Reliability Analysis of Multidisciplinary Analysis Systems," Structural and Multidisciplinary Optimization, 28(6), pp. 397-406.

[12] Ahn, J., and Kwon, J. H., 2006, "An Efficient Strategy for Reliability-Based Multidisciplinary Design Optimization Using Bliss," Structural and Multidisciplinary Optimization, 31(5), pp. 363-372.

[13] Du, X., and Chen, W., 2005, "Collaborative Reliability Analysis under the Framework of Multidisciplinary Systems Design," Optimization and Engineering, 6(1), pp. 63-84.

[14] Du, X., Guo, J., and Beeram, H., 2008, "Sequential Optimization and Reliability Assessment for Multidisciplinary Systems Design," Structural and Multidisciplinary Optimization, 35(2), pp. 117-130.

[15] Padmanabhan, D., and Batill, S., 2002, "Decomposition Strategies for Reliability Based Optimization in Multidisciplinary Systems Design [C]," 9th AIAA/USAF/NASA/ISSMO Symposium In Multidisciplinary Analysis & Optimization.

[16] Padmanabhan, D., and Batill, S., 2002, "Reliability Based Optimization Using Approximations with Applications to Multidisciplinary System Design," Reliability Based Optimization using Approximations with Applications to Multidisciplinary System Design.

[17] Sues, R. H., Oakley, D. R., and Rhodes, G. S., "Multidisciplinary Stochastic Optimization," pp. 934-937.

[18] Koch, P. N., Wujek, B., and Golovidov, O., 2000, "A Multi-Stage, Parallel Implementation of Probabilistic Design Optimization in an Mdo Framework," AIAA Paper AIAA, 2000(4805).

[19] Juncher Jensen, J., and Dogliani, M., 1996, "Wave-Induced Ship Full Vibrations in Stochastic Seaways," Marine Structures, 9(3), pp. 353-387.

[20] Bierbooms, W., and Cheng, P.-W., 2002, "Stochastic Gust Model for Design Calculations of Wind Turbines," Journal of Wind Engineering and Industrial Aerodynamics, 90(11), pp. 1237-1251.

[21] Hu, Z., and Du, X., 2011, "Time-Dependent Reliability Analysis with Joint Upcrossing Rates," Structural and Multidisciplinary Optimization, pp. 1-15.

[22] Hu, Z., Li, H., Du, X., and Chandrashekhara, K., 2012, "Simulation-Based Time-Dependent Reliability Analysis for Composite Hydrokinetic Turbine Blades," Structural and Multidisciplinary Optimization, pp. 1-17.

[23] Hu, Z., and Du, X., 2013, "A Sampling Approach to Extreme Value Distribution for Time-Dependent Reliability Analysis," Journal of Mechanical Design, 135(7), p. 071003.

[24] Wang, Z., and Wang, P., 2012, "A Nested Extreme Response Surface Approach for Time-Dependent Reliability-Based Design Optimization," Journal of Mechanical Design, 134, p. 121007.

[25] Du, X., 2013, "An Envelop Approach to Time-Dependent Mechanism Reliability," The ASME 2013 International Design Engineering Technical Conferences (IDETC) and Computers and Information in Engineering Conference (CIE), August 14-17, 2013 in Portland, OR.

[26] Li, J., and Mourelatos, Z. P., 2009, "Time-Dependent Reliability Estimation for Dynamic Problems Using a Niching Genetic Algorithm," Journal of Mechanical Design, Transactions of the ASME, 131(7), pp. 0710091-07100913.

[27] Singh, A., Mourelatos, Z., and Nikolaidis, E., 2011, "Time-Dependent Reliability of Random Dynamic Systems Using Time-Series Modeling and Importance Sampling," SAE International Journal of Materials and Manufacturing, 4(1), pp. 929-946.

[28] Singh, A., Mourelatos, Z. P., and Li, J., 2010, "Design for Lifecycle Cost Using Time-Dependent Reliability," Journal of Mechanical Design, Transactions of the ASME, 132(9), pp. 0910081-09100811.

[29] Pandey, V., and Mourelatos, Z. P., "Decision-Based Design Using Time-Varying Preferences Represented by Stochastic Processes," Proc. ASME 2012 International Design Engineering Technical Conferences and Computers and Information in Engineering Conference, American Society of Mechanical Engineers, pp. 123-130.

[30] Hu, Z., and Du, X., 2013, "Lifetime Cost Optimization with Time-Dependent Reliability," Engineering Optimization(ahead-of-print), pp. 1-22.

[31] Wang, Z., and Wang, P., 2014, "A Maximum Confidence Enhancement Based Sequential Sampling Scheme for Simulation-Based Design," Journal of Mechanical Design, Transactions of the ASME, 136(2).

[32] Wang, Z., Mourelatos, Z. P., Li, J., Baseski, I., and Singh, A., 2014, "Time-Dependent Reliability of Dynamic Systems Using Subset Simulation with Splitting over a Series of Correlated Time Intervals," Journal of Mechanical Design, Transactions of the ASME, 136(6).

[33] Wang, Z., and Wang, P., 2013, "A New Approach for Reliability Analysis with Time-Variant Performance Characteristics," Reliability Engineering & System Safety, 115(0), pp. 70-81.

[34] Nielsen, U. D., 2010, "Calculation of Mean Outcrossing Rates of Non-Gaussian Processes with Stochastic Input Parameters - Reliability of Containers Stowed on Ships in Severe Sea," Probabilistic Engineering Mechanics, 25(2), pp. 206-217.

[35] Do, D. M., Gao, W., Song, C., and Tangaramvong, S., 2014, "Dynamic Analysis and Reliability Assessment of Structures with Uncertain-but-Bounded Parameters under Stochastic Process Excitations," Reliability Engineering & System Safety, 132(0), pp. 46-59.

[36] Hu, Z., and Du, X., "Time-Dependent Reliability Analysis by a Sampling Approach to Extreme Values of Stochastic Processes," Proc. Proceedings of the ASME Design Engineering Technical Conference, pp. 1075-1086.

[37] Singh, A., Mourelatos, Z. P., and Nikolaidis, E., "An Importance Sampling Approach for Time-Dependent Reliability," Proc. Proceedings of the ASME Design Engineering Technical Conference, pp. 1077-1088.

[38] Rice, S. O., 1945, "Mathematical Analysis of Random Noise-Conclusion," Bell Systems Tech. J., Volume 24, p. 46-156, 24, pp. 46-156.

[39] Zhang, J., and Du, X., 2011, "Time-Dependent Reliability Analysis for Function Generator Mechanisms," Journal of Mechanical Design, Transactions of the ASME, 133(3).

[40] Breitung, K., and Hohenbichler, M., 1989, "Asymptotic Approximations for Multivariate Integrals with an Application to Multinormal Probabilities," Journal of Multivariate Analysis, 30(1), pp. 80-97.

[41] Madsen, P. H., and Krenk, S., 1984, "Integral Equation Method for the First-Passage Problem in Random Vibration," Journal of Applied Mechanics, Transactions ASME, 51(3), pp. 674-679.

[42] Li, C. C., Kiureghian, A. D.,, 1993, "Optimal Discretization of Random Fields," Journal of Engineering Mechanics, , 119(6), pp. 1136-1154.

[43] Du, X., and Zhang, Y., 2010, "An Approximation Approach to General Robustness Assessment for Multidisciplinary Systems," Journal of Computing and Information Science in Engineering, 10(1), pp. 1-9.

II. RELIABILITY ANALYSIS WITH MONTE CARLO SIMULATION AND DEPENDENT KRIGING PREDICTIONS

Zhifu Zhu and Xiaoping Du

Department of Mechanical and Aerospace Engineering

Missouri University of Science and Technology

ABSTRACT

Reliability analysis is time consuming, and high efficiency could be maintained through the integration of the Kriging method and Monte Carlo simulation (MCS). This Kriging-based MCS reduces the computational cost by building a surrogate model to replace the original limit-state function through MCS. The objective of this research is to further improve the efficiency of reliability analysis with a new strategy for building the surrogate model. The major approach used in this research is to refine (update) the surrogate model by accounting for the full information available from the Kriging method. The existing Kriging-based MCS uses only partial information. Higher efficiency is achieved by the following strategies: (1) a new formulation defined by the expectation of the probability of failure at all MCS sample points, (2) the use of a new learning function to choose training points. The learning function accounts for dependencies between Kriging predictions at all MCS samples, thereby resulting in more effective training points, and (3) the employment of a new convergence criterion. The new method is suitable for highly nonlinear limit-state functions for which the traditional First and Second Order Reliability Methods are not accurate. Its performance is compared with that of existing Kriging-based MCS method through five examples.

1. INTRODUCTION

Reliability analysis evaluates the likelihood of failure for components or systems in the presence of randomness [1]. Seeking for a good balance between accuracy and efficiency is always the focus on the methodology development of reliability analysis. Monte Carlo simulation (MCS) [2, 3] is commonly used for reliability analysis. MCS can produce high accuracy given a sufficiently large sample size. But it is computationally expensive if the sample size is too large. On the other hand, approximation methods, such as the First and Second Order Reliability Methods (FORM and SORM) [2, 4-6] are in general much more efficient, but may not be accurate for highly nonlinear limit-state functions. To this end, Design of Experiments (DoE) based MCS methods have been developed for high accuracy and efficiency.

DoE methods are used to generate initial training points, and a surrogate model is built for a limit-state function, then MCS is performed based on the surrogate model. The DoE methods for reliability analysis include response surface modeling [7-10], artificial neural networks (ANN) [7, 11], support vector machines [12], polynomial chaos expansions (PCE) [13], and Kriging [7, 14-17]. Most of these methods evaluate the limit-state function at a number of predefined points and then create a surrogate model to replace the limit-state function in the subsequent MCS.

The Kriging-based active learning reliability method is used to create the surrogate model in a sequential manner [18]. After the initial surrogate model is built with a small number of initial training points, more training points are added one by one until the surrogate model accurately represents the original limit-state function. A

learning function is employed in the model building process to select the best training points intelligently and refine the surrogate model in a most efficient fashion.

A learning function is a function that defines the criteria of selecting a best training point so that the surrogate model can be refined with improved accuracy. Different Kriging-based reliability methods use different learning functions. Based on the Efficient Global Optimization (EGO) [19], the Efficient Global Reliability Analysis (EGRA) [1] uses the expected feasibility function to determine training points, while the active learning reliability method combining Kriging and Monte Carlo Simulation (AK-MCS) [18] uses the probability of predicting the correct sign of the limit-state function as its learning function. Other leaning functions are also available [20, 21], and discussions on learning functions can be found in [22] and [23].

EGRA and AK-MCS have also been applied to system reliability [24, 25] and time-dependent reliability analyses [26, 27], and other improvements have been made [21, 22, 28-30]. The Kriging-based reliability methods can be further improved with respect to accuracy and efficiency because of the following reason: even though the responses predicted by Kriging are realizations of a Gaussian process and are therefore dependent on one another, the above methods do not account for the dependencies between the responses.

To further improve the efficiency of Kriging-based reliability methods, this work proposes a new Kriging-based reliability method. Its general process is similar to that of AK-MCS. An initial surrogate model is created with a small number of training points. Then the surrogate model is refined with more training points. Once the surrogate model becomes accurate, MCS is used to estimate the probability of failure. The contributions

of this research include the following new components that help select the new training points more efficiently.

(1) The method selects a new training point using the complete Gaussian process output of the surrogate model that is available from the Kriging method. It can therefore fully account for the correlations between output variables at all the MCS sample points.

(2) The new method calculates both the mean and variance of the estimated probability of failure with new formulas that involve the mean and covariance functions of the above Gaussian process. This makes it more effective to select new training points.

(3) Instead of focusing on the accuracy of the limit-state function, the new method focuses directly on the accuracy of the reliability estimate with a new convergence criterion. This improves the efficiency of the reliability analysis without jeopardizing the accuracy.

With the above new components, the new method is in general more effective than the methods that use independent Kriging predictions.

The remainder of this paper is organized as follows. Section 2 reviews the Kriging method and existing Kriging-based reliability methods. The new method and its implementation procedure are described in Section 3, followed by five examples in Section 4. Conclusions are made in Section 5.

2. BACKGROUND AND LITERATURE REVIEW

In this section, we review the definition of reliability and Kriging-based reliability methods.

2.1 RELIABILITY

A performance function is defined by

$$y = g(\mathbf{x}) \tag{1}$$

where $\mathbf{x}$ is a vector of random input variables, and y is a response. If $y > 0$, no failure occurs; if $y < 0$, a failure occurs. The threshold 0 is a limit state, and in this sense, $g(\mathbf{x}) = 0$ is called a limit-state function. Then the reliability is defined by the following probability

$$R = \Pr\{g(\mathbf{x}) > 0\} \tag{2}$$

And the probability of failure is defined by

$$p_f = \Pr\{g(\mathbf{x}) < 0\} \tag{3}$$

As we discussed previously, R or p_f can be estimated by MCS, surrogate MCS, FORM, and SORM.

2.2 KRIGING

Kriging is an interpolation method, which means that the prediction of an existing training point is the exact value of the response at the point. For a performance function $y = g(\mathbf{x})$, Kriging considers $y = g(\mathbf{x})$ being a realization of a Gaussian process, defined by [15]

$$G(\mathbf{x}) = \mathbf{f}(\mathbf{x})^T \boldsymbol{\beta} + Z(\mathbf{x}) \tag{4}$$

$\mathbf{f}(\mathbf{x})^T\boldsymbol{\beta}$ is a deterministic term, providing the estimate of the mean response, $\mathbf{f}(\mathbf{x}) = [f_1(\mathbf{x}), f_2(\mathbf{x}), \cdots, f_p(\mathbf{x})]^T$ is a vector of regression functions, and $\boldsymbol{\beta} = [\beta_1, \beta_2, \cdots, \beta_p]^T$ is a vector of regression coefficients. $Z(\cdot)$ is a stationary Gaussian process with zero mean and covariance

$$\text{Cov}[Z(\mathbf{x}_i), Z(\mathbf{x}_j)] = \sigma_Z^2 R(\mathbf{x}_i, \mathbf{x}_j) \tag{5}$$

in which σ_Z^2 is the process variance, and $R(\cdot, \cdot)$ is the correlation function. Due to the stochastic characteristics, Kriging provides not only the prediction of untried points, but also the variance of the prediction. The variance indicates the uncertainty of the prediction. At an untried point $\mathbf{x}$, the Kriging predictor $\hat{g}(\mathbf{x})$ follows a Gaussian distribution denoted by

$$\hat{g}(\mathbf{x}) \sim N(\mu_G(\mathbf{x}), \sigma_G^2(\mathbf{x})) \tag{6}$$

where $\mu_G(\cdot)$ and $\sigma_G^2(\cdot)$ are the Kriging prediction and Kriging variance, respectively. More details about Kriging method can be found in Appendix A and references [14, 15].

2.3 INDEPENDENT KRIGING METHODS

The output of the surrogate model from the Kriging method follows a Gaussian process. As a result, two output variables predicted by the surrogate model are two realizations of the Gaussian process and are likely dependent. The independent Kriging methods (IKM) ignore such dependence. In other words, the output variables are assumed independent. This assumption simplifies the process of building the surrogate model, but may adversely affect the efficiency of the model building process.

The other assumption of IKM is that the surrogate model at the limit state will produce an accurate reliability estimate if the surrogate model is accurate. Although this

assumption is valid, it emphasizes the accuracy of the surrogate model, instead of devoting effort directly to improving the accuracy of the reliability estimate. This may also affect the efficiency.

A sequential process is involved as the surrogate model is built iteratively with the help of MCS. After obtaining the accurate surrogate model, MCS is performed on it, and the Kriging predictions of the surrogate model are treated independently. The general idea of IKM is as follows.
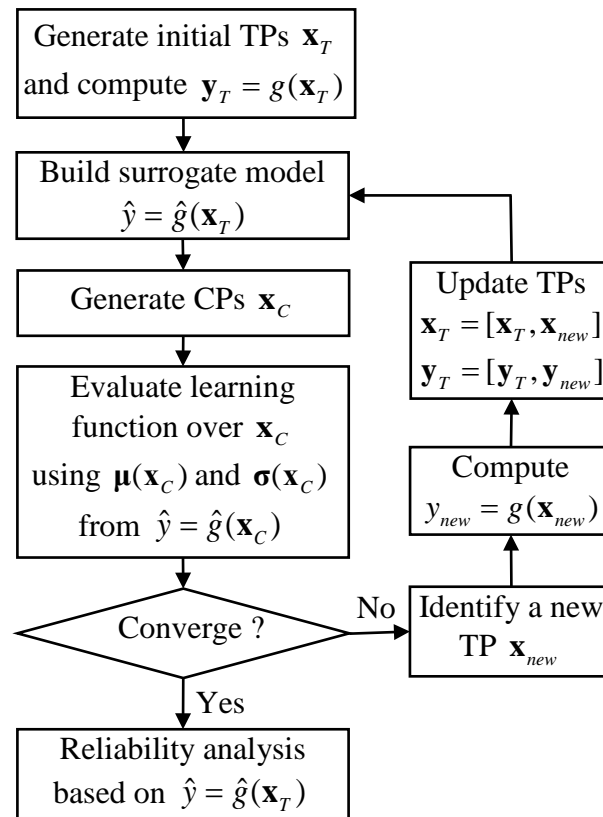
Figure 2.1 Flowchart of IKM

(1) Generate a small number of training points (TPs) for input random variables $\mathbf{x}$, denoted by $\mathbf{x}_T$. And build an initial surrogate model based on these TPs.

(2) Generate a large number of Monte Carlo sample points for $\mathbf{x}$. These points serve as candidates for the TPs and are called candidate points (CPs), denoted by $\mathbf{x}_C$.

(3) If the surrogate model is not accurate, a learning function is used to select the best TP to refine the surrogate model in a most efficient fashion.

(4) Add the new TP to the existing TPs, and then refine the surrogate model.

Steps (3) and (4) are repeated until convergence is attained. The flow chart of the process is provided in Figure 2.1. Note that the size of CPs may change during the process if the error of reliability analysis from MCS is large. The error can be found in [31].

The methods differ from one another by their learning functions. While the active learning reliability method combining Kriging and MCS (AK-MCS) [18] uses a probability measure in its learning function, the Efficient Global Reliability Analysis Method (EGRA) [1] uses the limit-state function value directly. Since the two methods have the similar performance [18], we will compare the proposed method with only AK-MCS, which is reviewed briefly next.

AK-MCS uses the probability of predicting the correct sign of the limit-state function in its learning function. With the surrogate model $\hat{y} = \hat{g}(\mathbf{x})$, the probability of failure is estimated by

$$p_f = \int_{\hat{g}(\mathbf{x})<0} f(\mathbf{x})d\mathbf{x} = \int I(\mathbf{x})f(\mathbf{x})d\mathbf{x} = \mathrm{E}\big(I(\mathbf{x})\big) \tag{7}$$

where E($\cdot$) stands for expectation, N_1 is the joint probability density function (PDF) of $\mathbf{x}$, and the indicator function $I(\cdot)$ is defined by

$$I(\mathbf{x}) = \begin{cases} 1, \ \hat{y} = \hat{g}(\mathbf{x}) < 0 \\ 0, \text{otherwise} \end{cases} \tag{8}$$

Thus, the accuracy of the reliability analysis depends on the accuracy of the indicator function or the correct sign of $\hat{g}(\mathbf{x})$. As $\hat{g}(\cdot)$ at $\mathbf{x}$ is normally distributed, the probability of a wrong sign is

$$p_w(\mathbf{x}) = \Phi\left(-\frac{|\mu(\mathbf{x})|}{\sigma(\mathbf{x})}\right) \tag{9}$$

where $\mu(\mathbf{x})$ and $\sigma(\mathbf{x})$ are mean and standard deviation of the Kriging prediction at $\mathbf{x}$, respectively.

The learning function of AK-MCS is defined by

$$U(\mathbf{x}) = \frac{|\mu(\mathbf{x})|}{\sigma(\mathbf{x})} \tag{10}$$

The smaller is U, the higher is p_w. Hence a new TP is identified with the minimum U among CPs. When U is sufficiently large, the surrogate model will be accurate at the limit state $g = 0$, and the process will then converge. $U = 2$ is used in AK-MCS [18], and it is equivalent to $p_w = 0.0228$.

As mentioned previously, the size of CPs varies during the analysis process. The coefficient of variation of p_f is used to determine the size and is given by

$$cov = \sqrt{\frac{1 - p_f}{N_C p_f}} \tag{11}$$

where N_C is the size of CPs. If $cov > 0.05$, N_C will be increased [18].

Upon convergence, the probability of failure is estimated by

$$p_f = \frac{1}{N_C} \sum_{i=1}^{N_C} I(\mathbf{x}_i) \tag{12}$$

The above equation shows that the estimate of p_f only uses the sign information of the predictions, and correlations between the predictions are not considered. The surrogate model built with Kriging, however, is a Gaussian process, and its output variables (the Kriging predictions) are dependent. This work develops a new method that accounts for such prediction dependency in order to improve the performance of IKM.

3. DEPENDENT KRIGING METHOD

We now discuss the new method that accounts for the dependencies between Kriging predictions. The method is referred to as the dependent Kriging method (DKM) for brevity.

3.1 OVERVIEW

The key points of DKM are as follows.

(1) DKM considers correlations between Kriging predictions at all CPs.

(2) As a result, DKM uses complete statistical characteristics of the Gaussian process, including not only the mean and standard deviation functions of the Gaussian process, but also its correlation function.

(3) DKM focuses directly on the accuracy of the estimate of reliability, instead of that of the limit-state function considered by IKM. DKM is therefore probability oriented, instead of function value oriented.

With the above considerations, new components of the proposed method are developed, including a new way to estimate p_f, a new learning function, a new convergence criterion, and a new procedure.

3.2 FUNDAMENTALS

We now discuss the aforementioned new components.

3.2.1 A New Way To Calculate p_f. Let the surrogate model be $\hat{y} = \hat{g}(\mathbf{x}) = \mu(\mathbf{x}) + \varepsilon(\mathbf{x})$. This model is the Kriging prediction given in Eq. (4), and $\varepsilon(\mathbf{x})$ is a Gaussian process with $N(0, \sigma^2(\mathbf{x}))$ and correlation $\mathbf{R}$. Thus

$$p_f = \int\limits_{\mu(\mathbf{x})+\varepsilon(\mathbf{x})<0} f(\mathbf{x})d\mathbf{x} = \int I(\mathbf{x})f(\mathbf{x})d\mathbf{x} = \mathrm{E}\left(I(\mathbf{x})\right) \tag{13}$$

Then

$$p_f = \frac{1}{N_C}\sum_{i=1}^{N_C}I(\mathbf{x}_i) = \frac{1}{N_C}\sum_{i=1}^{N_C}I_i \tag{14}$$

where $I_i = I(\mathbf{x}_i)$. The probability of failure at $\mathbf{x}_i$ is

$$\Pr\{I_i = 1\} = \Pr\{\hat{g}(\mathbf{x}_i) < 0\} = \Phi\left(-\mu_i/\sigma_i\right) = e_i \tag{15}$$

where $\mu_i = \mu(\mathbf{x}_i)$ and $\sigma_i = \sigma(\mathbf{x}_i)$. And

$$\Pr\{I_i = 0\} = 1 - e_i \tag{16}$$

The expectation of the indicator at $\mathbf{x}_i$ is then

$$\mathrm{E}(I_i) = 1\cdot\Pr\{I_i = 1\} + 0\cdot\Pr\{I_i = 0\} = \Pr\{I_i = 1\} = e_i \tag{17}$$

And its variance is

$$\mathrm{Var}(I_i) = \mathrm{E}(I_i^2) - \left(\mathrm{E}(I_i)\right)^2 = e_i - e_i^2 = e_i(1 - e_i) \tag{18}$$

The indicator function is a random variable because the integration region $\mu(\mathbf{x}) + \varepsilon(\mathbf{x}) < 0$ in Eq. (13) is random; p_f is also a random variable as suggested in Eq. (14).

The randomness comes from the uncertainty in Kriging predictions. Then we propose to use the expectation of p_f for the estimate of the probability of failure, which is given by

$$\mathrm{E}(p_f) = \frac{1}{N_C}\sum_{i=1}^{N_C}\mathrm{E}(I_i) = \frac{1}{N_C}\sum_{i=1}^{N_C}e_i \tag{19}$$

The error of the estimate can be measured by the variance of p_f, which is computed by

$$\mathrm{Var}(p_f) = \frac{1}{N_C^2}\mathrm{Var}\sum_{i=1}^{N_C}I_i = \frac{1}{N_C^2}\left[\sum_{i=1}^{N_C}\mathrm{Var}(I_i) + 2\sum_{j=1}^{N_C}\sum_{k>j}^{N_C}\mathrm{Cov}(I_j, I_k)\right] \qquad (20)$$

The variance accounts for the correlation between Kriging predictions through the term involving the covariance $\mathrm{Cov}(I_j, I_k)$, which is derived as follows.

$$\mathrm{Cov}(I_j, I_k) = \mathrm{E}(I_j I_k) - \mathrm{E}(I_j)\mathrm{E}(I_k) = \mathrm{Pr}(I_j = 1, I_k = 1) - \mathrm{E}(I_j)\mathrm{E}(I_k) = e_{jk} - e_j e_k \quad (21)$$

In the above equation, $e_{jk} = \mathrm{Pr}(\hat{g}(\mathbf{x}_j) < 0, \hat{g}(\mathbf{x}_k) < 0)$ is the cumulative distribution function (CDF) of the bivariate normal distribution defined by means $[\mu_j, \mu_k]$, standard deviations $[\sigma_j, \sigma_k]$, and correlation r_{jk}. Therefore,

$$\mathrm{Var}(p_f) = \frac{1}{N_C^2}\left[\sum_{i=1}^{N_C}e_i(1-e_i) + 2\sum_{j=1}^{N_C}\sum_{k>j}^{N_C}(e_{jk} - e_j e_k)\right] = \frac{1}{N_C^2}\sum_{i=1}^{N_C}c_i \qquad (22)$$

where

$$c_i = e_i(1-e_i) + \sum_{j=1, j\neq i}^{N_C}(e_{ij} - e_i e_j) \qquad (23)$$

The standard deviation of p_f is then given by

$$\sigma_{p_f} = \frac{1}{N_C}\sqrt{\sum_{i=1}^{N_C}c_i} \qquad (24)$$

3.2.2 A New Learning Function. The purpose of the learning function is to identify new TPs so that the error or $\mathrm{Var}(p_f)$ can be reduced. As indicated in Eq. (22), each CP contributes to $\mathrm{Var}(p_f)$, and the contribution is different. The sum of the terms involving $\mathbf{x}_i$ in $\mathrm{Var}(p_f)$ is c_i in Eq. (23). We therefore define c_i as the contribution to $\mathrm{Var}(p_f)$ and use c_i as the learning function. The learning function represents the contribution of the uncertainty of the Kriging prediction at $\mathbf{x}_i$ to the overall uncertainty

in the estimate of p_f. Note that the contribution also accounts for the correlation of the response at $\mathbf{x}_i$ with those at all the other CPs. Then we select the point that has the highest contribution to $\mathrm{Var}(p_f)$ as a new TP, which is therefore found by

$$\mathbf{x}_{new} = \mathbf{x}_{Ck}, \; k = \arg \max_{i=1,2,\cdots,N_C} \{c_i\} \tag{25}$$

In the above equation, $\mathbf{x}_{Ck}$ is the k-th point of CPs $\mathbf{x}_C = (\mathbf{x}_1, \mathbf{x}_2, \cdots, \mathbf{x}_{N_C})$. After the training point $\mathbf{x}_{new} = \mathbf{x}_{Ck}$ and its response $g(\mathbf{x}_{new})$ are added to train the surrogate model, the standard deviation σ_k becomes zero [14, 15, 32], and then

$$e_k = \Phi\left(-\frac{\mu_k}{\sigma_k}\right) = \begin{cases} 0, \text{if } \mu_k > 0 \\ 1, \text{if } \mu_k < 0 \end{cases} \tag{26}$$

Thus

$$e_k(1 - e_k) = 0 \tag{27}$$

$$e_{kj} = \mathrm{Pr}\{I_k = 1, I_j = 1, j = 1,2,\cdots,N_C\} = \begin{cases} 0, & \text{if } \mu_k > 0 \\ \mathrm{Pr}\{I_j = 1\} = e_j, \text{if } \mu_k < 0 \end{cases} \tag{28}$$

and

$$e_{kj} - e_k e_j = \begin{cases} 0 - 0, & \text{if } \mu_k > 0 \\ e_j - e_j, \text{if } \mu_k < 0 \end{cases} = 0 \tag{29}$$

Therefore,

$$c_k = 0 \tag{30}$$

This indicates that the contribution to $\mathrm{Var}(p_f)$ at the newly added TP becomes zero. Recall that this point has the highest contribution to $\mathrm{Var}(p_f)$ before it is added to TPs. Keep adding new TPs this way will provide the highest effectiveness way to reach convergence.

The learning function of DKM uses all the information of the Gaussian process, including its mean, variance, and correlation functions, while the IKM uses only the mean and variance functions of the Gaussian process. DKM is also more direct because it focuses on the probability of failure itself while IDM employs two steps – create an accurate surrogate model first and then calculate the probability of failure. As a result, the former method will be in general more effective than the latter method.

If correlations are neglected, the new learning function of DKM is equivalent to the learning function of IKM that has been discussed in Sec. 2.3. IKM can therefore be regarded as a special case of DKM. The proof is given in the Appendix B.

3.2.3 A New Convergence Criterion. If the error is small enough, the process of adding new TPs terminates, and then the final surrogate model is used to estimate the probability of failure. Let the allowable relative error of the probability of failure be ε. Assume the confidence is $1-\alpha$, and then the confidence interval of the estimate is given by $E(p_f) \pm \Phi^{-1}(\alpha/2)\sigma_{p_f}$. Thus, the relative error is computed by

$$\frac{\left| E(p_f) \pm \Phi^{-1}(\alpha/2)\sigma_{p_f} - E(p_f) \right|}{E(p_f)} = \left| \frac{\Phi^{-1}(\alpha/2)\sigma_{p_f}}{E(p_f)} \right| \tag{31}$$

Letting $\left| \Phi^{-1}(\alpha/2)\sigma_{p_f} / E(p_f) \right| < \varepsilon$, we obtain the following convergence criterion:

$$\frac{\sigma_{p_f}}{E(p_f)} \leq \left| \frac{\varepsilon}{\Phi^{-1}(\alpha/2)} \right| \tag{32}$$

The convergence criterion is therefore given by the ratio of σ_{p_f} to $E(p_f)$. This convergence criterion is directly linked to the error of the estimate of the probability of failure, and such a direct link does not exist in IKM.

3.3 IMPLEMENTATION

With the use of the full information of the Gaussian process, DKM will be in general more effective than IKM. Directly using the strategy of the new learning function, however, will be computationally intensive because of calculating the bivariate joint probabilities e_{ij} $(i, j = 1, 2, \cdots, N_C; i \neq j)$ for all CPs. The number of such calculations is $N_C(N_C + 1)/2$. If the size of the CPs is 10^5, the number of calculations will be $10^5(10^5 + 1)/2 \approx 5 \times 10^9$. (But note that e_{ij} does not require calling the original limit-state function.)

To avoid using all the CPs, we select a small portion of the CPs. The points in this small portion are called selected candidate points (SCPs). SCPs are selected based on two criteria: small errors in the estimate of p_f and high potential contributions to $\mathrm{Var}(p_f)$.

Let the size of SCPs be N_S and the number of failures estimated by the surrogate model be N_F in the domain of SCPs. Then the probability of failure using SCPs is approximately given by

$$\tilde{p}_f = \frac{N_F}{N_S} \tag{33}$$

The error of this estimate is proportional to $\sqrt{\dfrac{1 - \tilde{p}_f}{N_S \tilde{p}_f}}$, as indicated in Eq. (11). This shows that the higher is $\tilde{p}_f$, the smaller is the error. For the first criterion or a smaller error, we therefore prefer a larger N_F. Then we add all the CPs in the failure region to SCPs, and this means that SCPs contain all the CPs in the failure region. In

addition, to have a good balance between the two criteria, we make sure that 25% to 75% of the SCPs are in the failure region; namely

$$25\% \leq \frac{N_F}{N_S} \leq 75\% \tag{34}$$

The second criterion requires high potential contributions to $\mathrm{Var}(p_f)$. Recall that the contribution of a CP is given by $c_i = e_i(1 - e_i) + \sum_{j=1, j \neq i}^{N_C} (e_{ij} - e_i e_j)$. To avoid calculating the bivariate probabilities e_{ij} $(j = 1, 2, \cdots, N_C, j \neq i)$, we only consider the first term $e_i(1 - e_i)$, which is the variance of the indicator function at $\mathbf{x}_i$. As a result, the CPs that have the highest variances of indicator functions will be added to the set of SCPs, and the number of these points is $N_S - N_F$. The SCPs therefore consist of all the points in the failure region and other points with the highest indicator function variances in the safe region.

After the set of SCPs is formed, the learning function at each point of SCPs is calculated, and the SCP with the highest learning function value will be chosen as a new TP. Recall that evaluating the learning function needs to calculate bivariate probabilities. With the use of SCPs, the total number of bivariate probability calculations will be reduced to $N_S(N_S + 1) / 2$. If 200 SCPs are used, the total number of bivariate probability calculations will be $200(200 + 1) / 2 = 20,100$, which is much less than the number when all CPs are used.

We now discuss how to use the learning function to identify a new TP from SCPs.

The learning function now becomes

$$c_i = e_i(1-e_i) + \sum_{j=1, j\neq i}^{N_S} (e_{ij} - e_i e_j) \tag{35}$$

where $j = 1, 2, \cdots, N_S$. e_i is found using Eq. (17).

Denote the SCPs by $\mathbf{x}_S$. e_{ij} is the joint probability $\Pr\{\hat{g}(\mathbf{x}_{Si}) < 0, \hat{g}(\mathbf{x}_{Sj}) < 0\}$, which is the joint CDF of the bivariate normal distribution $N_2(\boldsymbol{\mu}_{ij}, \boldsymbol{\Sigma}_{ij})$ at $(0,0)$, and $\mathbf{x}_{Si}$ and $\mathbf{x}_{Sj}$ are the i-th and j-th components of $\mathbf{x}_S$, respectively. $\boldsymbol{\mu}_{ij}$ is given by

$$\boldsymbol{\mu}_{ij} = \left[\mu(\mathbf{x}_{Si}), \mu(\mathbf{x}_{Sj})\right] \tag{36}$$

and $\boldsymbol{\Sigma}_{ij}$ is given by

$$\boldsymbol{\Sigma}_{ij} = \begin{bmatrix} \sigma^2(\mathbf{x}_{Si}) & \mathrm{Cov}(\mathbf{x}_{Si}, \mathbf{x}_{Sj}) \\ \mathrm{Cov}(\mathbf{x}_{Sj}, \mathbf{x}_{Si}) & \sigma^2(\mathbf{x}_{Sj}) \end{bmatrix} \tag{37}$$

where $\mathrm{Cov}(\mathbf{x}_{Sj}, \mathbf{x}_{Si}) = \mathrm{Cov}(\mathbf{x}_{Si}, \mathbf{x}_{Sj})$, and $\mathrm{Cov}(\mathbf{x}_{Si}, \mathbf{x}_{Sj})$ is given by [33]

$$\mathrm{Cov}(\mathbf{x}_{Si}, \mathbf{x}_{Sj}) = \sigma^2 \left\{ \begin{array}{l} R(\mathbf{x}_{Si}, \mathbf{x}_{Sj}) - \mathbf{r}^T(\mathbf{x}_{Si})\mathbf{R}^{-1}\mathbf{r}(\mathbf{x}_{Sj}) \\ + \left[\mathbf{f}(\mathbf{x}_{Si}) - \mathbf{F}^T\mathbf{R}^{-1}\mathbf{r}(\mathbf{x}_{Si})\right]^T \left[\mathbf{F}^T\mathbf{R}^{-1}\mathbf{F}\right]^{-1} \\ \times \left[\mathbf{f}(\mathbf{x}_{Sj}) - \mathbf{F}^T\mathbf{R}^{-1}\mathbf{r}(\mathbf{x}_{Sj})\right] \end{array} \right\} \tag{38}$$

The symbols in the above equation are the same as those in Appendix A.
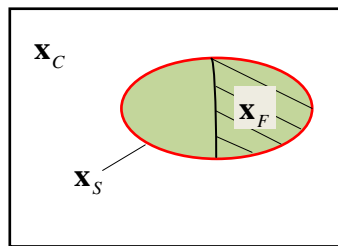
Figure 3.1 Domains of $\mathbf{x}_C$, $\mathbf{x}_S$ and $\mathbf{x}_F$

Figure 3.1 shows the domains of CPs, SCPs, and the failure region, denoted by $\mathbf{x}_C$, $\mathbf{x}_S$ and $\mathbf{x}_F$, respectively. From the figure, we have

$$p_f = \Pr(\mathbf{x} \in \mathbf{x}_F) = \Pr(\mathbf{x} \in \mathbf{x}_S, \mathbf{x} \in \mathbf{x}_F) = \Pr(\mathbf{x} \in \mathbf{x}_F \mid \mathbf{x} \in \mathbf{x}_S)\Pr(\mathbf{x} \in \mathbf{x}_S) \qquad (39)$$

where $\Pr(\mathbf{x} \in \mathbf{x}_F \mid \mathbf{x} \in \mathbf{x}_S)$ is the probability of failure in the domain of $\mathbf{x}_S$. Denoting it by p_{fS} and using Eqs. (19) and (24), we have

$$E(p_{fS}) = \frac{1}{N_S}\sum_{i=1}^{N_S} e_i \qquad (40)$$

and

$$\sigma_{p_{fS}} = \frac{1}{N_S}\sqrt{\sum_{i=1}^{N_S} c_i} \qquad (41)$$

For a given set of $\mathbf{x}_S$, $\Pr(\mathbf{x} \in \mathbf{x}_S)$ can be estimated by N_S/N_C and can be treated as a constant. Then

$$E(p_f) = E(p_{fS})\Pr(\mathbf{x} \in \mathbf{x}_S) \qquad (42)$$

$$\sigma_{p_f} = \sigma_{p_{fS}}\Pr(\mathbf{x} \in \mathbf{x}_S) \qquad (43)$$

The convergence criterion in Eq. (32) then becomes

$$\frac{\sigma_{p_{fS}}}{E(p_{fS})} = \frac{\sigma_{p_f}}{E(p_f)} \leq \left| \frac{\varepsilon}{\Phi^{-1}(\alpha/2)} \right| \qquad (44)$$

This means that we can just use the SCPs to determine the convergence criterion. After the convergence criterion is satisfied, MCS is performed on the final surrogate model to evaluate the probability of failure.

The DKM procedures discussed above are summarized below. The flow chart of the DKM is provided in Figure 3.2.
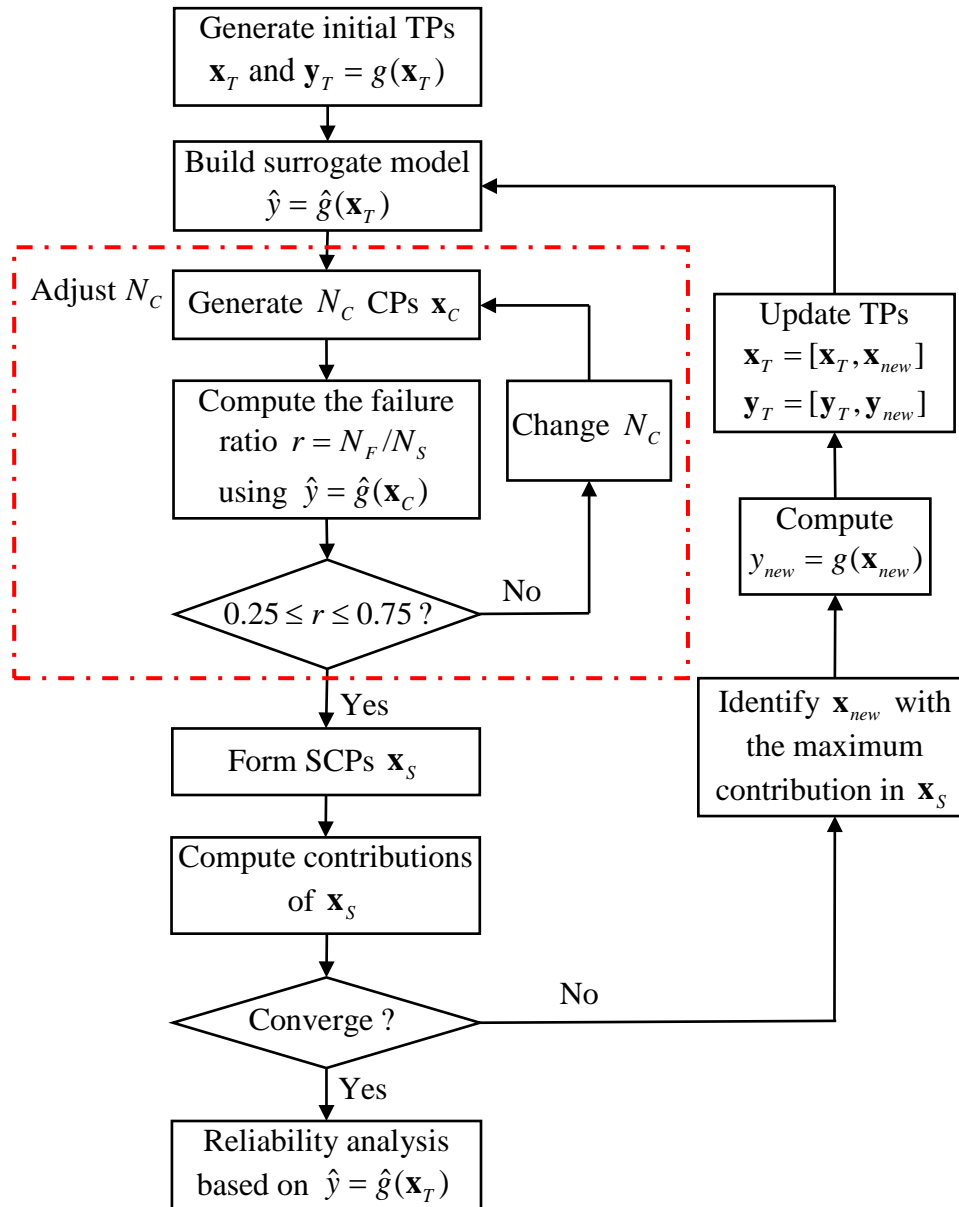
Figure 3.2 Flowchart of DKM

4. EXAMPLES

In this section, we present one numerical example and four engineering examples. These problems cover a wide range of applications. While the first example demonstrates the implementation process of DKM, the four other engineering problems evaluate the applicability of DKM for various situations, including vibration in Example 2, structural analysis in Example 3, mechanical component design in Example 4, and mechanism analysis in Example 5. All the five examples involve nonlinear limit-state functions. To build the initial surrogate model, we use Latin Hypercube sampling [34] to generate the initial TPs, and the sample size is 12 as suggested in [18]. We also use the number of limit-state function calls (N_{FC}) to measure the efficiency and the following percentage error to measure the accuracy:

$$\varepsilon = \frac{\left| p_f - p_f^{MCS} \right|}{p_f^{MCS}} \times 100\% \tag{45}$$

where p_f^{MCS} is from MCS with a large sample size and the original limit-state function. p_f^{MCS} is therefore regarded as an accurate solution for accuracy comparison. p_f is from a non-MCS method; namely, DKM, IKM, or AK-MCS. Since both DKM and IKM are based on random sampling, their results are also random. We therefore run DKM and IKM 20 times independently and then report their average results.

To have a fair comparison between DKM and IKM, ideally, we should incorporate the same convergence criteria. The direct equivalency of the convergence criteria between the two methods, however, does not exist. Thus, we implement the following strategy for the comparison.

1) For DKM, set the confidence in Eq. (31) to be 98%, or $\alpha = 0.02$, and the allowable error to be $\varepsilon = 0.02$. The number of SCPs is 200.

2) Run DKM until convergence, and record the number of function calls N_{FC}.

3) Use the same value of N_{FC} and initial TPs to run IKM. This means that if the total number of TPs reaches N_{FC}, IKM terminates.

Repeat the above steps 20 times and report the average p_f, ε, N_{FC}, and the standard deviation of p_f. With the above strategy, the accuracy of the two methods is compared with the same number of TPs or function calls.

As discussed previously, it is not easy to estimate the error of the estimated probability of failure if we use the existing Kriging-based reliability methods. DKM can easily overcome this drawback because the process of model training terminates once the estimated error of the probability of failure is small enough. To show this advantage, we also perform AK-MCS with its original procedure [18] 20 times using the same CPs as those of DKM. The parameters we use for AK-MCS are those in [18], and they are $U = 2$ and $cov = 5\%$. Then the results from MCS, DKM, IKM, and AK-MCS are put together in a table for an easy comparison.

The process of building the surrogate model actually takes place in the space of independent random variables that follow standard normal distributions. This means that all the random variables are transformed into standard normal variables during the analysis. This transformation makes programming the process more convenient, and it does not affect the performance, such as the accuracy and efficiency, of the reliability analysis.

4.1 EXAMPLE 1

A highly nonlinear performance function is defined by [1]

$$g(\mathbf{x}) = \sin\frac{5x_1}{2} + 2 - \frac{(x_1^2 + 4)(x_2 - 1)}{20} \tag{46}$$

where x_1 and x_2 are independently and normally distributed with $x_1 \sim N(1.5, 1^2)$, $x_2 \sim N(2.5, 1^2)$.

The contour of the limit-state function is plotted in Figure 4.1, which shows the high nonlinearity of the limit-state function. This figure also shows the initial TPs, added TPs, CPs, and SCPs in the last iteration for one of the 20 DKM runs. The procedure is as follows.

1) Generate 12 initial TPs, indicated by pentagrams in Figure 4.1, and use them to build an initial surrogate model.

2) Generate N_C sample points as CPs, denoted by solid dots in Figure 4.1. N_C is determined by Eq. (34), where $N_S = 200$ remains the same for all the examples. Then all the new SCPs and TPs, indicated by stars and circles, respectively, in Figure 4.1, will be selected from the CPs.

3) Select SCPs from CPs based on the state of each CP (either in the safe or failure region) and the variance of the indicator function.

4) Select a new TP from SCPs if the point has the highest contribution.

5) Add the new TP and its response to the existing set of TPs; update the surrogate model.

Steps 2) through 5) are repeated until convergence. The contour of the final surrogate model at the limit state is plotted in Figure 4.2, which shows that the surrogate model is accurate in the region where the random variables have high probability density and is less accurate in the region where the random variables have low probability density. This feature keeps the number of TPs minimum. Then Eq. (19) is used to calculate the probability of failure using the final surrogate model and the same CPs.
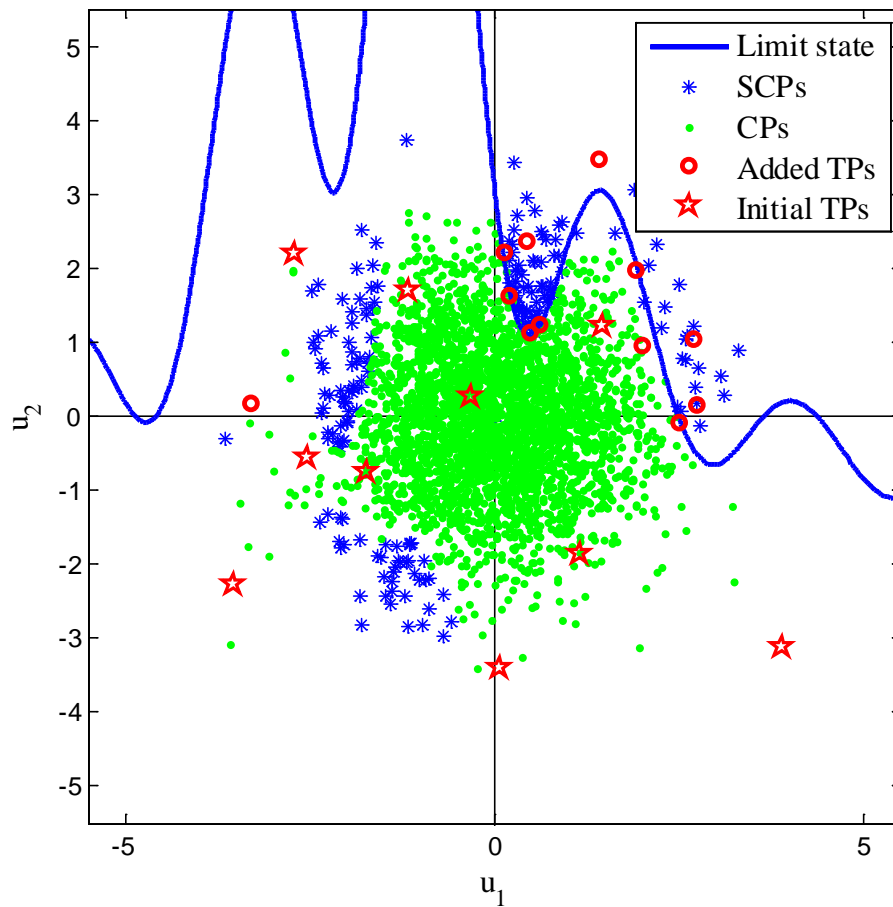
Figure 4.1 Sample points of DKM

After DKM is completed, the total number of limit-state function calls N_{FC}, which is also the total number of TPs, is recorded. Then with the same initial TPs, IKM is performed, and its TPs are added iteratively until the total number of TPs reaches the recoded number N_{FC}. Then Eq. (12) is used to calculate the probability of failure using the final surrogate model and the same CPs.
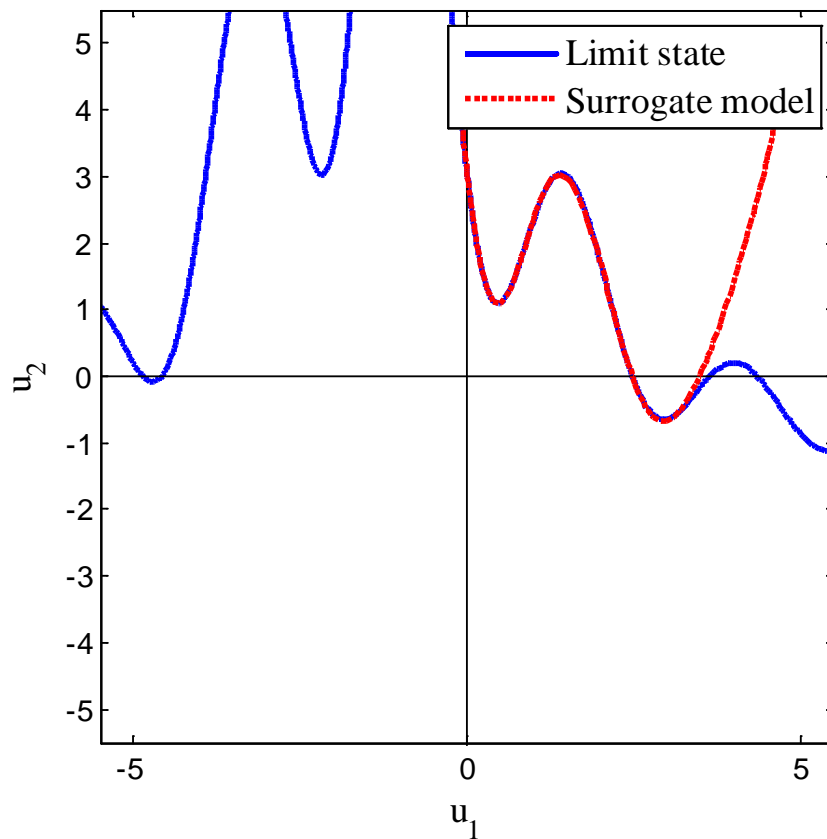
Figure 4.2 Final surrogate model

For comparison, the initial TPs, added TPs, and CPs of IKM are also plotted in Figure 4.3. By comparing Figures 4.1 and 4.3, we see that patterns of the added TPs of IKM and DKM are similar even though the two methods generate different TPs. The TPs

of IKM are generated to minimize the error of the wrong sign of the limit-state function while the TPs of DKM are generated to minimize the error in the estimate of the probability of failure. As discussed previously, both the two TP updating strategies help increase the accuracy, and this is the reason that the two patterns are similar; the two strategies also have different foci, and this is the reason that the individual TPs from the two strategies are different. As indicated in the results, the strategy of DKM makes the updating process more efficient.
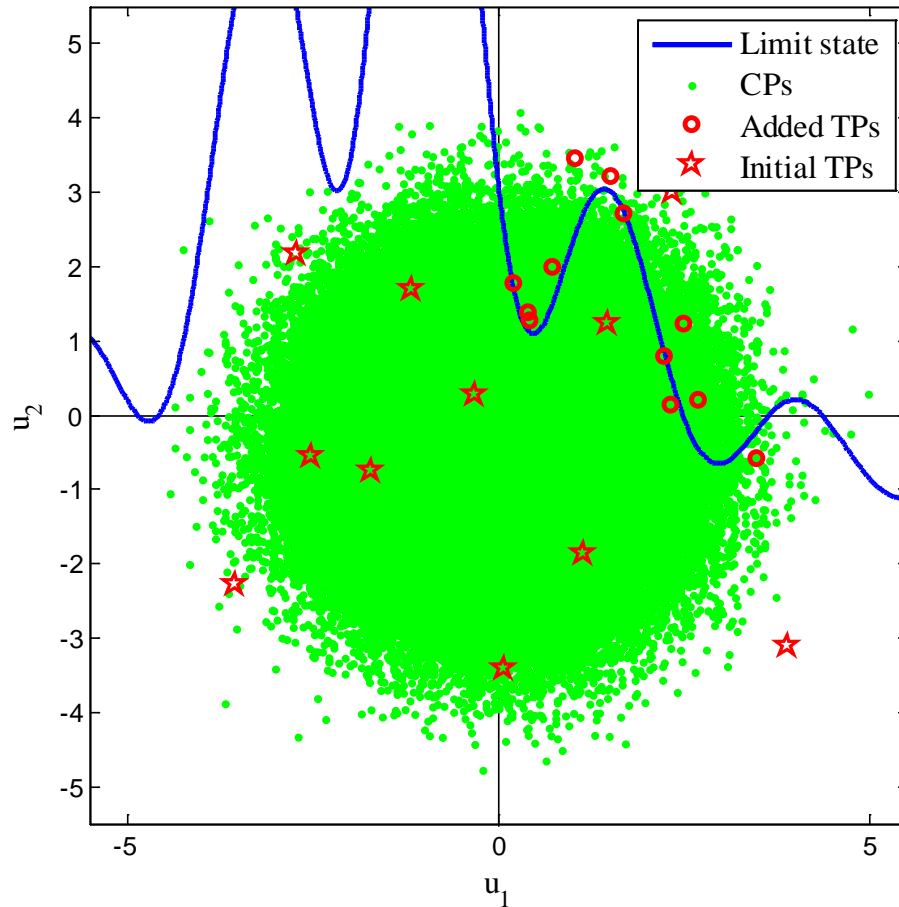
Figure 4.3 Sample points of IKM

After DKM and IKM are performed 20 times, the average results are calculated and are shown in the row of DKM and IKM, respectively, in Table 4.1. With the same average 26.3 function calls or the same efficiency, DKM is more accurate than IKM. The results also show that DKM is more robust since the standard deviation of p_f is smaller than that of IKM and AK-MCS.

The original AK-MCS is also performed 20 times with the same initial TPs as that of DKM or IKM. The results are given in the last row of Table 4.1. Both its average errors and number of function calls are larger than those of DKM and IKM. AK-MCS is less accurate for this problem because it requires a sample size smaller than that of DKM. AK-MCS is also less efficient because it requires a minimum value $U = 2$ (or the minimum probability of wrong sign = 0.0228). This requirement does not have a direct link to the error of probability of failure, and it is satisfied with more function calls than that of DKM.

Table 4.1 Average results of example one

Method	p_f	σ_{p_f}	ε (%)	N_{FC}
MCS	3.1293×10^{-2}	N/A	N/A	1×10^{6}
DKM	3.1393×10^{-2}	2.4064×10^{-4}	0.63	26.30
IKM	3.1315×10^{-2}	3.5857×10^{-4}	0.82	26.30
AK-MCS	3.1351×10^{-2}	4.8611×10^{-4}	1.24	39.45

4.2 EXAMPLE 2

Example 2 involves a nonlinear oscillator [18, 35-37] shown in Figure 4.4. With six independently and normally distributed random variables, the performance function reads as

$$g(\mathbf{x}) = 3r - \left| \frac{2F_1}{mw_0^2} \sin\left(\frac{w_0 t_1}{2} \right) \right| \tag{47}$$

where $\mathbf{x} = (m, c_1, c_2, r, F_1, t_1)$, and $w_0 = \sqrt{(c_1 + c_2)/m}$. Table 4.2 provides the distributions.

Table 4.2 Random variables of example two

Variable	Mean	Standard deviation	Distribution
m	1	0.05	Normal
c_1	1	0.1	Normal
c_2	0.1	0.01	Normal
r	0.5	0.05	Normal
F_1	1	0.2	Normal
t_1	1	0.2	Normal
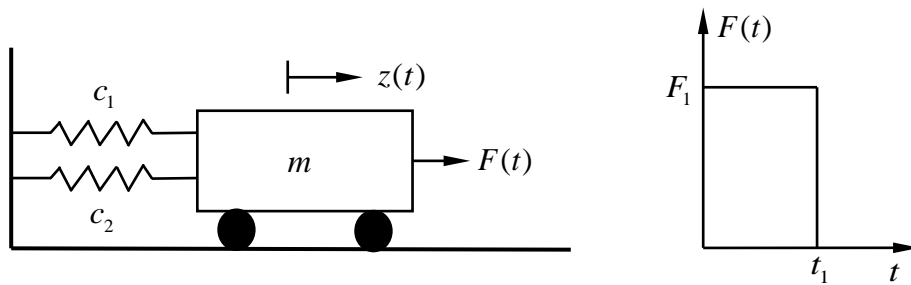
Figure 4.4 A nonlinear oscillator

The results are shown in Table 4.3, which indicate that DKM has higher accuracy than IKM, and both DKM and IKM outperform AK-MCS.

Table 4.3 Average results of example two

Method	p_f	σ_{p_f}	ε (%)	N_{FC}
MCS	2.8793×10^{-2}	N/A	N/A	2×10^6
DKM	2.8641×10^{-2}	3.1771×10^{-4}	0.83	40.95
IKM	2.8628×10^{-2}	2.4503×10^{-4}	0.96	40.95
AK-MCS	2.8430×10^{-2}	5.0794×10^{-4}	1.63	105.05

4.3 EXAMPLE 3

A roof truss structure [38, 39] is shown in Figure 4.5. Assume the truss bars bear a uniformly distributed load q, which can be transformed into nodal load $P = ql/4$.

Table 4.4 Random variables of example three

Variable	Mean	Standard deviation	Distribution
q (N/m)	20,000	1400	Normal
l (m)	12	0.12	Normal
A_s (m^2)	9.82×10^{-4}	5.982×10^{-5}	Normal
A_c (m^2)	0.04	0.0048	Normal
E_s (Pa)	1×10^{11}	6×10^9	Normal
E_c (Pa)	2×10^{10}	1.2×10^9	Normal

In Figure 4.5, A_c and A_s are the cross sectional areas of the reinforced concrete and steel bars, respectively, E_c and E_s are their corresponding elastic modulus, and l is the length of the truss.
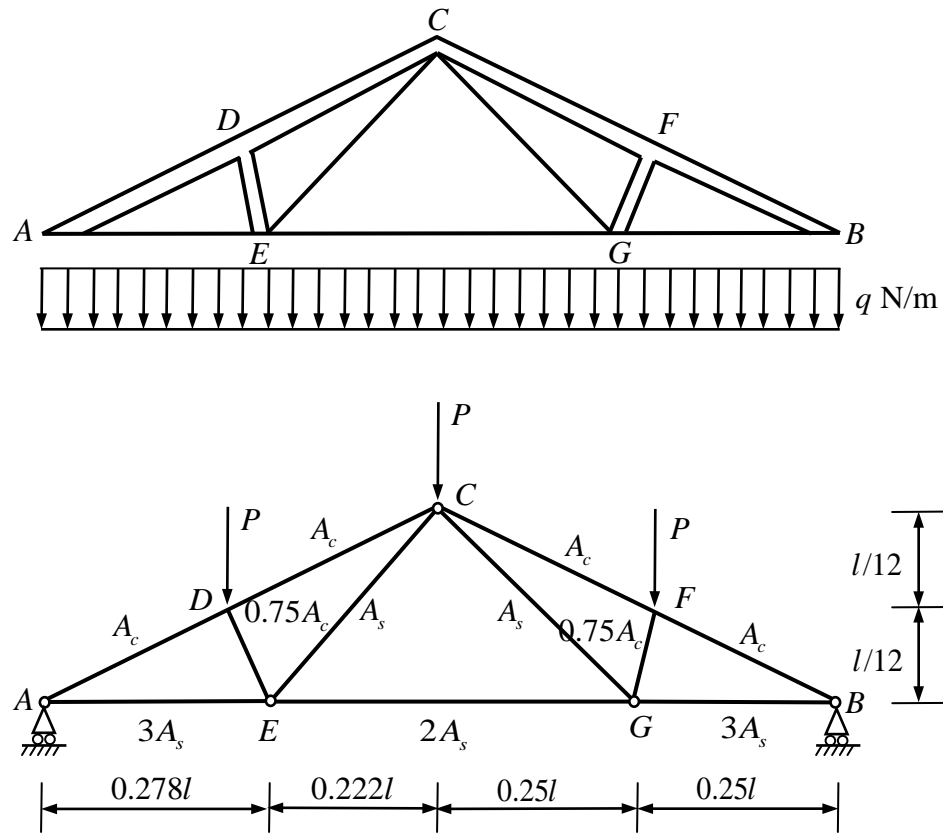
Figure 4.5 A roof truss structure

The perpendicular deflection of the truss peak node C is calculated by

$$\Delta C = \frac{ql^2}{2}\left(\frac{3.81}{A_c E_c} + \frac{1.13}{A_s E_s}\right) \tag{48}$$

A failure event occurs when the perpendicular deflection ΔC exceeds $3\,\text{cm}$. The performance function is then defined by

$$g(\mathbf{x}) = 0.03 - \frac{ql^2}{2}\left(\frac{3.81}{A_c E_c} + \frac{1.13}{A_s E_s}\right) \tag{49}$$

where $\mathbf{x} = (q, l, A_s, A_c, E_s, E_c)$. All the random variables are independent, and their distributions are given in Table 4.4.

Table 4.5 shows the average results from 20 runs, which indicate that DKM is more accurate than IKM and is also more accurate and efficient than AK-MCS.

Table 4.5 Average results of example three

Method	p_f	σ_{p_f}	ε (%)	N_{FC}
MCS	9.4890×10^{-3}	N/A	N/A	2×10^6
DKM	9.5482×10^{-3}	1.3699×10^{-4}	1.25	43.25
IKM	9.5570×10^{-3}	2.3177×10^{-4}	1.90	43.25
AK-MCS	9.3935×10^{-3}	2.7093×10^{-4}	2.31	92.40

4.4 EXAMPLE 4

The cantilever tube [40] shown in Figure 4.6 is subjected to external forces F_1, F_2, P, and torsion T. The performance function is defined as

$$g = S_y - \sigma_{\max} \tag{50}$$

in which S_y is the yield strength, σ_{max} is the maximum von Mises stress on the top surface of the tube at the origin and is given by

$$\sigma_{max} = \sqrt{\sigma_x^2 + 3\tau_{zx}^2} \tag{51}$$

The normal stress σ_x is calculated by

$$\sigma_x = \frac{P + F_1 \sin\theta_1 + F_2 \sin\theta_2}{A} + \frac{Md}{2I} \tag{52}$$

where the first term is the normal stress due to the axial forces, and the second term is the normal stress due to the bending moment M, which is given by

$$M = F_1 L_1 \cos\theta_1 + F_2 L_2 \cos\theta_2 \tag{53}$$

Table 4.6 Random variables of example four

Variable	Mean	Standard deviation	Distribution
t (mm)	5	0.1	Normal
d (mm)	42	0.5	Normal
L_1 (mm)	120	1.2	Normal
L_2 (mm)	60	0.6	Normal
F_1 (kN)	3	0.3	Normal
F_2 (kN)	3	0.3	Normal
P (kN)	12	1.2	Normal
T (N·m)	90	4	Lognormal
S_y (MPa)	145	6	Lognormal

The cross sectional area of the tube is $A = \dfrac{\pi}{4}\left[d^2 - (d - 2t)^2\right]$, and the moment of inertia

of the tube is $I = \dfrac{\pi}{64}\left[d^4 - (d - 2t)^4\right]$. The torsional stress τ_{zx} at the origin is $\tau_{zx} = \dfrac{Td}{2J}$,

where $J = 2I$. The distributions of the independent random variables are given in Table

4.6.

The results from Table 4.7 also show the higher accuracy of DKM.
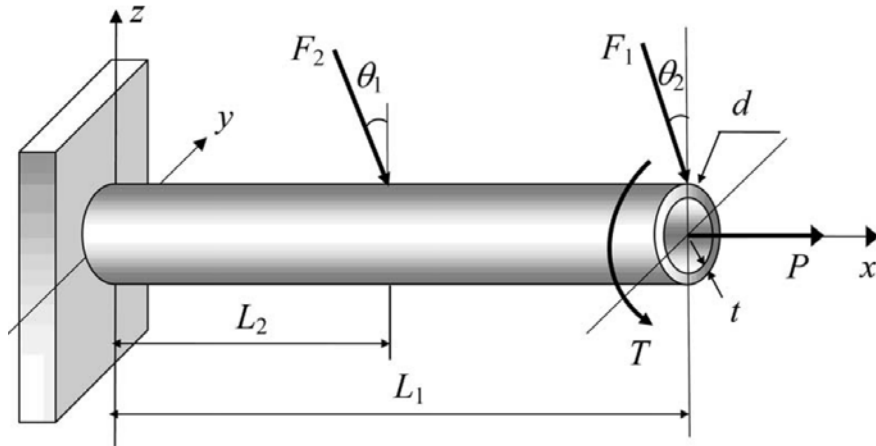
Figure 4.6 A cantilever tube

Table 4.7 Average results of example four

Method	p_f	σ_{p_f}	ε (%)	N_{FC}
MCS	6.1788×10^{-3}	N/A	N/A	5×10^6
DKM	6.1552×10^{-3}	7.8757×10^{-5}	0.92	68.65
IKM	6.1222×10^{-3}	7.1696×10^{-5}	1.15	68.65
AK-MCS	6.0815×10^{-3}	1.7590×10^{-4}	2.46	123.15

4.5 EXAMPLE 5

This example involves a slider-crank mechanism [27]. The crank is a disc with a radius of x_1 as shown in Figure 4.7. The angular velocity is $\omega = 1$ rad/s, and the length of the coupler is x_2. The motion output is the displacement of the slider, which is given by

$$S = x_1 \cos\theta + \sqrt{x_2^2 - (x_1 \sin\theta)^2} \qquad (54)$$

where x_1 and x_2 are independently and normally distributed with $x_1 \sim N(100, 0.1^2)$ mm and $x_2 \sim N(150, 0.1^2)$ mm. θ is the motion input defined by $\theta = \omega t$. The required motion output is the nominal displacements of the slider, given by

$$S_R = \mu_1 \cos\theta + \sqrt{\mu_2^2 - (\mu_1 \sin\theta)^2} \qquad (55)$$

where μ_1 and μ_2 are the mean values of x_1 and x_2, respectively.
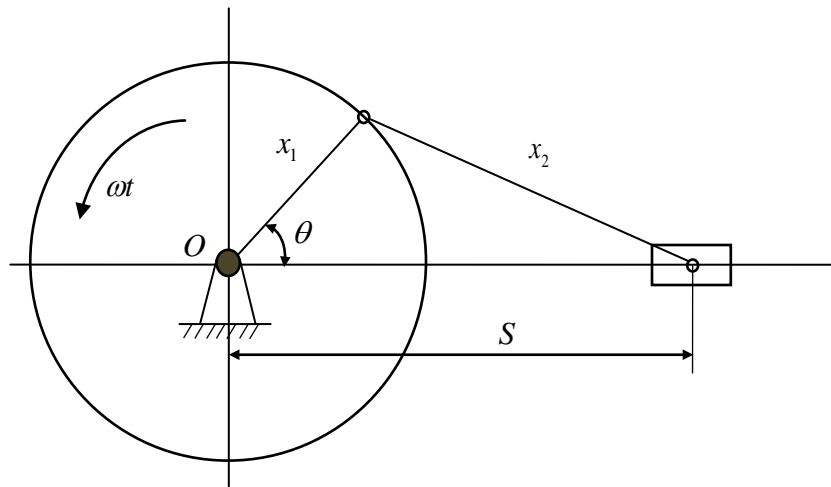
Figure 4.7 A slider-crank mechanism

The motion error should not be greater than the allowable motion error 0.55 mm. The system is required to produce accurate motion output within a full motion cycle $\theta \in [0, 2\pi]$. Thus, the motion error is

$$\Delta S = \left| S_R - S \right| \tag{56}$$
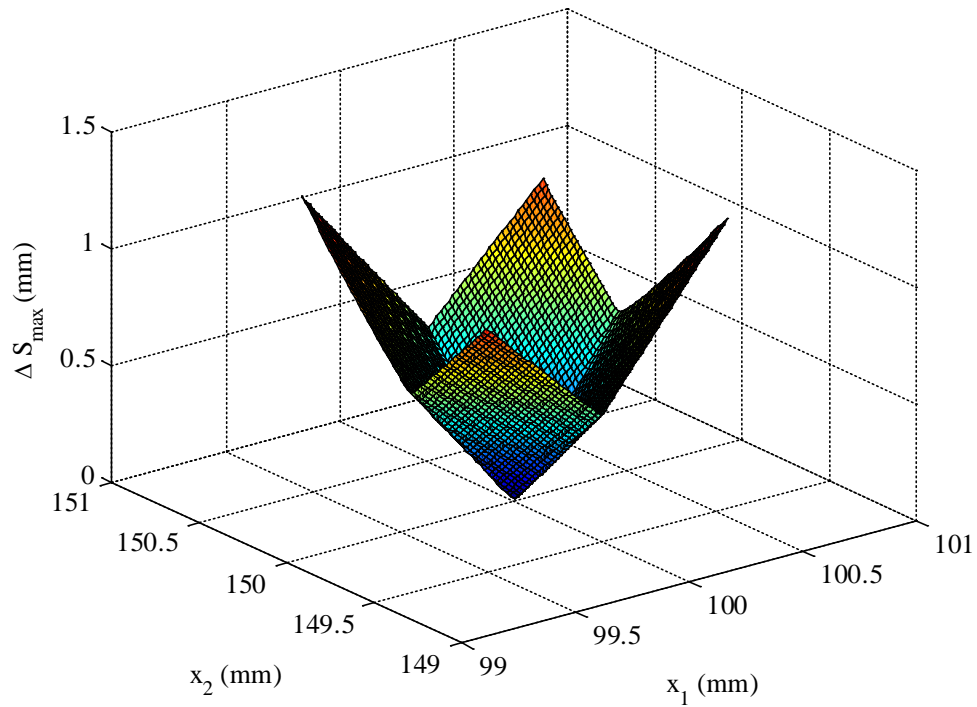
Figure 4.8 Maximum motion error of $[0, 2\pi]$ s

Table 4.8 Average results of example five

Method	p_f	σ_{p_f}	ε (%)	N_{FC}
MCS	1.2780×10^{-3}	N/A	N/A	2×10^7
DKM	1.2627×10^{-3}	1.8078×10^{-5}	1.45	33.60
IKM	1.2598×10^{-3}	2.5607×10^{-5}	1.81	33.60
AK-MCS	1.2935×10^{-3}	5.9168×10^{-5}	3.77	57.20

Thus, the maximum motion error on $[0, 2\pi]$ should not exceed 0.55 mm, and then the performance function is defined by

$$g(\mathbf{x}) = \varepsilon - \Delta S_{max}$$
$$= 0.55 - \max_{\theta} \left\{ \left| (\mu_1 - x_1) \cos\theta + \sqrt{\mu_2^2 - (\mu_1 \sin\theta)^2} - \sqrt{x_2^2 - (x_1 \sin\theta)^2} \right| \right\}, \theta \in [0, 2\pi] \quad (57)$$

The maximum motion error ΔS_{max} is shown in Figure 4.8, and the failure region is shown in Figure 4.9. The two figures indicate the irregularity and nonlinearity of the performance function and the failure region, for which traditional reliability methods, such as the FORM and SORM will not be accurate. The DKM works quite well for this problem, as indicated by the results in Table 4.8. The results show that DKM is more accurate than IKM.
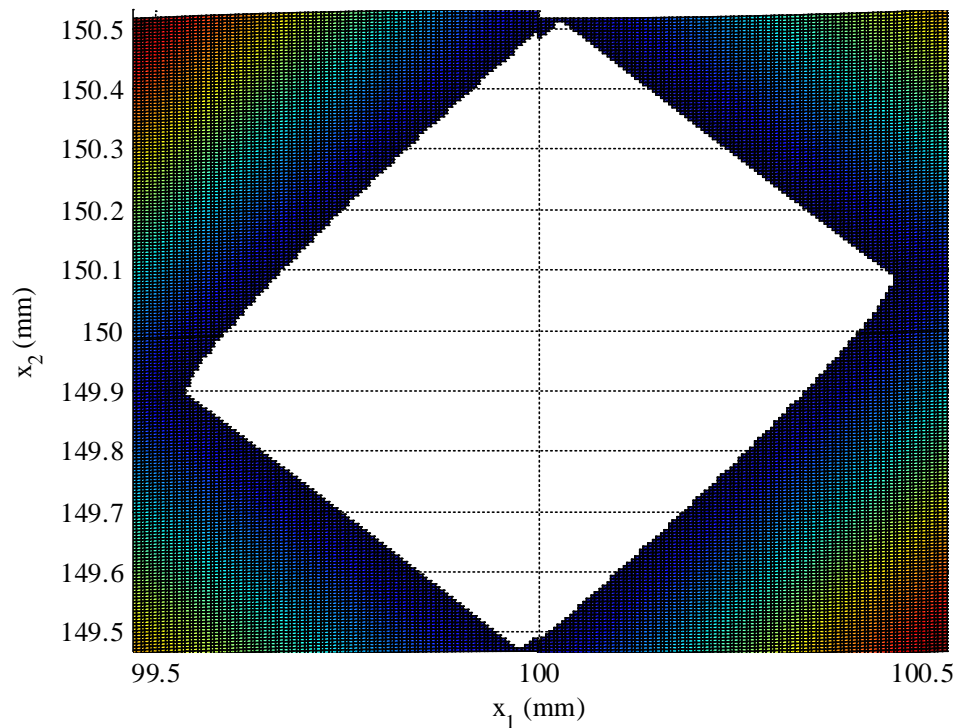
Figure 4.9 The failure region

5. CONCLUSIONS

The efficiency of reliability analysis is critical because it calls the associated limit-state function repeatedly. Kriging-based reliability methods are computationally efficient. As a result, they have increasingly been researched and applied, especially for highly nonlinear limit-state functions, for which the traditional First and Second Order Reliability Methods are not applicable. This study clearly demonstrates that the efficiency can be further improved by accounting for the dependencies between Kriging predictions.

The new dependent Kriging method (DKM) in this work improves the efficiency with its three new components. The first component is the new formula of calculating the probability of failure. The formula uses the average probability of failure at all the Monte Carlo samples, as well as both means and standard deviations of the Kriging predictions. The second component is the new learning function for selecting training points. For a single sample point, the learning function considers not only the contribution of the point itself to the error of the probability of failure, but also those of the dependencies from all the other points. The third component is the new stopping criterion that guarantees a good balance between accuracy and efficiency. The five examples indicate that DKM is more accurate than the Kriging-based methods that use only independent Kriging predictions.

The future work includes the following directions: (1) Improve the performance of DKM for problems with an extremely low probability of failure. (2) Extend DKM for system reliability analysis with at least two limit-state functions. (3) Incorporate DKM in reliability-based design, and (4) develop new DKM for time-dependent reliability analysis.

APPENDIX A

KRIGING METHOD

There are several models for the correlation function. In this work, we used the commonly used Gaussian correlation function defined by [14, 15, 32]

$$R(\mathbf{x}_i, \mathbf{x}_j) = \exp\left[-\sum_{k=1}^{d} \theta_k (x_{ik} - x_{jk})^2\right] \tag{58}$$

where x_{ik} and x_{jk} are the k-th coordinates of points $\mathbf{x}_i$ and $\mathbf{x}_j$, respectively. d is the dimensionality of $\mathbf{x}$, and θ_k indicates the correlation between the points in dimension k. The Kriging prediction and Kriging variance are computed by [14]

$$\mu_G(\mathbf{x}) = \mathbf{f}(\mathbf{x})^T \hat{\boldsymbol{\beta}} + \mathbf{r}(\mathbf{x})^T \mathbf{R}^{-1}(\mathbf{y} - \mathbf{F}\hat{\boldsymbol{\beta}}) \tag{59}$$

$$\sigma_G^2(\mathbf{x}) = \hat{\sigma}_Z^2 \left\{ \begin{aligned} &1 - \mathbf{r}(\mathbf{x})^T \mathbf{R}^{-1}\mathbf{r}(\mathbf{x}) \\ &+ \left[\mathbf{F}^T\mathbf{R}^{-1}\mathbf{r}(\mathbf{x}) - \mathbf{f}(\mathbf{x})\right]^T (\mathbf{F}^T\mathbf{R}^{-1}\mathbf{F})^{-1} \left[\mathbf{F}^T\mathbf{R}^{-1}\mathbf{r}(\mathbf{x}) - \mathbf{f}(\mathbf{x})\right] \end{aligned} \right\} \tag{60}$$

where $\mathbf{y}$ is a vector of responses at the training points, $\mathbf{F}$ is a $m \times p$ matrix with rows $\mathbf{f}(\mathbf{x})^T$, m is the number of sample points, $\mathbf{r}(\cdot)$ is the correlation vector containing the correlation between the $\mathbf{x}$ and each of the m training points

$$\mathbf{r}(\mathbf{x}) = \left[R(\mathbf{x},\mathbf{x}_1), R(\mathbf{x},\mathbf{x}_2), \cdots, R(\mathbf{x},\mathbf{x}_m)\right]^T \tag{61}$$

$\mathbf{R}$ is the correlation matrix, which is composed of correlation functions evaluated at each possible combination of the m sample points.

$$\mathbf{R} = \left[R(\mathbf{x}_i, \mathbf{x}_j)\right], 1 \leq i \leq m; 1 \leq j \leq m \tag{62}$$

$\hat{\boldsymbol{\beta}}$ is the generalized least square estimate of $\boldsymbol{\beta}$ given by [14, 15]

$$\hat{\boldsymbol{\beta}} = (\mathbf{F}^T\mathbf{R}^{-1}\mathbf{F})^{-1}\mathbf{F}^T\mathbf{R}^{-1}\mathbf{y} \tag{63}$$

and the Maximum Likelihood Estimation of the process variance is

$$\hat{\sigma}_Z^2 = \frac{1}{m}(\mathbf{y} - \mathbf{F}\hat{\boldsymbol{\beta}})^T \mathbf{R}^{-1}(\mathbf{y} - \mathbf{F}\hat{\boldsymbol{\beta}}) \tag{64}$$

APPENDIX B

IKM AS A SPECIAL CASE OF DKM

We herein show that the learning function of IKM (AK-MCS) is a special case of DKM. The learning function of DKM is $c_i = e_i(1-e_i) + \sum_{j=1, j\neq i}^{N} (e_{ij} - e_i e_j)$, which is maximized for searching for a new TP. If no correlations are considered, the learning function reduces to

$$c_i = e_i(1-e_i) \tag{65}$$
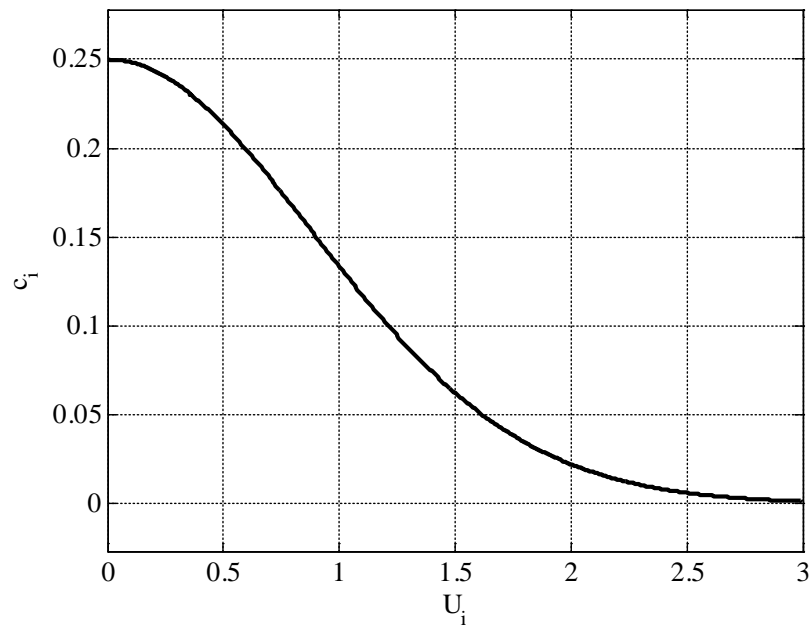
Figure A.1 The curve of c_i with respect to U_i

IKM (AK-MCS) uses the probability of wrong sign or $U_i = \dfrac{|\mu_i|}{\sigma_i}$ as its leaning

function. The leaning function is minimized for searching for a new TP. Recall that

$e_i = \Phi\left(-\mu_i/\sigma_i\right)$, and then

$$c_i = \begin{cases} \Phi(-U_i)\left[1-\Phi(-U_i)\right] & \text{if } \mu_i \geq 0 \\ \Phi(U_i)\left[1-\Phi(U_i)\right] & \text{otherwise} \end{cases} \tag{66}$$

Since $\Phi(-U_i) = 1 - \Phi(U_i)$, $\Phi(-U_i)\left[1-\Phi(-U_i)\right] = \left[1-\Phi(U_i)\right]\Phi(U_i)$, we have

$$c_i = \left[1-\Phi(U_i)\right]\Phi(U_i) \tag{67}$$

c_i is monotonic with respect to U_i as shown in Figure A.1. This indicates that

maximizing c_i in DKM without considering correlations is equivalent to minimizing U_i

in IKM. The learning function of IKM is therefore a special case of that of DKM.

ACKNOWLEDGEMENTS

REFERENCES

[1] Bichon, B. J., Eldred, M. S., Swiler, L. P., Mahadevan, S., and McFarland, J. M., "Multimodal Reliability Assessment for Complex Engineering Applications Using Efficient Global Optimization," Proc. Collection of Technical Papers - AIAA/ASME/ASCE/AHS/ASC Structures, Structural Dynamics and Materials Conference, pp. 3029-3040.

[2] Ditlevsen, O., and Madsen, H. O., 1996, Structural Reliability Methods, Wiley New York.

[3] Mourelatos, Z. P., Kuczera, R., and Latcha, M., "An Efficient Monte Carlo Reliability Analysis Using Global and Local Metamodels," Proc. Proceedings of 11th AIAA/ISSMO multidisciplinary analysis and optimization conference, September, Portsmouth, VA.

[4] Du, X., and Hu, Z., 2012, "First Order Reliability Method with Truncated Random Variables," Journal of Mechanical Design, Transactions of the ASME, 134(9), p. 091005.

[5] Zhu, Z., Hu, Z., and Du, X., 2015, "Reliability Analysis for Multidisciplinary Systems Involving Stationary Stochastic Processes," Proceedings of ASME 2015 Design Engineering Technical Conference, Paper DETC2015-46168, Boston, Massachusetts.

[6] Lee, I., Choi, K. K., and Gorsich, D., 2010, "Sensitivity Analyses of Form‐Based and Drm‐Based Performance Measure Approach (Pma) for Reliability‐Based Design Optimization (Rbdo)," International Journal for Numerical Methods in Engineering, 82(1), pp. 26-46.

[7] Simpson, T. W., Peplinski, J. D., Koch, P. N., and Allen, J. K., 2001, "Metamodels for Computer-Based Engineering Design: Survey and Recommendations," Engineering with Computers, 17(2), pp. 129-150.

[8] Gomes, H. M., and Awruch, A. M., 2004, "Comparison of Response Surface and Neural Network with Other Methods for Structural Reliability Analysis," Structural Safety, 26(1), pp. 49-67.

[9] Zou, T., Mourelatos, Z. P., Mahadevan, S., and Tu, J., 2008, "An Indicator Response Surface Method for Simulation-Based Reliability Analysis," Journal of Mechanical Design, 130(7), pp. 071401-071401.

[10] Youn, B. D., and Choi, K. K., 2004, "A New Response Surface Methodology for Reliability-Based Design Optimization," Computers & structures, 82(2), pp. 241-256.

[11] Viana, F. A. C., Simpson, T. W., Balabanov, V., and Toropov, V., 2014, "Metamodeling in Multidisciplinary Design Optimization: How Far Have We Really Come?," AIAA Journal, 52(4), pp. 670-690.

[12] Smola, A. J., and Schölkopf, B., 2004, "A Tutorial on Support Vector Regression," Statistics and Computing, 14(3), pp. 199-222.

[13] Xiu, D., and Karniadakis, G. E., 2003, "Modeling Uncertainty in Flow Simulations Via Generalized Polynomial Chaos," Journal of Computational Physics, 187(1), pp. 137-167.

[14] Lophaven, S. N., Nielsen, H. B., and Sondergaard, J., 2002, "Dace-a Matlab Kriging Toolbox, Version 2.0," Technical University of Denmark.

[15] Sacks, J., Welch, W. J., Toby, J. M., and Wynn, H. P., 1989, "Design and Analysis of Computer Experiments," Statistical Science, 4(4), pp. 409-423.

[16] Zhao, L., Choi, K., and Lee, I., 2011, "Metamodeling Method Using Dynamic Kriging for Design Optimization," AIAA Journal, 49(9), pp. 2034-2046.

[17] Joseph, V. R., Hung, Y., and Sudjianto, A., 2008, "Blind Kriging: A New Method for Developing Metamodels," Journal of Mechanical Design, 130(3), p. 031102.

[18] Echard, B., Gayton, N., and Lemaire, M., 2011, "Ak-Mcs: An Active Learning Reliability Method Combining Kriging and Monte Carlo Simulation," Structural Safety, 33(2), pp. 145-154.

[19] Jones, D., Schonlau, M., and Welch, W., 1998, "Efficient Global Optimization of Expensive Black-Box Functions," Journal of Global Optimization, 13(4), pp. 455-492.

[20] Lv, Z., Lu, Z., and Wang, P., 2015, "A New Learning Function for Kriging and Its Applications to Solve Reliability Problems in Engineering," Computers & Mathematics with Applications, 70(5), pp. 1182-1197.

[21] Wang, Z., and Wang, P., 2013, "A Maximum Confidence Enhancement Based Sequential Sampling Scheme for Simulation-Based Design," Journal of Mechanical Design, 136(2), pp. 021006-021006.

[22] Dubourg, V., Sudret, B., and Deheeger, F., 2013, "Metamodel-Based Importance Sampling for Structural Reliability Analysis," Probabilistic Engineering Mechanics, 33, pp. 47-57.

[23] Bect, J., Ginsbourger, D., Li, L., Picheny, V., and Vazquez, E., 2012, "Sequential Design of Computer Experiments for the Estimation of a Probability of Failure," Statistics and Computing, 22(3), pp. 773-793.

[24] Fauriat, W., and Gayton, N., 2014, "Ak-Sys: An Adaptation of the Ak-Mcs Method for System Reliability," Reliability Engineering and System Safety, 123, pp. 137-144.

[25] Bichon, B. J., McFarland, J. M., and Mahadevan, S., 2011, "Efficient Surrogate Models for Reliability Analysis of Systems with Multiple Failure Modes," Reliability Engineering and System Safety, 96(10), pp. 1386-1395.

[26] Hu, Z., and Du, X., 2015, "Mixed Efficient Global Optimization for Time-Dependent Reliability Analysis," Journal of Mechanical Design, 137(5), pp. 051401-051409.

[27] Zhu, Z., and Du, X., 2015, "Extreme Value Metamodeling for System Reliability with Time-Dependent Functions," Proceedings of ASME 2015 Design Engineering Technical Conference, Paper DETC2015-46162, Boston, Massachusetts.

[28] Viana, F. A. C., Haftka, R. T., and Watson, L. T., 2013, "Efficient Global Optimization Algorithm Assisted by Multiple Surrogate Techniques," Journal of Global Optimization, 56(2), pp. 669-689.

[29] Chaudhuri, A., and Haftka, R. T., 2014, "Efficient Global Optimization with Adaptive Target Setting," AIAA Journal, 52(7), pp. 1573-1577.

[30] Wang, Z., and Wang, P., 2015, "An Integrated Performance Measure Approach for System Reliability Analysis," Journal of Mechanical Design, 137(2), pp. 021406-021406.

[31] Koehler, E., Brown, E., and Haneuse, S. J. P. A., 2009, "On the Assessment of Monte Carlo Error in Simulation-Based Statistical Analyses," American Statistician, 63(2), pp. 155-162.

[32] Martin, J. D., and Simpson, T. W., 2005, "Use of Kriging Models to Approximate Deterministic Computer Models," AIAA Journal, 43(4), pp. 853-863.

[33] Arendt, P. D., Apley, D. W., and Chen, W., 2012, "Quantification of Model Uncertainty: Calibration, Model Discrepancy, and Identifiability," Journal of Mechanical Design, Transactions of the ASME, 134(10).

[34] Viana, F. A. C., Venter, G., and Balabanov, V., 2010, "An Algorithm for Fast Optimal Latin Hypercube Design of Experiments," International Journal for Numerical Methods in Engineering, 82(2), pp. 135-156.

[35] Schueremans, L., and Van Gemert, D., 2005, "Benefit of Splines and Neural Networks in Simulation Based Structural Reliability Analysis," Structural Safety, 27(3), pp. 246-261.

[36] Balesdent, M., Morio, J., and Marzat, J., 2013, "Kriging-Based Adaptive Importance Sampling Algorithms for Rare Event Estimation," Structural Safety, 44, pp. 1-10.

[37] Gayton, N., Bourinet, J. M., and Lemaire, M., 2003, "Cq2rs: A New Statistical Approach to the Response Surface Method for Reliability Analysis," Structural Safety, 25(1), pp. 99-121.

[38] Zhao, H., Yue, Z., Liu, Y., Gao, Z., and Zhang, Y., 2015, "An Efficient Reliability Method Combining Adaptive Importance Sampling and Kriging Metamodel," Applied Mathematical Modelling, 39(7), pp. 1853-1866.

[39] Song, S., Lu, Z., and Qiao, H., 2009, "Subset Simulation for Structural Reliability Sensitivity Analysis," Reliability Engineering and System Safety, 94(2), pp. 658-665.

[40] Du, X., 2008, "Unified Uncertainty Analysis by the First Order Reliability Method," Journal of Mechanical Design, Transactions of the ASME, 130(9), p. 091401.

III. A SYSTEM RELIABILITY METHOD WITH DEPENDENT KRIGING PREDICTIONS

Zhifu Zhu and Xiaoping Du

Department of Mechanical and Aerospace Engineering

Missouri University of Science and Technology

ABSTRACT

It is difficult to accurately estimate system reliability when component limit-state functions are highly nonlinear. This work develops a new system reliability method that combines Monte Carlo simulation (MCS) and the Kriging method to achieve high accuracy while maintaining good efficiency. Using the MCS sample points as potential training points, the proposed Kriging method creates cheaper surrogate models of component limit-state functions in order to reduce the error (variance) of the system reliability prediction. New training points are gradually added until the error is sufficiently small. The MCS point with the highest contribution to the variance of the system reliability prediction is selected as a new training point. Since the dependence between Kriging predictions at the MCS sample points is considered, the variance of the system reliability prediction is accurately calculated, producing an accurate estimation of the contribution of each MCS sampling point to the variance and therefore an accurate system reliability prediction. Good accuracy and efficiency are demonstrated by three examples.

1. INTRODUCTION

With the increasing complexity of engineering systems, the cost of system failures may also increase sharply. In order to maintain low lifecycle cost and avoid tragic system failures, it is vital to predict the system reliability accurately and efficiently in the design process. System reliability is the probability that a system performs its intended function without failures under given working conditions. With the system reliability available, designers can make more reliable decisions on the selection of design variables, system maintenance plans, and warranty policies [1, 2].

Tremendous efforts have been dedicated to accurate and efficient system reliability prediction. In general, system reliability analysis methods can be classified into two groups: analytical methods and sampling-based methods [3]. The most popular analytical methods are the First and Second Order Reliability Methods (FORM and SORM) [4-7] due to their good balance between accuracy and efficiency [8]. But for highly nonlinear limit-state functions, a significant error could be introduced using FORM and SORM.

Sampling-based methods include Monte Carlo simulation (MCS) [4], importance sampling [9], and surrogate model based methods [10]. MCS is easy to use and is accurate if sufficient samples are drawn regardless the nonlinearity of limit-state functions. Importance sampling methods [11-14] could be used to reduce the computational cost because it generates more samples in the failure region. Most importance sampling methods require the Most Probable Point (MPP) [4-7] to center the sample distributions. Searching for the MPP is expensive because of an optimization process.

Surrogate model based methods reduce the computational cost by creating surrogate models or metamodels [10] for limit-state functions. A surrogate model is much more computationally efficient than its original limit-state function model. The key of using a metamodel is to make it accurate at an affordable computational cost. The general process of metamodeling starts from generating a small number of initial sample (training) points by design of experiments (DOE) [15]. Based on these samples, an initial surrogate model is built. And then more training points are added to improve the accuracy. Learning functions are employed to select the best training points intelligently and refine the surrogate model in a most efficient manner.

Popular metamodeling techniques include the polynomial response surface [16], neural networks [17], support vector machines [18], polynomial chaos expansion [19, 20], and Kriging [21-23]. Kriging is an exact interpolation method, and this means that the prediction of an existing training point is the exact value of the response at the point. Besides, due to its stochastic characteristics, Kriging provides not only the prediction of an untried point, but also the variance of the prediction. The variance indicates the uncertainty of the prediction. Based on Kriging, Jones et al. developed the Efficient Global Optimization (EGO) method [24]. EGO uses the Expected Improvement Function (EIF) to achieve a balance between exploiting areas of the design space where good solutions have been found, and exploring the design space where the uncertainty is high. Based on EGO, the Efficient Global Reliability Analysis (EGRA) [25] method was proposed for system reliability analysis with multiple failure modes [26]. EGRA uses the Expected Feasibility Function (EFF) to choose new training points in the vicinity of the limit state and helps build an accurate surrogate model with less function evaluations.

EGRA needs global optimization to find the optimum training point. Recently, Echard et al. proposed an active learning method to avoid global optimization. The method takes advantage of Kriging and Monte Carlo simulation (AK-MCS) [27] by choosing new training points from a pre-sampled MCS population; as a result, no global optimization is needed. Fauriat and Gayton [28] then applied AK-MCS to the system reliability analysis.

Since the above mentioned methods treat Kriging predictions at different points independently, they are referred to as Independent Kriging Methods (IKM). As a matter of fact, the predictions of Kriging are realizations of a Gaussian process and therefore are dependent on one another. Considering the dependence could further improve the efficiency and accuracy. Based on this strategy, Zhu and Du proposed a component reliability method with Monte Carlo simulation and dependent Kriging predictions, called the Dependent Kriging Method (DKM) [29]. Accounting for dependence between Kriging predictions and focusing directly on the accuracy of reliability estimation, DKM achieves better accuracy and efficiency than IKM.

The existing DKM is applicable only for component reliability analysis where only one limit-state function is involved. The objective of the present study is to extend DKM to system reliability analysis. With multiple limit-state functions, the extension requires a significant further investigation. The significance of the new development in this work includes the following: (1) Create accurate surrogate models for only limit-state functions that contribute most to the system reliability. (2) Define a new learning function that identifies the best training points and the importance of limit-state functions so that the computational burden is lifted without jeopardizing the accuracy of reliability

estimation (3) Develop an efficient MCS procedure that accommodates dependent Kringing predictions at different MCS sample points.

We briefly review the Kriging method and DKM in Section 2. Then we discuss the proposed dependent Kriging method for systems (DKM-SYS) in Section 3 and present three examples in Section 4. Section 5 provides conclusions and future work.

2. LITERATURE REVIEW

In this section the three methods on which this study is based are reviewed.

2.1 KRIGING METHOD

In the Kriging method, a deterministic $y = g(\mathbf{x})$ is assumed to be a realization of a Gaussian process given by [21]

$$G(\mathbf{x}) = \mathbf{f}(\mathbf{x})^T \boldsymbol{\beta} + Z(\mathbf{x}) \tag{1}$$

stochastic component of the Gaussian is $Z(\cdot)$, which is a stationary Gaussian process with zero mean and the covariance defined by

$$Cov\left[Z(\mathbf{x}_i), Z(\mathbf{x}_j) \right] = \sigma_Z^2 R(\mathbf{x}_i, \mathbf{x}_j) \tag{2}$$

where σ_Z^2 is the variance of the Gaussian process, and $R(\cdot, \cdot)$ is the correlation function. In this study, we use the Gaussian correlation [21, 22] defined by

$$R(\mathbf{x}_i, \mathbf{x}_j) = \exp\left[-\sum_{k=1}^{d} \theta_k (x_{ik} - x_{jk})^2 \right] \tag{3}$$

where x_{ik} and x_{jk} are the k-th components of $\mathbf{x}_i$ and $\mathbf{x}_j$, respectively. d is the dimensionality of $\mathbf{x}$, and θ_k is a parameter that indicates the correlation between the points in dimension k. Then the response predicted by Kriging follows a Gaussian distribution [21]

$$\hat{y} = \hat{g}(\mathbf{x}) \sim N\left(\mu_G(\mathbf{x}), \sigma_G^2(\mathbf{x}) \right) \tag{4}$$

where the mean $\mu_G(\cdot)$ and $\sigma_G^2(\cdot)$ are given by [22]

$$\mu_G(\mathbf{x}) = h + \mathbf{r}(\mathbf{x})^T \mathbf{R}^{-1}(\mathbf{y} - \mathbf{1}h) \tag{5}$$

$$\sigma_G^2(\mathbf{x}) = \hat{\sigma}_Z^2 \left\{ 1 - \mathbf{r}(\mathbf{x})^T \mathbf{R}^{-1} \mathbf{r}(\mathbf{x}) + \frac{\left[1 - \mathbf{1}^T \mathbf{R}^{-1} \mathbf{r}(\mathbf{x}) \right]^2}{\mathbf{1}^T \mathbf{R}^{-1} \mathbf{1}} \right\} \tag{6}$$

in which $\mathbf{y}$ is a column vector of responses of current samples; $\mathbf{r}(\cdot)$ is the vector of cross-correlations between the m observations and the prediction, and $\mathbf{r}(\mathbf{x}) = \left[R(\mathbf{x},\mathbf{x}_1), \cdots, R(\mathbf{x},\mathbf{x}_m) \right]^T$; $\mathbf{R}$ is the correlation matrix defined by $\mathbf{R} = \left[R(\mathbf{x}_i, \mathbf{x}_j) \right], 1 \le i \le m; 1 \le j \le m$; and $\hat{\sigma}_Z^2$ is the maximum likelihood estimation of the process variance

$$\hat{\sigma}_Z^2 = \frac{1}{m}(\mathbf{y} - \mathbf{1}h)^T \mathbf{R}^{-1}(\mathbf{y} - \mathbf{1}h) \tag{7}$$

2.2 AK-SYS

AK-MCS [27] is a Kriging-based component reliability method. Its extension to system reliability is called AK-SYS [28]. The method creates an initial surrogate model with initial training points. New training points are then added one by one for updating the model. A new training point is selected by using a learning function, which is defined by [27, 28]

$$U(\mathbf{x}) = \frac{|\mu_G(\mathbf{x})|}{\sigma_G(\mathbf{x})} \tag{8}$$

U is related to the likelihood of making a mistake on the sign of the prediction. The smaller is U , the higher is the likelihood. Consequently, the sample point with the smallest U is selected as a new training point to eliminate the largest likelihood of wrong sign estimation. For a system with multiple components, composite learning function U^* is used and is given by $U^*(\mathbf{x}) = |\mu_G^*(\mathbf{x})| / \sigma_G^*(\mathbf{x})$. For series systems, $\mu_G^*(\mathbf{x})$ is the minimum value among the predictions of all components at point $\mathbf{x}$, and $\sigma_G^*(\mathbf{x})$ is the corresponding standard deviation.

The process of AK-SYS is as follows:

(1) Generate Monte Carlo samples for input random variables $\mathbf{x}_{MCS}$.

(2) Generate a small number of initial training points (TPs), denoted by $\mathbf{x}_{kT}$ and evaluate limit-state function $\mathbf{y}_{kT} = g_k(\mathbf{x}_{kT})$, where $k = 1, 2, \cdots, n$, and n is the number of components.

(3) Build surrogate models $\hat{y}_k = \hat{g}_k(\mathbf{x}_{kT})$.

(4) Evaluate the composite U function over $\mathbf{x}_{MCS}$ using the predictions and standard deviations from $\hat{y}_k = \hat{g}_k(\mathbf{x}_{kT})$.

(5) Find the minimum value of the composite learning function $U^*_{\min}$.

(6) Check the convergence. If converged, perform reliability analysis based on $\hat{y}_k = \hat{g}_k(\mathbf{x}_{kT})$; otherwise, go to Step (7).

(7) Identify a new TP $\mathbf{x}_{new}$ with the minimum composite learning function value $U^*_{\min}$.

(8) Calculate the component U value at $\mathbf{x}_{new}$ and check if $U_k < 2$.

(9) Evaluate the limit-state function at $\mathbf{x}_{new}$, $y_{k,new} = g_k(\mathbf{x}_{new})$ only if the component U value at this point is smaller than 2.

(10) Add $\mathbf{x}_{new}$ and the responses to the existing sample sets, and update the surrogate models.

Steps (3) through (10) are repeated until convergence. The flowchart of the process is provided in Figure 2.1.

The size of $\mathbf{x}_{MCS}$ is determined by the estimate of probability of system failure p_{Sf} and the coefficient of variation $COV_{p_{Sf}}$. The relationship is given by

$$COV_{p_{Sf}} = \sqrt{\frac{1-p_{Sf}}{p_{Sf}N_{MCS}}} \tag{9}$$

where N_{MCS} is the size of $\mathbf{x}_{MCS}$. N_{MCS} may vary so that $COV_{p_{Sf}} \leq 5\%$. N_{MCS} must be increased if $COV_{p_{Sf}}$ is greater than 5%. Note that for brevity, the step of adjusting N_{MCS} is not included in the above procedure and flowchart.
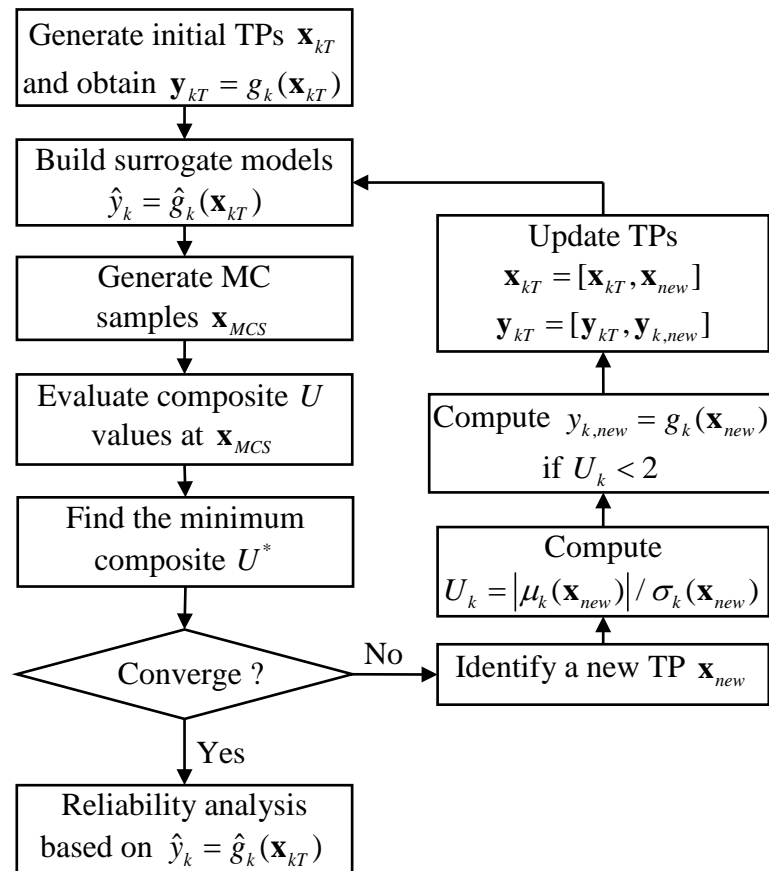
Figure 2.1 Flowchart of AK-SYS

2.3 DEPENDENT KRIGING METHOD FOR COMPONENT RELIABILITY

AK-MCS is an independent Kriging method (IKM) [29] because it does not consider the dependence between predictions at $\mathbf{x}_{MCS}$. The dependent Kriging method (DKM) [29] accounts for such dependence so that new training points can be selected more effectively.

Without considering the dependence, IKM uses the mean predictions only and it uses the following indicator function

$$I(\mathbf{x}) = \begin{cases} 1, \ \mu(\mathbf{x}) < 0 \\ 0, \ \text{otherwise} \end{cases} \tag{10}$$

Then p_f is estimated by

$$p_f = \frac{1}{N} \sum_{i=1}^{N} I(\mathbf{x}_i) \tag{11}$$

where N is the number of samples.

DKM uses all the information of the surrogate model $\hat{y} = \hat{g}(\mathbf{x}) = \mu(\mathbf{x}) + \varepsilon(\mathbf{x})$, where $\varepsilon(\mathbf{x})$ is a Gaussian process and $\varepsilon(\mathbf{x}) \sim N\left(0, \sigma^2(\mathbf{x})\right)$ with correlation $\mathbf{R}$. DKM computes p_f by

$$p_f = \int_{\mu(\mathbf{x}) + \varepsilon(\mathbf{x}) < 0} f(\mathbf{x}) d\mathbf{x} = \int I(\mathbf{x}) f(\mathbf{x}) d\mathbf{x} = \mathrm{E}\left[I(\mathbf{x})\right] \tag{12}$$

in which $I(\cdot)$ is the indicator function defined by

$$I(\mathbf{x}) = \begin{cases} 1, \ \hat{y} = \hat{g}(\mathbf{x}) = \mu(\mathbf{x}) + \varepsilon(\mathbf{x}) < 0 \\ 0, \ \text{otherwise} \end{cases} \tag{13}$$

p_f is a random variable since the domain of integration in Eq. (12) is random. The expectation of p_f is used as the estimate of the probability of failure [29]

$$E\left[p_f\right] = \frac{1}{N}\sum_{i=1}^{N} E[I_i] = \frac{1}{N}\sum_{i=1}^{N} e_i \tag{14}$$

where

$$e_i = \Phi\left(-\frac{\mu(\mathbf{x}_i)}{\sigma(\mathbf{x}_i)}\right) \tag{15}$$

in which $\Phi(\cdot)$ is the cumulative distribution function (CDF) of a standard normal random variable. The variance of p_f is used to measure the error of the estimate of p_f and is given by [29]

$$\mathrm{Var}\left[p_f\right] = \frac{1}{N^2}\sum_{i=1}^{N}\left[e_i(1-e_i) + \sum_{i=1,j\neq i}^{N}(e_{ij}-e_ie_j)\right] \tag{16}$$

in which $e_{ij} = \mathrm{Pr}\left\{\hat{g}(\mathbf{x}_i) < 0, \hat{g}(\mathbf{x}_j) < 0\right\}$ is the CDF of the bivariate normal distribution defined by means $[\mu_i, \mu_j]$, standard deviations $[\sigma_i, \sigma_j]$, and correlation r_{ij}. Eq. (16) indicates that the error or $\mathrm{Var}\left[p_f\right]$ is the sum of N terms of the N sample points. Each term can be considered as the contribution from each sample. The contribution of one sample is defined as the learning function

$$c_i = e_i(1-e_i) + \sum_{i=1,j\neq i}^{N}(e_{ij}-e_ie_j) \tag{17}$$

The learning function uses all the information of a Gaussian process, including its mean, variance, and correlation. As a result, it provides a more accurate and efficient way of selecting training points to build surrogate models. In [29], selected candidate points (SCPs) are also used to relieve the computational burden of the bivariate joint probability evaluation in Eq. (17). e_{ij} is not calculated for all points in $\mathbf{x}_{MCS}$, and a smaller number of points in $\mathbf{x}_{MCS}$ are selected to form the SCPs. Then the evaluations of e_{ij} is performed on

SCPs only. The SCPs are selected based on two criteria. The first criterion is a small error in the estimate of p_f, and this criterion requires a significant number of points fall into the failure region. The second criterion is a high contribution to $\text{Var}\left[p_f\right]$. Therefore the SCPs consist of all the points in the failure region and other points with the highest indicator function variances in the safe region. Details of the DKM implementation is given in [29].

3. DEPENDENT KRIGING METHOD FOR SYSTEM RELIABILITY

The new dependent Kriging method for systems (DKM-SYS) is the extension of component DKM [29] to system reliability analysis. Similar to the component DKM, DKM-SYS consists of the same components: the estimate of probability of failure, a learning function, a stopping criterion, and an implementation process.

3.1 ESTIMATE OF p_{Sf}

We now use a series system with three failure modes for demonstration. If one failure mode occurs, the system fails, and then the probability of system failure is defined by

$$p_{Sf} = \Pr\{g_1(\mathbf{x}) < 0 \cup g_2(\mathbf{x}) < 0 \cup g_3(\mathbf{x}) < 0\} \tag{18}$$

where $\cup$ denotes a union. The failure region Ω is therefore

$$\Omega = \{\mathbf{x} \mid g_1(\mathbf{x}) < 0 \cup g_2(\mathbf{x}) < 0 \cup g_3(\mathbf{x}) < 0\} \tag{19}$$

If a point $\mathbf{x}$ falls into Ω, the system fails. Thus p_{Sf} is computed by

$$p_{Sf} = \int_{\Omega} f(\mathbf{x})d\mathbf{x} = \int I_S(\mathbf{x})f(\mathbf{x})d\mathbf{x} = E[I_S(\mathbf{x})] \tag{20}$$

where the system indicator function is defined by

$$I_S(\mathbf{x}) = \begin{cases} 1, \mathbf{x} \in \Omega \\ 0, \text{otherwise} \end{cases} \tag{21}$$

Therefore, p_{Sf} becomes

$$p_{Sf} = \frac{1}{N}\sum_{i=1}^{N} I_S(\mathbf{x}_i) = \frac{1}{N}\sum_{i=1}^{N} I_{S_i} \tag{22}$$

where $I_{Si} = I_S(\mathbf{x}_i)$. The probability of system failure at $\mathbf{x}_i \in \mathbf{x}_{MCS}$ is

$$\Pr\{I_{S_i} = 1\} = \Pr\{\hat{g}_1(\mathbf{x}_i) < 0 \cup \hat{g}_2(\mathbf{x}_i) < 0 \cup \hat{g}_3(\mathbf{x}_i) < 0\} \tag{23}$$

We assume that the predictions of the three responses at the same point are independent, and the above equation then becomes

$$\Pr\{I_{S_i}=1\}=1-\left(1-\Pr\{\hat{g}_1(\mathbf{x}_i)<0\}\right)\left(1-\Pr\{\hat{g}_2(\mathbf{x}_i)<0\}\right)\left(1-\Pr\{\hat{g}_3(\mathbf{x}_i)<0\}\right) \qquad (24)$$

Since the probability of failure of component k $(k=1,2,3)$ at $\mathbf{x}_i$ is

$$\Pr\{\hat{g}_k(\mathbf{x}_i)<0\}=\Phi\left(-\frac{\mu_k(\mathbf{x}_i)}{\sigma_k(\mathbf{x}_i)}\right)=e_{k_i} \qquad (25)$$

Thus

$$\Pr\{I_{S_i}=1\}=1-(1-e_{1_i})(1-e_{2_i})(1-e_{3_i}) \qquad (26)$$

And

$$\Pr\{I_{S_i}=0\}=1-\Pr\{I_{S_i}=1\}=(1-e_{1_i})(1-e_{2_i})(1-e_{3_i}) \qquad (27)$$

The expectation of the system indicator at $\mathbf{x}_i$ is

$$E\left[I_{S_i}\right]=1\cdot\left(\Pr\{I_{S_i}=1\}\right)+0\cdot\left(\Pr\{I_{S_i}=0\}\right)=1-(1-e_{1_i})(1-e_{2_i})(1-e_{3_i}) \qquad (28)$$

And its variance is

$$\begin{aligned}
\mathrm{Var}\left[I_{S_i}\right]&=E\left[\left(I_{S_i}\right)^2\right]-\left(E\left[I_{S_i}\right]\right)^2\\
&=\left[1-(1-e_{1_i})(1-e_{2_i})(1-e_{3_i})\right]-\left[1-(1-e_{1_i})(1-e_{2_i})(1-e_{3_i})\right]^2\\
&=\left[1-(1-e_{1_i})(1-e_{2_i})(1-e_{3_i})\right](1-e_{1_i})(1-e_{2_i})(1-e_{3_i})
\end{aligned} \qquad (29)$$

Since p_{Sf} is a random variable, its expectation is used for the estimate of the probability of system failure; namely

$$E\left[p_{Sf}\right]=\frac{1}{N}\sum_{i=1}^{N}E\left[I_{S_i}\right]=\frac{1}{N}\sum_{i=1}^{N}\left[1-(1-e_{1_i})(1-e_{2_i})(1-e_{3_i})\right] \qquad (30)$$

And the variance of p_{Sf} is calculated by

$$\text{Var}\left[p_{Sf}\right] = \frac{1}{N^2}\text{Var}\sum_{i=1}^{N} I_{S_i} = \frac{1}{N^2}\left[\sum_{i=1}^{N}\text{Var}\left[I_{S_i}\right] + 2\sum_{i=1}^{N}\sum_{j>i}^{N}\text{Cov}\left(I_{S_i},I_{S_j}\right)\right] \tag{31}$$

The above equation accounts for the correlation between Kriging predictions through the

covariance $\text{Cov}\left(I_{S_i},I_{S_j}\right)$, which is given by

$$\text{Cov}\left(I_{S_i},I_{S_j}\right) = E\left[I_{S_i}I_{S_j}\right] - E\left[I_{S_i}\right]E\left[I_{S_j}\right] = \Pr\left\{I_{S_i}=1,I_{S_j}=1\right\} - E\left[I_{S_i}\right]E\left[I_{S_j}\right] \tag{32}$$

where

$$\Pr\left\{I_{S_i}=1,I_{S_j}=1\right\} = \Pr\left\{\begin{matrix}\left[\hat{g}_1(\mathbf{x}_i)<0 \cup \hat{g}_2(\mathbf{x}_i)<0 \cup \hat{g}_3(\mathbf{x}_i)<0\right]\\ \cap\left[\hat{g}_1(\mathbf{x}_j)<0 \cup \hat{g}_2(\mathbf{x}_j)<0 \cup \hat{g}_3(\mathbf{x}_j)<0\right]\end{matrix}\right\} \tag{33}$$

and

$$E\left[I_{S_i}\right]E\left[I_{S_j}\right] = \left[1-(1-e_{1_i})(1-e_{2_i})(1-e_{3_i})\right]\left[1-(1-e_{1_j})(1-e_{2_j})(1-e_{3_j})\right] \tag{34}$$

Let $H = \Pr\left\{I_{S_i}=1,I_{S_j}=1\right\}$, Eq. (31) becomes

$$\text{Var}\left[p_{Sf}\right] = \frac{1}{N^2}\left[\begin{matrix}\sum_{i=1}^{N}\left[1-(1-e_{1_i})(1-e_{2_i})(1-e_{3_i})\right]\times(1-e_{1_i})(1-e_{2_i})(1-e_{3_i})\\ +2\sum_{i=1}^{N}\sum_{j>i}^{N}\left(\begin{matrix}H-\left[1-(1-e_{1_i})(1-e_{2_i})(1-e_{3_i})\right]\\ \times\left[1-(1-e_{1_j})(1-e_{2_j})(1-e_{3_j})\right]\end{matrix}\right)\end{matrix}\right] \tag{35}$$

The derivation of H is given in the Appendix. The above equation can be

rewritten as

$$\text{Var}\left[p_{Sf}\right] = \frac{1}{N^2}\sum_{i=1}^{N}\left[\begin{matrix}\left[1-(1-e_{1_i})(1-e_{2_i})(1-e_{3_i})\right](1-e_{1_i})(1-e_{2_i})(1-e_{3_i})\\ +\sum_{j=1,j\neq i}^{N}\left(\begin{matrix}H-\left[1-(1-e_{1_i})(1-e_{2_i})(1-e_{3_i})\right]\\ \times\left[1-(1-e_{1_j})(1-e_{2_j})(1-e_{3_j})\right]\end{matrix}\right)\end{matrix}\right] \tag{36}$$

or

$$\mathrm{Var}\left[p_{Sf}\right]=\frac{1}{N^2}\sum_{i=1}^{N}c_i \tag{37}$$

where

$$c_i = \left[1-(1-e_{1_i})(1-e_{2_i})(1-e_{3_i})\right](1-e_{1_i})(1-e_{2_i})(1-e_{3_i})$$
$$+\sum_{j=1,j\neq i}^{N}\left(\begin{array}{c}H-\left[1-(1-e_{1_i})(1-e_{2_i})(1-e_{3_i})\right]\\ \times\left[1-(1-e_{1_j})(1-e_{2_j})(1-e_{3_j})\right]\end{array}\right) \tag{38}$$

Therefore, the standard deviation of p_{Sf} is

$$\sigma_{p_{Sf}}=\frac{1}{N}\sqrt{\sum_{i=1}^{N}c_i} \tag{39}$$

3.2 LEARNING FUNCTION

A learning function is used to select new training points to refine the surrogate model. As indicated in Eq. (37), each point contributes to $\mathrm{Var}\left[p_{Sf}\right]$. The sum of terms involving $\mathbf{x}_i$ in $\mathrm{Var}\left[p_{Sf}\right]$ is c_i in Eq. (38). Thus, we use c_i as the learning function. Maximizing c_i identifies a new training point that has the highest contribution to the uncertainty of the estimate of failure probability; namely

$$\mathbf{x}_{new}=\mathbf{x}_h,\, h=\arg\max_{i=1,2,\cdots,N_{MCS}}\{c_i\} \tag{40}$$

where $\mathbf{x}_h$ is the h-th point of a pre-sampled MC population $\mathbf{x}_{MCS}$. In [29], it is proved that adding the highest contribution point as new training point is the most effective way to refine the surrogate model and reach convergence.

3.3 STOPPING CRITERION

When the variance of p_{Sf} is small enough, no more new training points are needed. Then the surrogate models are used to calculate p_{Sf}. Let the confidence of the

probability of system failure be $1 - \alpha$, and the allowable relative error is ε, then the confidence interval of the estimate is computed by $E\left[p_{Sf}\right] \pm \Phi^{-1}(\alpha/2)\sigma_{p_{Sf}}$. Therefore, the relative error is

$$\eta = \frac{\left|E\left[p_{Sf}\right] \pm \Phi^{-1}(\alpha/2)\sigma_{p_{Sf}} - E\left[p_{Sf}\right]\right|}{E\left[p_{Sf}\right]} = \left|\frac{\Phi^{-1}(\alpha/2)\sigma_{p_{Sf}}}{E\left[p_{Sf}\right]}\right| \tag{41}$$

When η is smaller than the allowable error, the process terminates. Thus, the stopping criterion is given by

$$\frac{\sigma_{p_{Sf}}}{E\left[p_{Sf}\right]} \leq \left|\frac{\eta}{\Phi^{-1}(\alpha/2)}\right| \tag{42}$$

3.4 IMPLEMENTATION

Accounting for the dependences between Kriging predictions needs to calculate the bivariate joint probabilities

$$e_{k_{ij}} = \Pr\left\{\hat{g}_k(\mathbf{x}_i) < 0 \bigcap \hat{g}_k(\mathbf{x}_j) < 0\right\}, (k = 1,2,3; i, j = 1,2,\cdots,N, i \neq j) \tag{43}$$

Calculating $e_{k_{ij}}$ will be computationally intensive. For a system with three components, if the size of $\mathbf{x}_{MCS}$ is 10^5, the number of calculations needed for $e_{k_{ij}}$ is

$$M = \frac{N(N+1)k}{2} = \frac{10^5(10^5+1)(3)}{2} \approx 1.5 \times 10^{10} \tag{44}$$

To relieve the computational burden of considering correlations, we use the so-called selected candidate points (SCPs), denoted by $\mathbf{x}_S$. $\mathbf{x}_S$ is a smaller number of points selected from $\mathbf{x}_{MCS}$. To ensure a significant number of points fall into the failure region

so that the error in the estimate of probability of failure is small, we adjust the size of SCPs N_{Sel} to guarantee

$$25\% \le r = \frac{N_{F,Sel}}{N_{Sel}} \le 75\% \tag{45}$$

where $N_{F,Sel}$ is the number of failure points in the SCPs.

Therefore, SCPs consists of all points in the failure region and the other points with the highest indicator function variances in the safe region. Using SCPs, the computational effort needed is greatly reduced. In the examples in Sec. 4, we use 200 SCPs, and the number of calculations needed for $e_{k_{ij}}$ becomes

$$M' = \frac{N_{Sel}(N_{Sel}+1)k}{2} = \frac{200(200+1)(3)}{2} = 60300 \tag{46}$$

The stopping criterion in Eq. (42) needs to be modified accordingly. The probability of system failure using $\mathbf{x}_S$ is calculate by

$$E\left[p_{Sf,Sel}\right] = \frac{1}{N_{Sel}} \sum_{i=1}^{N_{Sel}} e_i \tag{47}$$

and

$$\sigma_{p_{Sf,Sel}} = \frac{1}{N_{Sel}} \sqrt{\sum_{i=1}^{N_{Sel}} c_i} \tag{48}$$

The stopping criterion becomes

$$\frac{\sigma_{p_{Sf,Sel}}}{E\left[p_{Sf,Sel}\right]} \le \left| \frac{\eta}{\Phi^{-1}(\alpha/2)} \right| \tag{49}$$

Details about how to use SCPs can be found in [29]. The flowchart of the DKM-

SYS is provided in Figure 3.1.
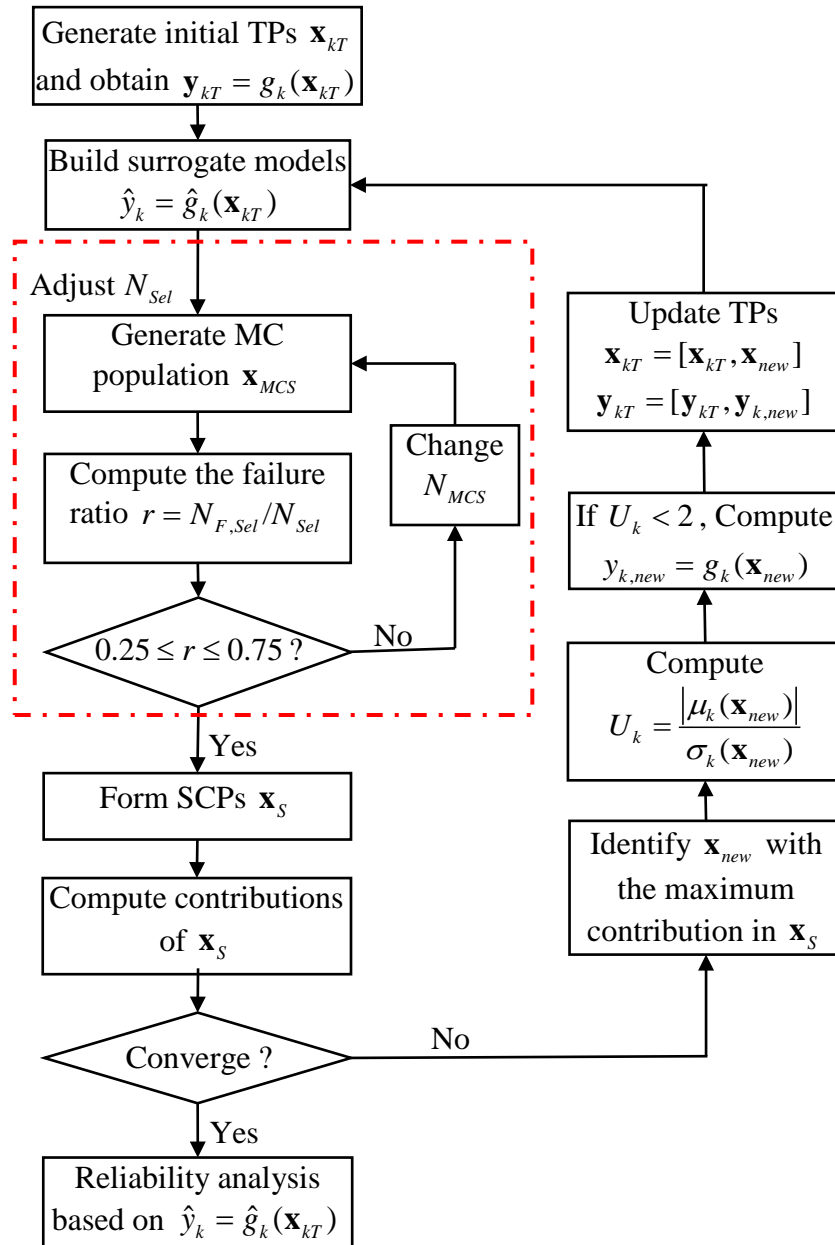
Figure 3.1 Flowchart of DKM-SYS

4. EXAMPLES

In this section, the proposed method is applied to three problems. The first numerical example is used to demonstrate the procedure of DKM-SYS while the other two examples show possible engineering applications.

In all examples, initial training points (TPs) are generated by the Latin Hypercube sampling [30], and the initial sample size is 12. The efficiency of the new method is measured by the number of limit-state function calls N_k for limit-state function k. And the accuracy is measured by the percentage error, which is calculated by

$$\varepsilon = \frac{\left| p_{Sf} - p_{Sf}^{MCS} \right|}{p_{Sf}^{MCS}} \times 100\% \tag{50}$$

where p_{Sf}^{MCS} and p_{Sf} are probabilities of system failure from MCS and a non-MCS method, respectively. Kriging-based reliability methods are stochastic methods, we therefore run each method 20 times independently, and the average results from the 20 independent runs are used for comparison. The standard deviation of function calls and probabilities of system failure are provided also. A smaller standard deviation of the probability of system failure means that the results are concentrated close to the mean value, which indicates that the method tends to produce stable results. We therefore use the standard deviation as an indicator of robustness of the method.

4.1 EXAMPLE 1

There are two random variables in this example, and the limit-state functions are given by [31, 32]

$$g_1(\mathbf{x}) = x_1^2 x_2 / 20 - 1 \tag{51}$$

$$g_2(\mathbf{x}) = (x_1 + x_2 - 5)^2 / 30 + (x_1 - x_2 - 12)^2 / 120 - 1 \tag{52}$$

$$g_3(\mathbf{x}) = 80 / (x_1^2 + 8x_2 - 5) - 1 \tag{53}$$

where $x_i \sim N(4, 0.7^2)$, $i = 1, 2$, and $g_k < 0$ indicates a failure. Figures 4.1 and 4.2 show the TPs and surrogate models using AK-SYS and DKM-SYS from one run, respectively.

(a) Training points   (b) Final surrogate models
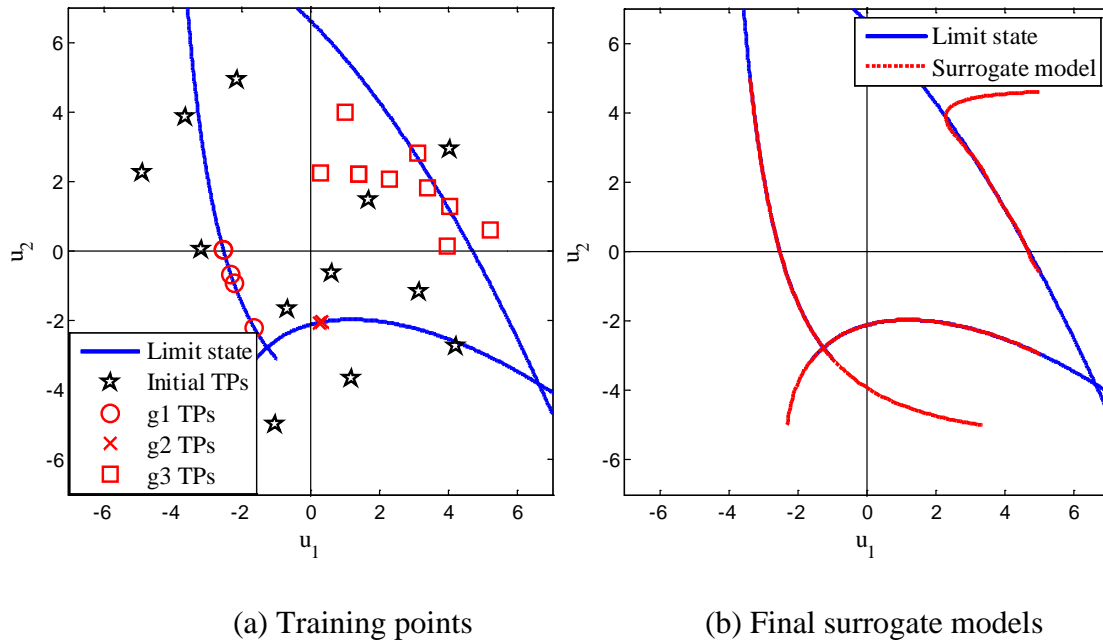
Figure 4.1 Training points and surrogate models of AK-SYS

In Figures 4.1 and 4.2, the initial training points are denoted by black pentagrams. The red circle, cross and square denote training points generated from limit-state function

1, 2 and 3, respectively. AK-SYS needs more training points to converge, while the results in Table 4.1 show that DKM-SYS has better accuracy. In Table 4.1, we provide the average results from 20 independent runs, and the standard deviation of function calls and probability of system failure are also provided to show the robustness of the two methods.

Table 4.1 Average results of example one

Method	N_1 (Std. Dev.)	N_2 (Std. Dev.)	N_3 (Std. Dev.)	p_{Sf} (Std. Dev.)	ε (%)
MCS	5×10^6	5×10^6	5×10^6	2.4553×10^{-2}	N/A
AK-SYS	3.80 (1.20)	1.20 (0.70)	13.75 (14.74)	2.4438×10^{-2} (3.95×10^{-4})	1.38
DKM-SYS	1.30 (0.92)	0.05 (0.22)	8.50 (11.02)	2.4506×10^{-2} (1.88×10^{-4})	0.60
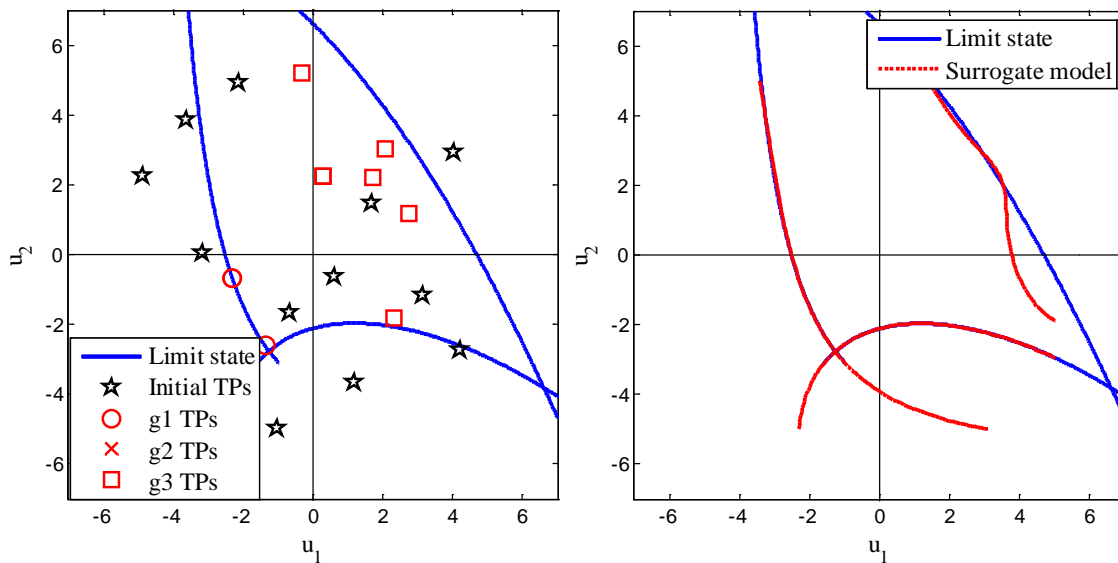
(a) Training points

(b) Final surrogate models

Figure 4.2 Training points and surrogate models of DKM-SYS

As shown in Table 4.1, DKM-SYS has better efficiency than AK-SYS since DKM-SYS has smaller average function calls and standard deviations for all three limit-state functions. Limit-state function 3 is far away from the origin and it is hard to obtain an accurate surrogate model, as shown by Figures 4.1 and 4.2. This function consumes the majority of the computational efforts by both AK-SYS and DKM-SYS. The results also show that DKM-SYS has better accuracy than AK-SYS. DKM-SYS has smaller standard deviation of the probability of system failure, and this means that DKM-SYS is more robust than AK-SYS since DKM-SYS tends to produce stable reliability analysis results.

4.2 EXAMPLE 2

A liquid hydrogen fuel tank is used on a space launch vehicle [26, 33, 34]. The tank has a honeycomb sandwich design. The tank is subjected to stresses caused by ullage pressure, head pressure, axial forces due to acceleration, and bending and shear stresses due to the weight of the fuel.

Table 4.2 Random variables of example two

Variable	Mean	Standard deviation	Distribution
t_{plate}	0.07443	0.005	Normal
t_h	0.1	0.01	Normal
N_x	13	60	Normal
N_y	4751	48	Normal
N_{xy}	-684	11	Normal

There are three failure modes related to von Mises strength, isotropic strength, and honeycomb buckling. The limit-state functions for the von Mises and isotropic strength are given by

$$g_{vM} = \frac{84000t_{plate}}{\sqrt{N_x^2 + N_y^2 - N_x N_y + 3N_{xy}^2}} - 1 \tag{54}$$

$$g_{ISO} = \frac{84000t_{plate}}{|N_y|} - 1 \tag{55}$$

The limit-state function of honeycomb buckling is defined by a response surface generated from the structural sizing program HyperSizer [35], and is given by [26, 34]

$$\begin{aligned} g_{HB} = {} &0.847 + 0.96x_1 + 0.986x_2 - 0.216x_3 + 0.077x_1^2 \\ &+ 0.11x_2^2 + 0.007x_3^2 + 0.378x_1 x_2 - 0.106x_1 x_3 - 0.11x_2 x_3 \end{aligned} \tag{56}$$

where

$$x_1 = 4(t_{plate} - 0.075) \tag{57}$$

$$x_2 = 20(t_h - 0.1) \tag{58}$$

$$x_3 = -6000\left(\frac{1}{N_{xy}} + 0.003\right) \tag{59}$$

Table 4.3 Average results of example two

Method	N_1 (Std. Dev.)	N_2 (Std. Dev.)	N_3 (Std. Dev.)	p_{Sf} (Std. Dev.)	ε (%)
MCS	2×10^7	2×10^7	2×10^7	6.9855×10^{-4}	N/A
AK-SYS	0 (0)	19.50 (1.28)	0.60 (0.82)	6.9756×10^{-4} (1.29×10^{-5})	1.52
DKM-SYS	0 (0)	6.30 (1.56)	0.25 (0.55)	7.0×10^{-4} (5.39×10^{-6})	0.65

The five independent random variables are given in Table 4.2. The reliability analysis results are provided in Table 4.3.

Table 4.3 shows that the average total function call of AK-MCS is $19.5 + 0.6 = 20.1$, while the average number of DKM-SYS is $6.30 + 0.25 = 6.55$. This shows that DKM-SYS is more efficient than AK-SYS. With better efficiency, DKM-SYS still has better accuracy than AK-SYS. Since DKM-SYS has smaller standard deviation of probability of system failure, DKM-SYS is more robust than AK-SYS.

4.3 EXAMPLE 3

As shown in Figure 4.3, a cantilever beam [8] is subjected to external forces F_1 and F_2, external moments M_1 and M_2, and external distributed loads denoted by (q_{L1}, q_{R1}) and (q_{L2}, q_{R2}). These forces, moments, distributed loads, together with the yield strength S and the maximum allowable shear stress $\tau_{\max}$ are normally distributed random variables. Their information is given in Table 4.4.

First, the maximum normal stress of the beam should be smaller than its yield strength, and this is given by

$$g_1 = S - \frac{6M}{wh^2} \tag{60}$$

where the bending moment at the left end point of the beam is

$$M = \sum_{i=1}^{2} M_i + \sum_{i=1}^{2} F_i b_i + \sum_{i=1}^{2} \frac{q_{Li}(d_i - c_i)(d_i + c_i)}{2}$$
$$+ \sum_{i=1}^{2} \frac{(q_{Ri} - q_{Li})(d_i - c_i)(2d_i + c_i)}{6} \tag{61}$$

Second, the deflection of the right end point of the beam should not greater than the allowable deflection $\delta_{allowable} = 2$ cm.

$$g_2 = \delta - \delta_{allowable} \tag{62}$$

where δ is computed by

$$\delta = \frac{1}{EI}\left[\begin{array}{l} \dfrac{ML^2}{2} + \dfrac{RL^3}{6} + \sum_{i=1}^{2}\dfrac{M_i(L-a_i)^2}{2} - \sum_{i=1}^{2}\dfrac{F_i(L-b_i)^3}{6} - \sum_{i=1}^{2}\dfrac{q_{Li}(L-c_i)^4}{24} \\[4mm] - \sum_{i=1}^{2}\dfrac{(q_{Ri}-q_{Li})(L-c_i)^5}{120(d_i-c_i)} + \sum_{i=1}^{2}\dfrac{q_{Ri}(L-d_i)^4}{24} + \sum_{i=1}^{2}\dfrac{(q_{Ri}-q_{Li})(L-d_i)^5}{120(d_i-c_i)} \end{array}\right] \tag{63}$$

in which the Young's modulus is $E = 2 \times 10^{11}$ Pa , and the moment of inertia is $I = wh^3/12$.

R is the reaction force at the fixed end, which is given by

$$R = \sum_{i=1}^{2}F_i + \sum_{i=1}^{2}q_{Li}(d_i-c_i) + \sum_{i=1}^{2}\frac{(q_{Ri}-q_{Li})(d_i-c_i)}{2} \tag{64}$$
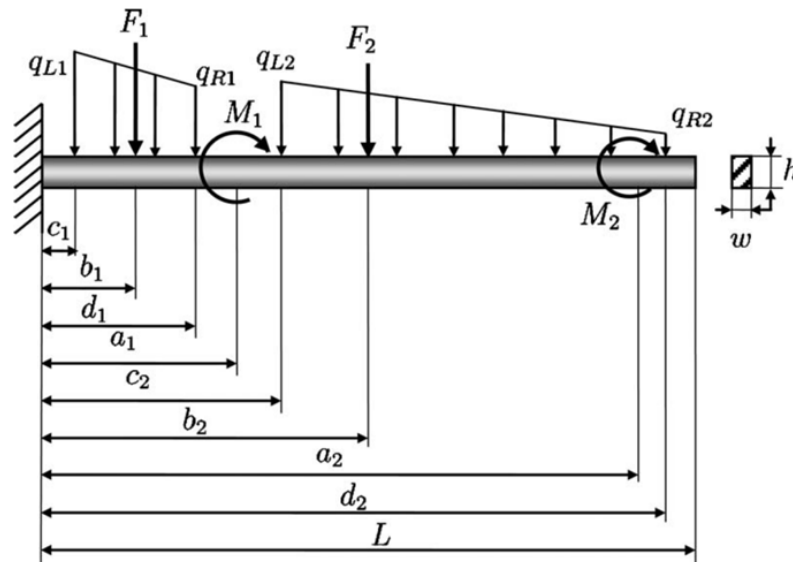
Figure 4.3 A cantilever beam

The last limit-state function specifies that the shear stress should not be greater than the maximum allowable shear stress

$$g_3 = \tau_{\max} - \tau = \tau_{\max} - \frac{3R}{2wh} \tag{65}$$

The average results of this example are given in Table 4.5.

Table 4.4 Random variables of example three

Variable	Mean	Standard deviation	Distribution
M_1 (Nm)	5×10^4	5×10^3	Normal
M_2 (Nm)	3×10^4	3×10^3	Normal
F_1 (N)	1.8×10^4	2×10^3	Normal
F_2 (N)	3×10^4	3×10^3	Normal
q_{L1} (N/m)	3×10^4	1×10^3	Normal
q_{R1} (N/m)	2×10^4	1×10^3	Normal
q_{L2} (N/m)	2×10^4	1×10^3	Normal
q_{R2} (N/m)	1×10^3	10	Normal
S (Pa)	4.5×10^7	4.5×10^6	Normal
$\tau_{\max}$ (Pa)	3.5×10^6	5×10^5	Normal

The results from example three show that DKM-SYS has better performance than AK-SYS in accuracy, efficiency and robustness. The significant advantage of DKM-SYS over AK-SYS in this example is the efficiency.

On average, AK-SYS needs about 312 function calls to converge, while DKM-SYS just needs 67 function calls. DKM-SYS reduces the computational burden greatly.

Table 4.5 Average results of example three

Method	N_1 (Std. Dev.)	N_2 (Std. Dev.)	N_3 (Std. Dev.)	p_{Sf} (Std. Dev.)	ε (%)
MCS	1×10^7	1×10^7	1×10^7	5.2567×10^{-3}	N/A
AK-SYS	228.30 (97.40)	0 (0)	83.75 (22.72)	5.2509×10^{-3} (1.29×10^{-4})	1.80
DKM-SYS	41.85 (8.13)	0 (0)	25.20 (9.45)	5.3276×10^{-3} (7.17×10^{-5})	1.49

5. CONCLUSIONS

This paper presents the extension of the component dependent Kriging method (DKM) to system reliability analysis. The proposed method considers the dependence between Kriging predictions. High efficiency and accuracy are achieved through the following components: 1) the estimate of the probability of system failure with both the mean and standard deviation of the Kriging prediction, instead of just the sign of prediction used by the independent Kriging method, 2) a learning function, which takes advantage of all the information to define a Gaussian process, including the mean, standard deviation and correlation, and 3) a stopping criterion, which achieves a good balance between accuracy and efficiency. The proposed method is applied to three examples from literature; the results indicate that the new method has much better performance than the independent Kriging method.

Though this work is based on series systems with three components, it can be extended to systems with more components with different configurations. This is our future work. Our future work also includes the following: improve the accuracy of the system DKM for systems with a large number of input random variables and extremely high reliabilities, and extend the results to general systems with time-dependent uncertainty.

ACKNOWLEDGEMENTS

APPENDIX

CALCULATION OF H

In Eq. (35), H is defined as

$$H = \Pr\{I_{S_i} = 1, I_{S_j} = 1\} = \Pr\left\{\begin{array}{l} [\hat{g}_1(\mathbf{x}_i) < 0 \cup \hat{g}_2(\mathbf{x}_i) < 0 \cup \hat{g}_3(\mathbf{x}_i) < 0] \\ \cap [\hat{g}_1(\mathbf{x}_j) < 0 \cup \hat{g}_2(\mathbf{x}_j) < 0 \cup \hat{g}_3(\mathbf{x}_j) < 0] \end{array}\right\} \qquad (66)$$

The above equation indicates the probability that the system fails at both points $\mathbf{x}_i$ and $\mathbf{x}_j$. This probability can be illustrated by the two subsystems in Figure A.1, where k_i and k_j represent component k at points $\mathbf{x}_i$ and $\mathbf{x}_j$, respectively.
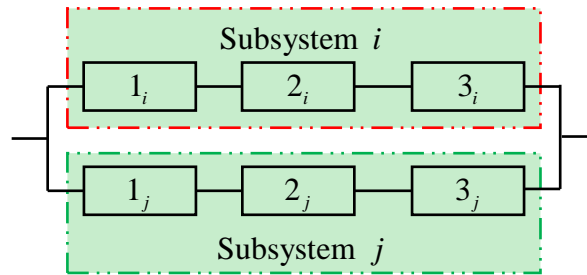
Figure A.1 A parallel-series system

$$\begin{aligned} \Pr\{I_{S_i} = 1, I_{S_j} = 1\} &= 1 - \Pr\{I_{S_i} = 0 \cup I_{S_j} = 0\} \\ &= 1 - \Pr\{\hat{g}_1(\mathbf{x}_i) > 0 \cap \hat{g}_2(\mathbf{x}_i) > 0 \cap \hat{g}_3(\mathbf{x}_i) > 0\} \\ &\quad - \Pr\{\hat{g}_1(\mathbf{x}_j) > 0 \cap \hat{g}_2(\mathbf{x}_j) > 0 \cap \hat{g}_3(\mathbf{x}_j) > 0\} \\ &\quad + \Pr\left\{\begin{array}{l} [\hat{g}_1(\mathbf{x}_i) > 0 \cap \hat{g}_2(\mathbf{x}_i) > 0 \cap \hat{g}_3(\mathbf{x}_i) > 0] \\ \cap [\hat{g}_1(\mathbf{x}_j) > 0 \cap \hat{g}_2(\mathbf{x}_j) > 0 \cap \hat{g}_3(\mathbf{x}_j) > 0] \end{array}\right\} \end{aligned} \qquad (67)$$

There are four cases for the probability:

Case 1, $k_i = 1$, $k_j = 1$

$$\Pr\{g_{k_i} < 0 \cap g_{k_j} < 0\} = e_{k_{ij}} \qquad (68)$$

Case 2, $k_i = 1$, $k_j = 0$

$$\Pr\left\{g_{k_i} < 0 \cap g_{k_j} > 0\right\} = \Pr\left\{g_{k_i} < 0\right\} - \Pr\left\{g_{k_i} < 0 \cap g_{k_j} < 0\right\} = e_{k_i} - e_{k_{ij}}$$ (69)

Case 3, $k_i = 0$, $k_j = 1$

$$\begin{aligned}
\Pr\left\{g_{k_i} > 0 \cap g_{k_j} < 0\right\} &= \Pr\left\{g_{k_j} < 0 \cap g_{k_i} > 0\right\} \\
&= \Pr\left\{g_{k_j} < 0\right\} - \Pr\left\{g_{k_j} < 0 \cap g_{k_i} < 0\right\} = e_{k_j} - e_{k_{ij}}
\end{aligned}$$ (70)

Case 4, $k_i = 0$, $k_j = 0$

$$\begin{aligned}
&\Pr\left\{g_{k_i} > 0 \cap g_{k_j} > 0\right\} \\
&= 1 - \Pr\left\{g_{k_i} < 0 \cap g_{k_j} < 0\right\} - \Pr\left\{g_{k_i} < 0 \cap g_{k_j} > 0\right\} - \Pr\left\{g_{k_i} > 0 \cap g_{k_j} < 0\right\} \\
&= 1 - e_{k_{ij}} - (e_{k_i} - e_{k_{ij}}) - (e_{k_j} - e_{k_{ij}}) \\
&= 1 - e_{k_i} - e_{k_j} + e_{k_{ij}}
\end{aligned}$$ (71)

Therefore, the probability of system safety is given by

$$\begin{aligned}
&\Pr\left\{I_{S_i} = 0 \cup I_{S_j} = 0\right\} \\
&= (e_{1_i} + e_{1_j} - 2e_{1_{ij}})(1 - e_{2_i} - e_{2_j} + e_{2_{ij}})(1 - e_{3_i} - e_{3_j} + e_{3_{ij}}) \\
&\quad + (1 - e_{1_i} - e_{1_j} + e_{1_{ij}})(e_{2_i} + e_{2_j} - 2e_{2_{ij}})(1 - e_{3_i} - e_{3_j} + e_{3_{ij}}) \\
&\quad + (1 - e_{1_i} - e_{1_j} + e_{1_{ij}})(1 - e_{2_i} - e_{2_j} + e_{2_{ij}})(e_{3_i} + e_{3_j} - 2e_{3_{ij}}) \\
&\quad + \left[(e_{1_i} - e_{1_{ij}})(e_{2_i} - e_{2_{ij}}) + (e_{1_j} - e_{1_{ij}})(e_{2_j} - e_{2_{ij}})\right](1 - e_{3_i} - e_{3_j} + e_{3_{ij}}) \\
&\quad + \left[(e_{1_i} - e_{1_{ij}})(e_{3_i} - e_{3_{ij}}) + (e_{1_j} - e_{1_{ij}})(e_{3_j} - e_{3_{ij}})\right](1 - e_{2_i} - e_{2_j} + e_{2_{ij}}) \\
&\quad + \left[(e_{2_i} - e_{2_{ij}})(e_{3_i} - e_{3_{ij}}) + (e_{2_j} - e_{2_{ij}})(e_{3_j} - e_{3_{ij}})\right](1 - e_{1_i} - e_{1_j} + e_{1_{ij}}) \\
&\quad + (e_{1_i} - e_{1_{ij}})(e_{2_i} - e_{2_{ij}})(e_{3_i} - e_{3_{ij}}) + (e_{1_j} - e_{1_{ij}})(e_{2_j} - e_{2_{ij}})(e_{3_j} - e_{3_{ij}}) \\
&\quad + (1 - e_{1_i} - e_{1_j} + e_{1_{ij}})(1 - e_{2_i} - e_{2_j} + e_{2_{ij}})(1 - e_{3_i} - e_{3_j} + e_{3_{ij}})
\end{aligned}$$ (72)

Then

$$H = 1 - \Pr\left\{I_{S_i} = 0 \cup I_{S_j} = 0\right\}$$ (73)

REFERENCES

[1] Singh, A., Mourelatos, Z. P., and Li, J., 2010, "Design for Lifecycle Cost Using Time-Dependent Reliability," Journal of Mechanical Design, 132(9), pp. 091008-091008.

[2] Hu, Z., and Du, X., 2014, "Lifetime Cost Optimization with Time-Dependent Reliability," Engineering Optimization, 46(10), pp. 1389-1410.

[3] Park, C., Kim, N. H., and Haftka, R. T., 2015, "The Effect of Ignoring Dependence between Failure Modes on Evaluating System Reliability," Structural and Multidisciplinary Optimization, 52(2), pp. 251-268.

[4] Ditlevsen, O., and Madsen, H. O., 1996, Structural Reliability Methods, Wiley New York.

[5] Lee, I., Choi, K. K., and Gorsich, D., 2010, "Sensitivity Analyses of Form‐Based and Drm‐Based Performance Measure Approach (Pma) for Reliability‐Based Design Optimization (Rbdo)," International Journal for Numerical Methods in Engineering, 82(1), pp. 26-46.

[6] Du, X., and Hu, Z., 2012, "First Order Reliability Method with Truncated Random Variables," Journal of Mechanical Design, Transactions of the ASME, 134(9), p. 091005.

[7] Zhu, Z., Hu, Z., and Du, X., 2015, "Reliability Analysis for Multidisciplinary Systems Involving Stationary Stochastic Processes," Proceedings of ASME 2015 Design Engineering Technical Conference, Paper DETC2015-46168, Boston, Massachusetts.

[8] Du, X., 2010, "System Reliability Analysis with Saddlepoint Approximation," Structural and Multidisciplinary Optimization, 42(2), pp. 193-208.

[9] Helton, J. C., Johnson, J. D., Sallaberry, C. J., and Storlie, C. B., 2006, "Survey of Sampling-Based Methods for Uncertainty and Sensitivity Analysis," Reliability Engineering & System Safety, 91(10), pp. 1175-1209.

[10] Viana, F. A. C., Simpson, T. W., Balabanov, V., and Toropov, V., 2014, "Metamodeling in Multidisciplinary Design Optimization: How Far Have We Really Come?," AIAA Journal, 52(4), pp. 670-690.

[11] Dubourg, V., Sudret, B., and Deheeger, F., 2013, "Metamodel-Based Importance Sampling for Structural Reliability Analysis," Probabilistic Engineering Mechanics, 33, pp. 47-57.

[12] Balesdent, M., Morio, J., and Marzat, J., 2013, "Kriging-Based Adaptive Importance Sampling Algorithms for Rare Event Estimation," Structural Safety, 44, pp. 1-10.

[13] Echard, B., Gayton, N., Lemaire, M., and Relun, N., 2013, "A Combined Importance Sampling and Kriging Reliability Method for Small Failure Probabilities with Time-Demanding Numerical Models," Reliability Engineering and System Safety, 111, pp. 232-240.

[14] Singh, A., Mourelatos, Z., and Nikolaidis, E., 2011, "Time-Dependent Reliability of Random Dynamic Systems Using Time-Series Modeling and Importance Sampling," SAE Technical Paper.

[15] Kleijnen, J. P., 2008, Design and Analysis of Simulation Experiments, Springer.

[16] Youn, B. D., and Choi, K. K., 2004, "A New Response Surface Methodology for Reliability-Based Design Optimization," Computers & structures, 82(2), pp. 241-256.

[17] Simpson, T. W., Peplinski, J. D., Koch, P. N., and Allen, J. K., 2001, "Metamodels for Computer-Based Engineering Design: Survey and Recommendations," Engineering with Computers, 17(2), pp. 129-150.

[18] Smola, A. J., and Schölkopf, B., 2004, "A Tutorial on Support Vector Regression," Statistics and Computing, 14(3), pp. 199-222.

[19] Schöbi, R., Sudret, B., and Marelli, S., 2016, "Rare Event Estimation Using Polynomial-Chaos Kriging," ASCE-ASME Journal of Risk and Uncertainty in Engineering Systems, Part A: Civil Engineering, p. D4016002.

[20] Xiu, D., and Karniadakis, G. E., 2003, "Modeling Uncertainty in Flow Simulations Via Generalized Polynomial Chaos," Journal of Computational Physics, 187(1), pp. 137-167.

[21] Sacks, J., Welch, W. J., Toby, J. M., and Wynn, H. P., 1989, "Design and Analysis of Computer Experiments," Statistical Science, 4(4), pp. 409-423.

[22] Lophaven, S. N., Nielsen, H. B., and Sondergaard, J., 2002, "Dace-a Matlab Kriging Toolbox, Version 2.0," Technical University of Denmark.

[23] Martin, J. D., and Simpson, T. W., 2005, "Use of Kriging Models to Approximate Deterministic Computer Models," AIAA Journal, 43(4), pp. 853-863.

[24] Jones, D. R., Schonlau, M., and Welch, W. J., 1998, "Efficient Global Optimization of Expensive Black-Box Functions," Journal of Global Optimization, 13(4), pp. 455-492.

[25] Bichon, B., Eldred, M., Swiler, L., Mahadevan, S., and McFarland, J., 2007, "Multimodal Reliability Assessment for Complex Engineering Applications Using Efficient Global Optimization," AIAA Paper No. AIAA-2007-1946.

[26] Bichon, B. J., McFarland, J. M., and Mahadevan, S., 2011, "Efficient Surrogate Models for Reliability Analysis of Systems with Multiple Failure Modes," Reliability Engineering and System Safety, 96(10), pp. 1386-1395.

[27] Echard, B., Gayton, N., and Lemaire, M., 2011, "Ak-Mcs: An Active Learning Reliability Method Combining Kriging and Monte Carlo Simulation," Structural Safety, 33(2), pp. 145-154.

[28] Fauriat, W., and Gayton, N., 2014, "Ak-Sys: An Adaptation of the Ak-Mcs Method for System Reliability," Reliability Engineering and System Safety, 123, pp. 137-144.

[29] Zhu, Z., and Du, X., 2016, "Reliability Analysis with Monte Carlo Simulation and Dependent Kriging Predictions," ASME Journal of Mechanical Design.

[30] Viana, F. A. C., Venter, G., and Balabanov, V., 2010, "An Algorithm for Fast Optimal Latin Hypercube Design of Experiments," International Journal for Numerical Methods in Engineering, 82(2), pp. 135-156.

[31] Wang, Z., and Wang, P., 2015, "An Integrated Performance Measure Approach for System Reliability Analysis," Journal of Mechanical Design, 137(2), pp. 021406-021406.

[32] Youn, B. D., and Wang, P., 2009, "Complementary Intersection Method for System Reliability Analysis," Journal of Mechanical Design, 131(4), pp. 041004-041004.

[33] McDonald, M., and Mahadevan, S., 2008, "Design Optimization with System-Level Reliability Constraints," Journal of Mechanical Design, 130(2), p. 021403.

[34] Smith, N., and Mahadevan, S., 2005, "Integrating System-Level and Component-Level Designs under Uncertainty," Journal of spacecraft and rockets, 42(4), pp. 752-760.

[35] Collier, C., Yarrington, P., and Pickenheim, M., "The Hypersizing Method for Structures," Proc. NAFEMS World Congress, pp. 25-28.

IV. A KRIGING METHOD FOR TIME-DEPENDENT SYSTEM RELIABILITY ANALYSIS

Zhifu Zhu and Xiaoping Du

Department of Mechanical and Aerospace Engineering

Missouri University of Science and Technology

ABSTRACT

Time-dependent system reliability is the probability a system performs its intended function without failures in a time period. Estimating such a probability is challenging when system responses are highly nonlinear and dependent. Many current time-dependent system reliability methods rely on extreme system responses, which require time-consuming global optimization. The distributions of the extreme responses may also be highly nonlinear and more irregular than their original functions. As a result, the efficiency of the time-dependent system reliability analysis is of great interest. This work develops a new time-dependent system reliability method that generates surrogate models for general time-dependent limit-state functions with respect to input variables in the form of random variables, stochastic processes, and time. By removing global optimization and combining the surrogate model building process with Monte Carlo simulation, the new method is efficient and accurate. As the proposed method does not rely on any assumptions or simplifications, it is applicable to systems with highly nonlinear and highly dependent system responses. Four examples, including series and parallel configurations, are used to demonstrate the effectiveness of the proposed method.

1. INTRODUCTION

Engineering systems are usually subjected to time-variant loads and deterioration of material properties, and the system reliability is therefore a function of time. Time-dependent system reliability is evaluated by the probability that the responses of a system do not exceed given failure thresholds in a given period of time. Since the accurate and efficient estimate of system reliability is crucial in decision makings associated with system performance degradation [1], lifetime cost estimation, maintenance [2, 3], and so on, time-dependent reliability analysis has gained significant attention during the past decades. The difficulty of time-dependent system reliability analysis comes from time-variant working conditions and system characteristics and also from dependent responses. Although many progresses have been made, time-dependent system reliability analysis is still very challenging.

Upcrossing rate methods, extreme value methods, and sampling-based methods are the most commonly used time-dependent system reliability methods. Upcrossing rate methods estimate the probability that the response exceeds its failure threshold for the first time in a period of time. When the response reaches its threshold, an upcrossing event happens. The upcrossing rate is the rate of change in upcrossing probability with respect to time. Based on the Rice's formula [4], many methods have been developed to estimate component reliability. For example, Breitung [5] proposed an asymptotic outcrossing rate method for stationary Gaussian process; Andrieu-Renaud et. al [6] proposed the PHI2 method which can take advantage of classical time-independent reliability tools, like the First/Second Order Reliability Method (FORM/SORM) [7], to estimate time-dependent reliability; Hu and Du developed an upcrossing rate method for

hydrokinetic turbine blades [8] and a joint upcrossing rate method [9] which relaxes the independent upcrossing assumption. Later, they extended the joint upcrossing rate method to systems with two responses [10]. Upcrossing rate methods have good efficiency, but the linearization of performance function may introduce large errors for highly nonlinear and multimodal problems; and for problems with strong dependent upcrossings, the independent upcrossing assumption does not hold, which will bring large errors to reliability analysis results.

Without the linearization and approximation in upcrossing rate methods, extreme value methods are extensively studied. Extreme value methods use the extreme responses from a performance function with respect to time. If the distribution of extreme values can be accurately estimated, extreme value methods are more accurate than upcrossing rate methods [11]. For example, Li et al. [12] proposed the equivalent extreme value event method for structural system reliability; Wang and Wang [13] developed a nested extreme response surface method for time-dependent reliability based design optimization; Hu and Du [14] proposed a sampling method to extreme value distribution for time-dependent reliability analysis. Extreme value methods generally require a double-loop procedure: the outer loop builds surrogate models of extreme values, and the inner loop performs global optimization to identify the extreme responses over the time period of interest. The double-loop procedure has two main drawbacks: (1) The distributions of extreme values are usually highly nonlinear and multimodal, even though the original performance functions are smooth and unimodal. The increased nonlinearity and irregularity of extreme values may introduce errors to reliability analysis, and the accuracy of global optimization in the inner loop will affect the accuracy of extreme

value surrogate modeling in the outer loop. (2) Identifying extreme values in the inner loop for problems with stochastic processes over a long time period is computationally expensive since the realizations of stochastic processes might be multimodal.

Sampling methods generate samples where performance functions are evaluated. Since these methods do not rely on approximations of performance functions, they are accurate when sufficient samples are used. Monte Carlo Simulation [15] is the most widely used sampling method, but is too computationally expensive. To reduce the computational cost, one may build cheaper surrogate models for performance functions and use them in reliability analysis. Many methods have been proposed recently with various surrogate models. For example, Zou et al. [16] proposed an indicator response surface method for simulation-based reliability analysis; with the help of Kriging model [17, 18] and the Efficient Global Optimization (EGO) [19] method, Hu and Du [11] developed a mixed EGO method which draws samples of random variables and time simultaneously, then Zhu and Du [20] extends the mixed EGO method to system problems. Surrogate models, such as artificial neural networks (ANN) [21], support vector machine (SVM) [22], polynomial chaos expansion (PCE) [23] and their combinations [24-28] are studied by many researchers. Among the various surrogate models, Kriging model [18, 29] has been extensively studied due to its characteristics that the model provides not only a prediction for an untried point, but also the uncertainty of the prediction. This is really helpful for adaptive modeling and uncertainty control in reliability analysis. A good discussion of surrogate modeling can be found in [30] and [31]. In the effort to reduce computational cost of sampling methods, there is an interesting trend that some methods are developed combining surrogate modeling and

importance sampling [32-35], which makes reliability estimate of rare events become affordable.

With the aforementioned surrogate modeling methods, Wang and Wang [36] developed a double-loop adaptive sampling method for dynamic systems. Later, Hu and Mahadevan [37] proposed a single-loop component method to overcome the drawbacks of double-loop procedure. Inspired by Hu and Mahadevan's method, this work develops a new surrogate modeling method for time-dependent system reliability analysis. The new method does not need global optimization to find extreme responses. The proposed surrogate modeling method is investigated for systems with and without stochastic processes, and this makes the method applicable to general time-dependent problems with any system configurations and any types of input in performance functions. Thus, the contributions of the paper are twofold: (1) a new perspective for surrogate-based time-dependent system reliability analysis, and (2) a new procedure to build surrogate models for general time-dependent systems.

The remainder of this paper is organized as follows: Section 2 reviews the background of time-dependent system reliability analysis and the system mixed EGO method. The proposed method and its implementation procedures are developed in Section 3. Section 4 demonstrates the effectiveness of proposed method with four examples. Conclusions are drawn in Section 5.

2. BACKGROUND

2.1 TIME-DEPENDENT SYSTEM RELIABILITY ANALYSIS

For a general time-dependent system with n components, $k = 1, 2, \cdots, n$, the inputs include: random variables $\mathbf{X}$, stochastic processes $\mathbf{Y}(t)$, and time t. The performance function of component k is defined as

$$y_k(t) = g_k(\mathbf{X}, \mathbf{Y}(t), t) \tag{1}$$

For a period of time $[t_0, t_s]$, the reliability of component k over the time period is defined as

$$R^k(t_0, t_s) = \Pr\{g_k(\mathbf{X}, \mathbf{Y}(t), t) < 0, \forall t \in [t_0, t_s]\} \tag{2}$$

in which $\Pr\{\cdot\}$ stands for a probability, and "$\forall$" means "for all". The probability of failure of this component is therefore

$$p_f^k(t_0, t_s) = \Pr\{g_k(\mathbf{X}, \mathbf{Y}(t), t) > 0, \exists t \in [t_0, t_s]\} \tag{3}$$

in which "$\exists$" means "there exists".

Systems can be grouped into three categories: series systems, parallel systems, and combined systems. The time-dependent probabilities of failure for a series system and parallel system are defined as follows:

$$p_f^{\text{series}}(t_0, t_s) = \Pr\left\{ \bigcup_k g_k(\mathbf{X}, \mathbf{Y}(t), t) > 0, \exists t \in [t_0, t_s] \right\} \tag{4}$$

$$p_f^{\text{parallel}}(t_0, t_s) = \Pr\left\{ \bigcap_k g_k(\mathbf{X}, \mathbf{Y}(t), t) > 0, \exists t \in [t_0, t_s] \right\} \tag{5}$$

respectively, where $\bigcup$ is union, and $\bigcap$ is intersection.

For extreme value methods, the above equations can be rewritten as

$$p_f^{\text{series}}(t_0,t_s) = \Pr\left\{\bigcup_k y_k^{\max} = \max_{t_i \in [t_0,t_s]} g_k(\mathbf{X},\mathbf{Y}(t_i),t_i) > 0, \exists t_i \in [t_0,t_s]\right\} \tag{6}$$

$$p_f^{\text{parallel}}(t_0,t_s) = \Pr\left\{\bigcap_k y_k^{\max} = \max_{t_i \in [t_0,t_s]} g_k(\mathbf{X},\mathbf{Y}(t_i),t_i) > 0, \exists t_i \in [t_0,t_s]\right\} \tag{7}$$

Mixed system EGO method (mSEGO) [20] is a typical time-dependent system reliability analysis method that builds surrogate models for extreme values. The method developed in [20] is for systems whose performance functions are explicit functions of random variables and time. Next, we will review the procedure of mSEGO method. The proposed method is compared with mSEGO method in terms of accuracy and efficiency.

2.2 REVIEW OF MIXED SYSTEM EGO METHOD

Mixed system EGO method [20] deals with problems have random variables and time as inputs in their performance functions. The probability of failure of component k is defined as

$$p_f^k(t_0,t_s) = \Pr\left\{\hat{g}_k(\mathbf{X},t) > 0, \exists t \in [t_0,t_s]\right\} \tag{8}$$

The general idea of mSEGO is to construct extreme value surrogate models of performance functions, and use the extreme value surrogate models to replace original performance functions for reliability analysis. The surrogate models map input random variables to extreme responses, and the above equation therefore becomes

$$p_f^k(t_0,t_s) = \Pr\left\{\hat{y}^{\text{extreme}} = \hat{g}_k^{\text{extreme}}(\mathbf{X}) > 0\right\} \tag{9}$$

in which $\hat{g}_k^{\text{extreme}}(\mathbf{X})$ is the extreme response over $[t_0,t_s]$. For any given $\mathbf{X} = \mathbf{x}$, where $\mathbf{x}$ is a realization of random variables $\mathbf{X}$, $\hat{g}_k^{\text{extreme}}(\mathbf{x})$ is defined by

$$\hat{g}_k^{\text{extreme}}(\mathbf{x}) = \max_{t \in [t_0,t_s]}\left\{g_k(\mathbf{x},t)\right\} \text{ or } \min_{t \in [t_0,t_s]}\left\{g_k(\mathbf{x},t)\right\}, \forall \mathbf{X} = \mathbf{x} \tag{10}$$

After obtaining the above extreme value surrogate models of each component, time-dependent system reliability analysis is transformed to its time-independent counterpart. Estimating system reliability based on extreme value surrogate models is efficient and easy to implement.

Table 2.1 Major steps of mSEGO method

Step	Description
1	Construct initial surrogate models $\hat{y}_k = \hat{g}_k(\mathbf{X},t)$
	(a) Generate N_0 initial training points $\mathbf{x}_k^T$.
	(b) Divide time period $[t_0, t_s]$ into n_t time instants, $\mathbf{t} = [t_1 = t_0, t_2, \cdots, t_{n_t} = t_s]$, and randomly select N_0 time instants as initial training points $\mathbf{t}_k^T$.
	(c) Calculate $\mathbf{y}_k^T = g_k(\mathbf{x}_k^T, \mathbf{t}_k^T)$ and build initial surrogate models $\hat{y}_k = \hat{g}_k(\mathbf{X},t)$.
2	Construct initial extreme value surrogate models $\hat{y}_k^{\text{extreme}} = \hat{g}_k^{\text{extreme}}(\mathbf{X})$
	(d) Let $\mathbf{x}_k^{\text{extreme}} = \mathbf{x}_k^T$, $\mathbf{t}_k^{\text{extreme}} = \mathbf{t}_k^T$ and $\mathbf{y}_k^{\text{extreme}} = \mathbf{y}_k^T$.
	(e) For each component k, $k = 1,2,\cdots,n$
	(f) For each training point in $(\mathbf{x}_k^{\text{extreme}}, \mathbf{t}_k^{\text{extreme}})$, compute $\mathbf{U}_k$ and $\boldsymbol{\sigma}_k$ using $\hat{y}_k = \hat{g}_k(\mathbf{X},t)$
	End
	(g) Calculate the values of expected feasibility function (EFF) using Eq. (11).
	(h) Find the point with the maximum EFF value as new training point $(\mathbf{x}_{\text{new}}, t_{\text{new}})$.
	(i) Calculate the U value at $(\mathbf{x}_{\text{new}}, t_{\text{new}})$ for all components, and calculate $\mathbf{y}_k = g_k(\mathbf{x}_{\text{new}}, t_{\text{new}})$ when $U_k < 2$.
	(j) Update surrogate models $\hat{y}_k = \hat{g}_k(\mathbf{X},t)$ and $\hat{y}_k^{\text{extreme}} = \hat{g}_k^{\text{extreme}}(\mathbf{X})$.
	Continue steps (e) through (j) until the stopping criterion of EFF is satisfied.

Table 2.1 Major steps of mSEGO method (cont.)

3	Refine surrogate models by adding more training points
	(k) Generate N_C candidate Monte Carlo samples $\mathbf{x}_{MCS}$
	(l) Calculate the composite U value U^* at every point in $\mathbf{x}_{MCS}$ using $\hat{y}_k^{\text{extreme}} = \hat{g}_k^{\text{extreme}}(\mathbf{X})$.
	(m) Find a new point $(\mathbf{x}_{\text{new}}^*, t_{\text{new}}^*)$ with the minimum composite U value $U_{\min}^*$.
	(n) Calculate U values at $(\mathbf{x}_{\text{new}}^*, t_{\text{new}}^*)$ for all components, and calculate $\mathbf{y}_k = g_k(\mathbf{x}_{\text{new}}^*, t_{\text{new}}^*)$ when $U_k < 2$.
	(o) Update surrogate models $\hat{y}_k = \hat{g}_k(\mathbf{X}, t)$ and $\hat{y}_k^{\text{extreme}} = \hat{g}_k^{\text{extreme}}(\mathbf{X})$.
	Continue steps (l) through (o) until $U_{\min}^* > 2$.
4	Time-dependent system reliability analysis based on $\hat{y}_k^{\text{extreme}} = \hat{g}_k^{\text{extreme}}(\mathbf{X})$.
	(p) Calculate $p_f^{\text{system}}(t_0, t_s)$ using $\hat{y}_k^{\text{extreme}} = \hat{g}_k^{\text{extreme}}(\mathbf{X})$.
	(q) Compute COV_{p_f} and increase N_C if $COV_{p_f} > 0.05$; otherwise, stop.

The key problem here now is how to build surrogate model $\hat{g}_k^{\text{extreme}}(\mathbf{X})$. The extreme value surrogate modeling is a double-loop process, which is summarized as below.

- Outer loop: Construct surrogate models of $\hat{g}_k^{\text{extreme}}(\mathbf{X})$ using adaptive sampling approach and the learning function U from AK-MCS paper [38].

- Inner loop: Construct surrogate models of $\hat{g}_k(\mathbf{X}, t)$ to select new training points from a pre-sampled Monte Carlo sample pool and find the corresponding extreme responses $g_k^{\text{extreme}}(\mathbf{x})$ using mixed EGO method [11].

Next, we review the double-loop process of building extreme response surrogate models. The major steps of mSEGO method are summarized in Table 2.1.

In Table 2.1, the expected feasibility function (EFF) is used as an indication of how well the true value of a response at a new point is expected to satisfy the equality constraint $g(\mathbf{x},t) = e$ over a region defined by $e \pm \varepsilon$. EFF is defined as [39]

$$
\begin{aligned}
EFF\left(\hat{g}(\mathbf{x},t)\right) = (\mu - e) & \left[2\Phi\left(\frac{e-\mu}{\sigma}\right) - \Phi\left(\frac{e^{-}-\mu}{\sigma}\right) - \Phi\left(\frac{e^{+}-\mu}{\sigma}\right) \right] \\
& - \sigma \left[2\phi\left(\frac{e-\mu}{\sigma}\right) - \phi\left(\frac{e^{-}-\mu}{\sigma}\right) - \phi\left(\frac{e^{+}-\mu}{\sigma}\right) \right] \\
& + \varepsilon \left[\Phi\left(\frac{e^{+}-\mu}{\sigma}\right) - \Phi\left(\frac{e^{-}-\mu}{\sigma}\right) \right]
\end{aligned}
\tag{11}
$$

in which μ and σ are the mean and standard deviation provided by Kriging model at point $(\mathbf{x},t)$, respectively. e is the failure threshold, $\varepsilon = 2\sigma$, e^{+} and e^{-} denote $e \pm \varepsilon$. $\Phi(\cdot)$ and $\phi(\cdot)$ are cumulative distribution function and probability density function of a standard normal distribution, respectively.

The EFF function is called a learning function, which is used as a criterion of selecting new training points to update surrogate models so that the accuracy of surrogate models can be improved in a most efficient manner. The other learning function used in Table 2.1 is the U function defined by [38]

$$
U(\mathbf{x},t) = \frac{\left|\mu(\mathbf{x},t)\right|}{\sigma(\mathbf{x},t)}
\tag{12}
$$

For a system with several components, the contribution of each component may be significantly different. For example, some components have big contributions to the system reliability estimate, while some components may do not contribute to system

reliability at all. Thus treating all components equally by adding all new training points to each component is a waste of computational efforts. The good practice is to add large number of training points to performance functions that have significant contribution to system reliability estimate. The composite U value U^* in Step (l) is used for this purpose. This is called the composite criterion approach of updating system surrogate models. The detailed discuss of the three system approaches can be found in [40, 41]. U^* is calculated using the above equation with composite mean value and its corresponding composite standard deviation. The selection of composite mean value is given in Table 2.2.

Table 2.2 Selection of composite mean value

System topology	$g_k < 0$ is a failure	$g_k > 0$ is a failure
Series system	$\mu^* = \min(\mathbf{\mu})$	$\mu^* = \max(\mathbf{\mu})$
Parallel system	$\mu^* = \max(\mathbf{\mu})$	$\mu^* = \min(\mathbf{\mu})$

The coefficient of variation of reliability analysis result is used in Step (q) to account for the statistical uncertainty in Monte Carlo simulation. It is defined by

$$COV_{p_f} = \sqrt{\frac{1 - p_f^{\text{system}}(t_0, t_s)}{N_C p_f^{\text{system}}(t_0, t_s)}} \tag{13}$$

3. NEW METHOD

This section discusses the development of the new method and how it overcomes the two drawbacks of double-loop procedure extreme value methods.

3.1 OVERVIEW

The basic idea of the proposed method is to build surrogate models $\hat{g}_k(\mathbf{X}, \mathbf{Y}, t)$ to perform time-dependent system reliability analysis instead of using a double-loop procedure. The new method does not require the distributions of extreme responses and eliminates global optimization completely. For simplicity, we use a series system without stochastic processes as an example to demonstrate how the proposed method works. The method will be extended to problems with stochastic processes later. Based on the principle of MCS, the probability of system failure can be rewritten as

$$p_f^{\text{series}}(t_0, t_s) = \Pr\left\{\bigcup_k y_k^{\max} = \max_{t_i \in [t_0, t_s]} g_k(\mathbf{X}, t_i) > 0, \exists t_i \in [t_0, t_s]\right\} = \sum_{j=1}^{N} I_t^*(\mathbf{x}^{(j)}) / N \qquad (14)$$

where N is the number of MCS samples, and $I_t^*(\mathbf{x}^{(j)})$ is the time-dependent system failure indicator at point $\mathbf{x}^{(j)}$

$$I_t^*(\mathbf{x}^{(j)}) = \begin{cases} 1, \text{if } \max_{k=1,2,\cdots,n} \left\{g_k(\mathbf{x}^{(j)}, t^{(i)})\right\} > 0, \forall i = 1, 2, \cdots, n_t \\ 0, \text{ otherwise} \end{cases} \qquad (15)$$

The above equations indicate that the accuracy of time-dependent system reliability analysis is determined by the accuracy of surrogate models $\hat{y}_k(t) = \hat{g}_k(\mathbf{X}, t)$. Now the problem becomes how to construct and refine $\hat{y}_k(t) = \hat{g}_k(\mathbf{X}, t)$ so that they can be used to accurately estimate system reliability.

3.2 SURROGATE MODEL $\hat{y}_k(t) = \hat{g}_k(\mathbf{X}, t)$

The first step of proposed surrogate modeling method is to construct initial surrogate models for each component. N_0 initial training points of random variables $\mathbf{X}$ are generated using Latin Hypercube Sampling (LHS) method [42], and N_0 time instants are randomly selected from discretized time interval $\mathbf{t} = [t_1 = t_0, t_2, \cdots, t_{n_t} = t_s]$. The initial training point matrix for component k is

$$\left[\mathbf{x}_k^T, \mathbf{t}_k^T \right] = \begin{bmatrix} x_1^{(1)} & x_2^{(1)} & \cdots & x_m^{(1)} & t^{(1)} \\ x_1^{(2)} & x_2^{(2)} & \cdots & x_m^{(2)} & t^{(2)} \\ \vdots & \vdots & \ddots & \vdots & \vdots \\ x_1^{(N_0)} & x_2^{(N_0)} & \cdots & x_m^{(N_0)} & t^{(N_0)} \end{bmatrix} \tag{16}$$

in which $x_i^{(j)}$ is the j-th training point of the i-th random variable.

The responses of each component at these initial points are obtained by calling their performance functions $y_k(t) = g_k(\mathbf{X}, t)$, and based on these training points and responses, initial surrogate models $\hat{y}_k(t) = \hat{g}_k(\mathbf{X}, t)$ are built using the Kriging method [17, 18]. The output of a Kriging model at an untried point $(\mathbf{x}, t)$ follows a normal distribution

$$\hat{y}_k(t) \sim N\left(\mu_{\hat{g}_k}(\mathbf{x}, t), \sigma_{\hat{g}_k}^2(\mathbf{x}, t) \right) \tag{17}$$

where $\mu_{\hat{g}_k}(\mathbf{x}, t)$ and $\sigma_{\hat{g}_k}^2(\mathbf{x}, t)$ are the Kriging prediction and Kriging variance, respectively. As Kriging model is well studied and widely used by engineers and researcher, we are not reviewing it in this paper. The details of how to build Kriging models and how these outputs are calculated can be found in [17, 18].

When surrogate models $\hat{y}_k(t) = \hat{g}_k(\mathbf{X}, t)$ are well trained and accurate enough for reliability analysis, the time-dependent probability of system failure is calculated by

$$p_f^{\text{series}}(t_0, t_s) = \sum_{i=1}^{N} I\left(\max_{j=1,2,\cdots,n_t} \left(\max_{k=1,2,\cdots,n} \left\{ \mu_{\hat{g}_k}(\mathbf{x}^{(i)}, t^{(j)}) \right\} \right) \right) / N \qquad (18)$$

Table 3.1 Procedure of refining surrogate models

Step	Description
1	Generate N_C candidate points $\mathbf{x}_C$ and discretize $[t_0, t_s]$ into n_t time instants $\mathbf{t} = [t_1 = t_0, t_2, \cdots, t_{n_t} = t_s]$.
2	For each $\mathbf{x}^{(i)}$ in $\mathbf{x}_C$, $i = 1, 2, \cdots, N_C$ (a) For each component surrogate model $\hat{y}_k = \hat{g}_k(\mathbf{X}, t)$, $k = 1, 2, \cdots, n$ (b) Compute Kriging predictions $\boldsymbol{\mu}_k^{(i)} = \left[\hat{g}_k(\mathbf{x}^{(i)}, t^{(1)}), \hat{g}_k(\mathbf{x}^{(i)}, t^{(2)}), \cdots, \hat{g}_k(\mathbf{x}^{(i)}, t^{(n_t)}) \right]$ at each $(\mathbf{x}^{(i)}, t^{(j)})$. End (c) Find the system maximum prediction at $\mathbf{x}^{(i)}$, $\mu_{\max}^{(i)} = \max_{k=1,2,\cdots,n} \left(\boldsymbol{\mu}_k^{(i)} \right)$, and the corresponding $\sigma_{\max}^{(i)}$. (d) Calculate $U_{\max}^{(i)} = \left| \mu_{\max}^{(i)} \right| / \sigma_{\max}^{(i)}$. End
3	Find the point with minimum system U value $U_{\min}^* = \min_{i=1,2,\cdots,N_C} \left\{ U_{\max}^{(i)} \right\}$, and identify a new training point $(\mathbf{x}_{\text{new}}, t_{\text{new}})$ corresponding to $U_{\min}^*$.
4	Update surrogate models by adding new training points (e) Calculate U value at $(\mathbf{x}_{\text{new}}, t_{\text{new}})$ for all components. (f) If $U_k < 2$, calculate $\mathbf{y}_k = g_k(\mathbf{x}_{\text{new}}, t_{\text{new}})$. (g) Update surrogate models $\hat{y}_k = \hat{g}_k(\mathbf{X}, t)$ Continue steps (2) through (4) until $U_{\min}^* > 2$.

When surrogate models $\hat{y}_k(t) = \hat{g}_k(\mathbf{X}, t)$ are not accurate enough to substitute original performance functions for reliability analysis, more training points need to be added to refine the models. In order to remove global optimization, N_C sample points are generated based on the distributions of random variables, and these samples are served as candidates for new training points; they are therefore called candidate points (CP) $\mathbf{x}_C$. For each candidate point $\mathbf{x}^{(i)}$ in $\mathbf{x}_C$, the Kriging prediction and its variance can be obtained by using existing surrogate models $\hat{y}_k(t) = \hat{g}_k(\mathbf{X}, t)$, and the maximum prediction $\mu_{\max}^{(i)}$ and its corresponding standard deviation $\sigma_{\max}^{(i)}$ at this point are available.

$$\mu_{\max}^{(i)} = \max_{j=1,2,\cdots,n_t} \left(\max_{k=1,2,\cdots,n} \left\{ \mu_{\hat{g}_k}(\mathbf{x}^{(i)}, t^{(j)}) \right\} \right) \tag{19}$$

The U value at $\mathbf{x}^{(i)}$ is calculated with Eq. (12). The U value indicates the probability that surrogate models $\hat{y}_k(t) = \hat{g}_k(\mathbf{X}, t)$ correctly predicts the sign of $y_k(t) = g_k(\mathbf{X}, t)$. The smaller is the U value, the lower is the probability of correctness. Therefore, the point with the minimum U value has the greatest probability of making a wrong prediction, and adding this point to training points improves the accuracy of surrogate models to the most extent. This provides the most efficient way of refining surrogate models and achieving convergence.

$$\mathbf{x}_{\text{new}} = \arg \min_{i=1,2,\cdots,N_C} \left(\mu_{\max}^{(i)} / \sigma_{\max}^{(i)} \right) \tag{20}$$

After identifying the new training point and its corresponding time instant $(\mathbf{x}_{\text{new}}, t_{\text{new}})$, the U values of each component at this point is evaluated. If $U_k(\mathbf{x}_{\text{new}}, t_{\text{new}}) < 2$, evaluate the original performance function of this component and obtain the true response at the new training point. Then add the new training point and its

response to existing training points and update the surrogate model. If $U_k(\mathbf{x}_{\text{new}}, t_{\text{new}}) > 2$,

this means that adding the new training point does not improve the model accuracy of

component k significantly. Therefore, calling of original performance function of this

component is not needed.

The above process is continued until the stopping criterion is satisfied. The

detailed procedure is provided in Table 3.1.

3.3 EXTENSION TO PROBLEMS WITH STOCHASTIC PROCESSES

The surrogate modeling method developed above is for problems without

stochastic processes. For a general time-dependent system, the components performance

functions are in form of $y_k(t) = g_k(\mathbf{X}, \mathbf{Y}(t), t)$, where $\mathbf{Y}(t)$ are the stochastic processes.

To employ the proposed method, $\mathbf{Y}(t)$ need to be represented as a function of

independent random variables. This transformation is achieved by Karhunen-Loeve

expansion [43]. For a stochastic process $Y_i(t)$, the Karhunen-Loeve expansion is given

by

$$Y_i(t) = \mu_{Y_i(t)} + \sigma_{Y_i(t)} \sum_{j=1}^{n_e} \sqrt{\lambda_j} \xi_j f_j(t) \tag{21}$$

where $\mu_{Y_i(t)}$ and $\sigma_{Y_i(t)}$ are the mean and standard deviation of the stochastic process, λ_j

and $f_j(t)$ are eigenvalues and eigenvectors of the covariance function of the stochastic

process, ξ_j are independent standard random variables, and n_e is the number of

eigenvectors used to represent the stochastic process.

After the Karhunen-Loeve expansion, the stochastic processes $\mathbf{Y}(t)$ are

represented by a function of independent standard random variables ξ, the performance

functions therefore become $y_k(t) = g_k(\mathbf{X}, \xi, t)$. To accurately represent $\mathbf{Y}(t)$, a large number of random variables are needed, especially when the time period of interest is large. Because of the high dimensionality of $y_k(t) = g_k(\mathbf{X}, \xi, t)$, building their extreme value surrogate models $\hat{y}_k^{\text{extreme}} = \hat{g}_k^{\text{extreme}}(\mathbf{X}, \xi)$ using the double-loop process reviewed in Section 2.2 is very time consuming. In the proposed method, we build surrogate models for $y_k(t) = g_k(\mathbf{X}, \mathbf{Y}(t), t)$ directly so that the Karhunen-Loeve expansion will not increase the dimension of the surrogate modeling.

Table 3.2 Procedure of refining surrogate models with stochastic processes

Step	Description
1	Generate N_C candidate points $\mathbf{x}_C$ and ξ, and discretize $[t_0, t_s]$ into n_t time instants.
2	For each $\mathbf{x}^{(i)}$ and $\xi^{(i)}$, $i = 1, 2, \cdots, N_C$ (a) Convert $\xi^{(i)}$ to $[\mathbf{Y}(t^{(1)}), \mathbf{Y}(t^{(2)}), \cdots, \mathbf{Y}(t^{(n_t)})]$. (b) For each component surrogate model $\hat{y}_k = \hat{g}_k(\mathbf{X}, \mathbf{Y}, t)$, $k = 1, 2, \cdots, n$ (c) Compute Kriging prediction $\mathbf{\mu}_k^{(i)} = \left[\hat{g}_k(\mathbf{x}^{(i)}, t^{(1)}), \hat{g}_k(\mathbf{x}^{(i)}, t^{(2)}), \cdots, \hat{g}_k(\mathbf{x}^{(i)}, t^{(n_t)}) \right]$ at each $(\mathbf{x}^{(i)}, \mathbf{Y}(t^{(j)}), t^{(j)})$. End (d) Find the system maximum prediction at $\mathbf{x}^{(i)}$, $\mu_{\max}^{(i)} = \max\limits_{k=1,2,\cdots,n} \left(\mathbf{\mu}_k^{(i)} \right)$, and find the corresponding $\sigma_{\max}^{(i)}$ (e) Calculate $U_{\max}^{(i)} = \left| \mu_{\max}^{(i)} \right| / \sigma_{\max}^{(i)}$ End

Table 3.2 Procedure of refining surrogate models with stochastic processes (cont.)

3	Find the point with minimum system U value $U_{\min}^* = \min\limits_{i=1,2,\cdots,N_C}\{U_{\max}^{(i)}\}$, and identify a new training point $(\mathbf{x}_{new}, Y_{new}, t_{new})$ corresponding to $U_{\min}^*$.

4	Update surrogate models by adding new training points
	
	    (f) Calculate U value at $(\mathbf{x}_{new}, Y_{new}, t_{new})$ for all components.
	
	    (g) If $U_k < 2$, calculate $\mathbf{y}_k = g_k(\mathbf{x}_{new}, Y_{new}, t_{new})$.
	
	    (h) Update surrogate models $\hat{y}_k(t) = \hat{g}_k(\mathbf{X}, \mathbf{Y}, t)$
	
	Continue steps (2) through (4) until $U_{\min}^* > 2$.

Similar to the surrogate modeling process of $\hat{y}_k(t) = \hat{g}_k(\mathbf{X},t)$, N_0 initial training points are generated for $\mathbf{X}$, ξ, and t.

$$\left[\mathbf{x}_k^T, \xi_k^T, \mathbf{t}_k^T\right] = \begin{bmatrix} \mathbf{x}^{(1)} & \xi^{(1)} & t^{(1)} \\ \vdots & \vdots & \vdots \\ \mathbf{x}^{(N_0)} & \xi^{(N_0)} & t^{(N_0)} \end{bmatrix} \tag{22}$$

And then using Eq. (21), the responses of $\mathbf{Y}(t)$ are obtained. The training points are therefore become

$$\left[\mathbf{x}_k^T, \mathbf{Y}_k^T, \mathbf{t}_k^T\right] = \begin{bmatrix} \mathbf{x}^{(1)} & \mathbf{Y}^{(1)} & t^{(1)} \\ \vdots & \vdots & \vdots \\ \mathbf{x}^{(N_0)} & \mathbf{Y}^{(N_0)} & t^{(N_0)} \end{bmatrix} \tag{23}$$

Based on these initial training points, surrogate models of $\hat{y}_k(t) = \hat{g}_k(\mathbf{X},\mathbf{Y},t)$ are built. Then we generate N_C candidate points for $\mathbf{X}$ and ξ, and $[t_0,t_s]$ is divided into n_t time instants. The candidate points of ξ are transformed to candidate points of $\mathbf{Y}(t)$

using Eq. (21). The procedure of refining surrogate models for problems with stochastic processes is provided in Table 3.2.

Since the dimensionality of surrogate models $\hat{y}_k(t) = \hat{g}_k(\mathbf{X}, \mathbf{Y}, t)$ is much lower than that of the extreme value surrogate models $\hat{y}_k^{\text{extreme}} = \hat{g}_k^{\text{extreme}}(\mathbf{X}, \boldsymbol{\xi})$, the proposed method has better efficiency in surrogate modeling than extreme value methods.

4. EXAMPLES

In this section, four examples are used to demonstrate the effectiveness of the proposed method. The performance functions of the first three examples have random variables and time as inputs, example 4 deals with random variables, time, and stochastic processes. The efficiency of a method is measured by number of function calls (N_{FC}), and its accuracy is measured by the following percentage error

$$\varepsilon\% = \left| p_f^{\text{system}}(t_0,t_s) - p_{f,\text{MCS}}^{\text{system}}(t_0,t_s) \right| / p_{f,\text{MCS}}^{\text{system}}(t_0,t_s) \times 100\% \tag{24}$$

where $p_{f,\text{MCS}}^{\text{system}}(t_0,t_s)$ is the time-dependent probability of system failure using MCS. $p_{f,\text{MCS}}^{\text{system}}(t_0,t_s)$ is obtained from the brute force MCS performed on original response functions with a large sample size, and is therefore used as accurate solution for accuracy comparison. $p_f^{\text{system}}(t_0,t_s)$ is obtained using mSEGO and the proposed method.

For all examples in this paper, we use $N_0 = 12$ initial training points to construct initial surrogate models, as suggested by [38]. Since both mSEGO method and the proposed method are based on random sampling, their results are also random. We therefore run both methods 20 times independently and use their average function calls and probability of failures for accuracy and efficiency comparison.

4.1 EXAMPLE 1

The first example is a numerical example with three components. The performance functions are defined by

$$g_1(\mathbf{X},t) = x_1^2 x_2 - 0.2 x_1 \sqrt{t} \tag{25}$$

$$g_2(\mathbf{X},t) = (x_1 + x_2)^2 - (x_1 - x_2)t^2 / 15 \tag{26}$$

$$g_3(\mathbf{X},t) = 3x_1 - x_2 \sin t \tag{27}$$

where $x_1 \sim N(1,0.1^2)$, $x_2 \sim N(1,0.1^2)$. It is a series system, thus, the probability of system failure is defined as:

$$p_f^{\text{system}}(t_0,t_s) = \Pr\left\{g_1(\mathbf{X},t) < 0 \bigcup g_2(\mathbf{X},t) < 0 \bigcup g_3(\mathbf{X},t) < 0, \exists t \in [0,10]\right\} \qquad (28)$$

The average results of $p_f^{\text{system}}(t_0,t_s)$, ε, standard deviation of $p_f^{\text{system}}(t_0,t_s)$, and N_{FC} from 20 independent runs are reported in Table 4.1 for comparison.

The results show that the proposed method has much better efficiency and accuracy than mSEGO method. As the proposed method has smaller standard deviation of $p_f^{\text{system}}(t_0,t_s)$ than that of mSEGO method, which means the new method tends to produce stable reliability analysis results, the new method is more robust than mSEGO method.

Table 4.1 Average results of example 1

Methods	$p_f^{\text{system}}(t_0,t_s)$	$\sigma_{p_f^{\text{system}}(t_0,t_s)}$	ε (%)	N_{FC}		
MCS	2.2996×10^{-3}	N/A	N/A	1×10^8	1×10^8	1×10^8
mSEGO	2.2568×10^{-3}	5.58×10^{-5}	2.72	720.30	35.60	24.00
New method	2.2956×10^{-3}	2.72×10^{-5}	0.85	21.39	16.14	12.05

4.2 EXAMPLE 2

A function generator mechanism system consists of two four-bar linkage mechanisms is shown in Figure 4.1 [44, 45]. The two mechanisms generate a sine and a logarithm function, respectively.

The motion input and output of the sine function generator are θ and $\kappa = \kappa_a(\mathbf{B}, \theta)$, respectively, where $\mathbf{B} = [B_1, B_2, \cdots, B_7]$ are the lengths of linkages of the mechanism. The required motion output is given by

$$\kappa_d(\theta) = 60° + 60° \sin\left(0.75(\theta - 97°)\right) \tag{29}$$

For the logarithm function generator, the motion input and output are χ and $\eta = \eta_a(\mathbf{B}, \chi)$, respectively. The required motion output is given by

$$\eta_d(\chi) = 60° \log_{10}\left[(\chi + 15°)/60°\right] / \log_{10}(2) \tag{30}$$

And the motion errors of the two mechanisms are given by

$$\varepsilon_\kappa(\mathbf{B}, \theta) = \kappa_a(\mathbf{B}, \theta) - \kappa_d(\theta) \tag{31}$$

$$\varepsilon_\eta(\mathbf{B}, \chi) = \eta_a(\mathbf{B}, \chi) - \eta_d(\chi) \tag{32}$$

As linkages B_2 and B_5 are welded together, their input angles have the following relation
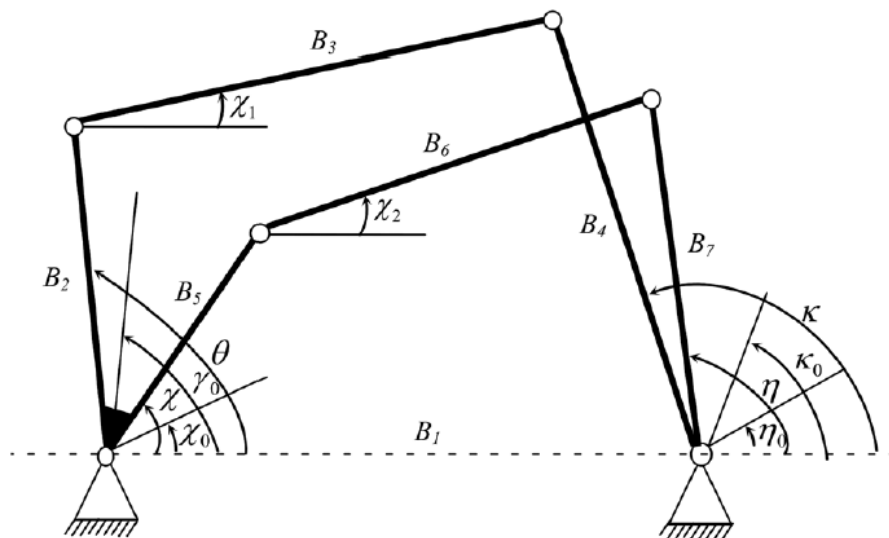
$$\theta = 62° + \chi \tag{33}$$

Figure 4.1 A function generator mechanism system

From the mechanism analysis of this system, the following equations can be obtained:

$$\kappa_a(\mathbf{B}, \theta) = 2\arctan\left(\frac{-E_\kappa \pm \sqrt{E_\kappa^2 + D_\kappa^2 - F_\kappa^2}}{F_\kappa - D_\kappa}\right) \tag{34}$$

in which $D_\kappa = 2B_4(B_1 - B_2\cos\theta)$, $E_\kappa = -2B_2B_4\sin\theta$, and

$F_\kappa = B_1^2 + B_2^2 + B_4^2 - B_3^2 - 2B_1B_2\cos\theta$.

$$\eta_a(\mathbf{B}, \chi) = 2\arctan\left(\frac{-E_\eta \pm \sqrt{E_\eta^2 + D_\eta^2 - F_\eta^2}}{F_\eta - D_\eta}\right) \tag{35}$$

in which $D_\eta = 2B_7(B_1 - B_5\cos\chi)$, $E_\eta = -2B_5B_7\sin\chi$, and

$F_\eta = B_1^2 + B_5^2 + B_7^2 - B_6^2 - 2B_1B_5\cos\chi$.

The distributions of random variables are given in Table 4.2.

Table 4.2 Random variables of example 2

Variable	Mean	Standard deviation	Distribution
B_1 (mm)	100	0.3	Normal
B_2 (mm)	55.5	0.005	Normal
B_3 (mm)	144.1	0.005	Normal
B_4 (mm)	72.5	0.005	Normal
B_5 (mm)	79.5	0.005	Normal
B_6 (mm)	203	0.005	Normal
B_7 (mm)	150.8	0.005	Normal

This system is a series system since the system fails if any motion error of the two function generators is greater than its allowable error.

The system is desired to perform its function over $[\chi_0, \chi_s] = [45°, 105°]$. The probability of system failure is therefore defined as

$$p_f^{\text{system}}(\chi_0, \chi_s) = \Pr\left\{\varepsilon_\kappa(\mathbf{B}, \chi_i) - \varepsilon_1 > 0 \cup \varepsilon_\eta(\mathbf{B}, \chi_j) - \varepsilon_2 > 0, \exists \chi_i, \chi_j \in [\chi_0, \chi_s]\right\} \quad (36)$$

where $\varepsilon_1 = 1.4°$ and $\varepsilon_2 = 1.4°$ are the allowable motion errors of the two function generators.

The average results are shown in Table 4.3, which indicate that the proposed method and mSEGO method have similar accuracy and robustness, but the proposed method has better efficiency.

Table 4.3 Average results of example 2

Methods	$p_f^{\text{system}}(t_0, t_s)$	$\sigma_{p_f^{\text{system}}(t_0, t_s)}$	ε (%)	N_{FC}	
MCS	2.6264×10^{-3}	N/A	N/A	6×10^8	6×10^8
mSEGO	2.6478×10^{-3}	2.23×10^{-5}	0.93	38.79	62.35
New method	2.6115×10^{-3}	2.40×10^{-5}	0.89	31.80	17.69

4.3 EXAMPLE 3

As shown in Figure 4.2, the slider-crank mechanism system consists of three slider-crank mechanisms [20]. The three cranks are attached to the disc by the revolute joints, and the three cranks therefore have the same angular velocity and the same length, which is the radius of the disc X_c. The angular velocity is $\omega = 1$ rad/s. The lengths of the

three couplers are X_1, X_2, and X_3, respectively. All the lengths are independent random

variables, and their distributions are given in Table 4.4.
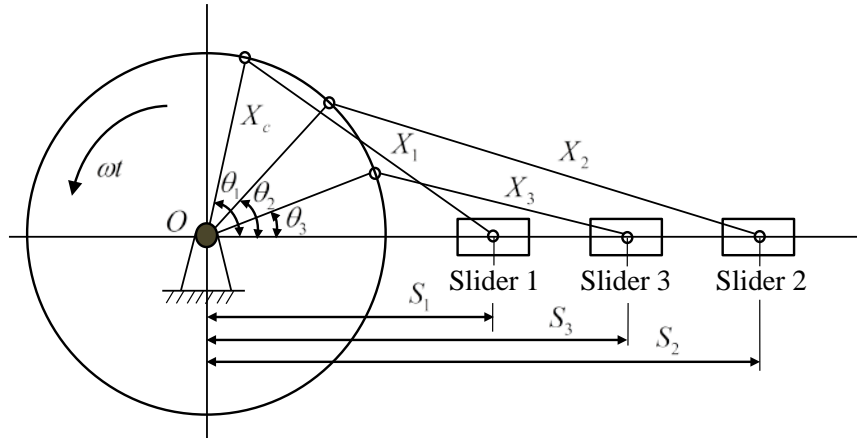
Figure 4.2 A system of crank slider mechanisms

Table 4.4 Random variables of example 3

Variable	Mean (mm)	Standard deviation (mm)	Distribution
X_c	100	0.1	Normal
X_1	150	0.1	Normal
X_2	250	0.1	Normal
X_3	200	0.1	Normal

The motion outputs are the displacements of the three sliders, denoted by S_i

($i = 1, 2, 3$). They are given by

$$S_i = X_c \cos \theta_i + \sqrt{X_i^2 - (X_c \sin \theta_i)^2} \tag{37}$$

where θ_i are the motion inputs as shown in Figure 4.2. The required motion outputs are the nominal displacements of the sliders and are given by

$$S_{R_i} = \mu_c \cos\theta_i + \sqrt{\mu_i^2 - (\mu_c \sin\theta_i)^2} \tag{38}$$

where μ_c and μ_i are the mean values of X_c and X_i, respectively.

The motion errors are

$$\Delta S_i = \left| S_{R_i} - S_i \right| \tag{39}$$

The motion errors of the mechanisms should not be greater than the allowable motion errors ε_i given by the customer, which are $\varepsilon_1 = 0.4$ mm, $\varepsilon_2 = 0.4$ mm, and $\varepsilon_3 = 0.4$ mm, respectively. Given the motion inputs to be $\theta_1 = \omega t$, $\theta_2 = \omega t - \pi/6$, and $\theta_3 = \omega t - \pi/3$, the limit-state functions are

$$g_i(\mathbf{X},t) = \varepsilon_i - \left| (X_c - \mu_c)\cos\theta_i + \sqrt{X_i^2 - (X_c \sin\theta_i)^2} - \sqrt{\mu_i^2 - (\mu_c \sin\theta_i)^2} \right| \tag{40}$$

Since the motions of mechanisms are periodical, we investigate the time interval $[0, \pi/2]$ seconds in this paper. The time-dependent component probability of failure over this time interval is

$$p_{f_i} = \Pr\left\{ y_i = \varepsilon_i - \left| S_{R_i}(t) - S_i(\mathbf{X},t) \right| < 0,\ \exists t[0,\pi/2] \right\} \tag{41}$$

where $\mathbf{X} = (X_c, X_1, X_2, X_3)$.

If any one of the three mechanisms produces a large motion error, the system failure occurs; and the system is therefore a series system. The probability of system failure is then defined by

$$p_f^{\text{system}}(t_0,t_s) = \Pr\left\{ g_1(\mathbf{X},t) < 0 \cup g_2(\mathbf{X},t) < 0 \cup g_3(\mathbf{X},t) < 0,\ \exists t \in [0,\pi/2] \right\} \tag{42}$$

The average results are shown in Table 4.5, which indicate that the proposed method outperforms mSEGO method in accuracy, efficiency, and robustness.

Table 4.5 Average results of example 3

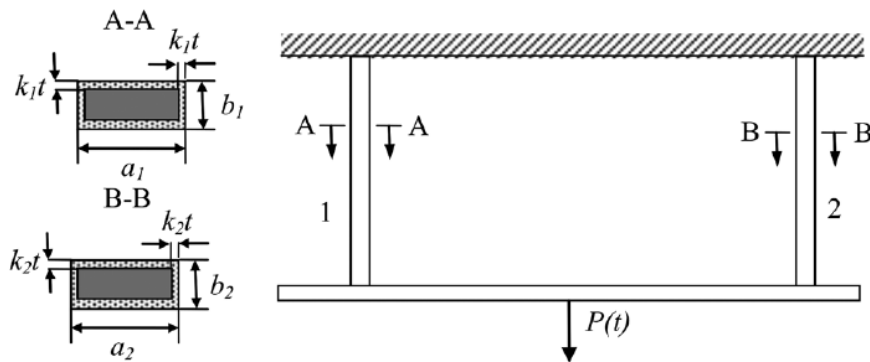| Methods	$p_f^{\text{system}}(t_0,t_s)$	$\sigma_{p_f^{\text{system}}(t_0,t_s)}$	$\varepsilon\,(\%)$	N_{FC}		
MCS	2.5518×10^{-2}	N/A	N/A	2.25×10^{8}	2.25×10^{8}	2.25×10^{8}
mSEGO	2.5372×10^{-2}	1.67×10^{-4}	0.70	142.95	68.79	83.90
New method	2.5339×10^{-2}	7.91×10^{-5}	0.69	52.89	33.79	38.25

Figure 4.3 A Daniels system with two components

4.4 EXAMPLE 4

The last example is a Daniels system subjected to a stochastic process load [45]. As shown in Figure 4.3, the widths and heights of the components decrease over time at rates of k_1 and k_2, respectively. Each component resists half of the load $P(t)$. The time-

dependent probability of system failure is defined as the occurrence of both components yields, which reads as

$$p_f^{\text{system}}(t_0, t_s) = \Pr\left\{g_1(\mathbf{X}, \mathbf{Y}(\chi), \chi) > 0 \bigcap g_2(\mathbf{X}, \mathbf{Y}(\tau), \tau) > 0, \exists \chi \text{ and } \tau \in [t_0, t_s]\right\} \quad (43)$$

in which

$$g_i(\mathbf{X}, \mathbf{Y}(t), t) = P(t)/2 - (a_i - 2k_i t)(b_i - 2k_i t)\sigma_{b_i}, \text{ where } i = 1, 2 \quad (44)$$

in which $[t_0, t_s] = [0, 10]$ years , $\mathbf{X} = [a_1, b_1, a_2, b_2, \sigma_{b_1}, \sigma_{b_2}]$, $\mathbf{Y}(t) = P(t)$, and

$k_1 = 5 \times 10^{-4}$ in./yr , $k_2 = 3 \times 10^{-4}$ in./yr . σ_{b_1} and σ_{b_2} are the yield strengths of components 1 and 2, respectively.

Table 4.6 Parameters and variables in example 4

Variable	Mean	Standard deviation	Distribution	Autocorrelation
a_1	1.3 in.	0.01 in.	Normal	N/A
b_1	1.2 in.	0.01 in.	Normal	N/A
a_2	1.3 in.	0.05 in.	Normal	N/A
b_2	1.2 in.	0.05 in.	Normal	N/A
$\sigma_{b_1}, \sigma_{b_2}$	36 kpsi	0.36 kpsi	Normal	N/A
$P(t)$	85 kpsi	8 kpsi	Gaussian process	Eq. (45)

The autocorrelation function of the stochastic process $P(t)$ is given by

$$\rho(t_1, t_2) = \exp\left[-(t_2 - t_1)^2 / \zeta^2\right] \quad (45)$$

in which $\zeta = 0.5\,\mathrm{yr}$ is the correlation length. The information of parameters and variables are provided in Table 4.6.

The average results are reported in Table 4.7. The results show that the proposed method has much better performance in accuracy, efficiency and robustness than mSEGO method. All four examples demonstrate that the proposed method works well for time-dependent systems with or without stochastic processes in their inputs. They also demonstrate that distributions of extreme values and global optimization are not indispensable in time-dependent system reliability analysis.

Table 4.7 Average results of example 4

Methods	$p_f^{\text{system}}(t_0,t_s)$	$\sigma_{p_f^{\text{system}}(t_0,t_s)}$	$\varepsilon\,(\%)$	N_{FC}	
MCS	1.3134×10^{-3}	N/A	N/A	1.2×10^{8}	1.2×10^{8}
mSEGO	1.3034×10^{-3}	6.48×10^{-4}	4.16	34.39	243.55
New method	1.3097×10^{-3}	6.79×10^{-5}	0.45	28.94	31.00

5. CONCLUSIONS

Time-dependent system reliability analysis is time-consuming and challenging, while it is critical to have accurate estimate of system reliability in decision makings on system performance degradation, lifetime cost estimation and maintenance, etc. The widely used extreme value methods employ a double-loop procedure which is used to obtain the distribution of extreme values. As it is difficult to get accurate distribution of extreme values, and computational cost is high to estimate system reliability for problems with stochastic processes over a long time period.

This work develops a new surrogate modeling method that is applicable to general time-dependent systems that have random variables, stochastic processes and time in performance functions. By removing global optimization and building surrogate models for performance functions directly, the proposed method is more efficient than extreme value methods. Four examples are used to demonstrate the effectiveness of the proposed method. The results show that the proposed method is applicable to systems with or without stochastic processes, and to both series and parallel systems with good accuracy, efficiency, and robustness.

ACKNOWLEDGEMENTS

REFERENCES

[1] Stewart, M. G., 2001, "Reliability-Based Assessment of Ageing Bridges Using Risk Ranking and Life Cycle Cost Decision Analyses," Reliability Engineering & System Safety, 74(3), pp. 263-273.

[2] Singh, A., Mourelatos, Z. P., and Li, J., 2010, "Design for Lifecycle Cost Using Time-Dependent Reliability," Journal of Mechanical Design, 132(9), pp. 091008-091008.

[3] Hu, Z., and Du, X., 2014, "Lifetime Cost Optimization with Time-Dependent Reliability," Engineering Optimization, 46(10), pp. 1389-1410.

[4] Rice, S. O., 1945, "Mathematical Analysis of Random Noise," Bell System Technical Journal, The, 24(1), pp. 46-156.

[5] Breitung, K., 1988, "Asymptotic Crossing Rates for Stationary Gaussian Vector Processes," Stochastic processes and their applications, 29(2), pp. 195-207.

[6] Andrieu-Renaud, C., Sudret, B., and Lemaire, M., 2004, "The Phi2 Method: A Way to Compute Time-Variant Reliability," Reliability Engineering & System Safety, 84(1), pp. 75-86.

[7] Zhu, Z., Hu, Z., and Du, X., 2015, "Reliability Analysis for Multidisciplinary Systems Involving Stationary Stochastic Processes," Proceedings of ASME 2015 Design Engineering Technical Conference, Paper DETC2015-46168, Boston, Massachusetts.

[8] Hu, Z., and Du, X., 2012, "Reliability Analysis for Hydrokinetic Turbine Blades," Renewable Energy, 48, pp. 251-262.

[9] Hu, Z., and Du, X., 2013, "Time-Dependent Reliability Analysis with Joint Upcrossing Rates," Structural and Multidisciplinary Optimization, 48(5), pp. 893-907.

[10] Hu, Z., Zhu, Z., and Du, X., 2015, "Time-Dependent Reliability Analysis for Bivariate Responses," Proceedings of ASME 2015 International Mechanical Engineering Conference & Exposition, Paper IMECE2015-53441, Houston, Texas.

[11] Hu, Z., and Du, X., 2015, "Mixed Efficient Global Optimization for Time-Dependent Reliability Analysis," Journal of Mechanical Design, 137(5), pp. 051401-051409.

[12] Li, J., Chen, J.-b., and Fan, W.-l., 2007, "The Equivalent Extreme-Value Event and Evaluation of the Structural System Reliability," Structural Safety, 29(2), pp. 112-131.

[13] Wang, Z., and Wang, P., 2012, "A Nested Extreme Response Surface Approach for Time-Dependent Reliability-Based Design Optimization," Journal of Mechanical Design, Transactions of the ASME, 134(12).

[14] Hu, Z., and Du, X., 2013, "A Sampling Approach to Extreme Value Distribution for Time-Dependent Reliability Analysis," Journal of Mechanical Design, Transactions of the ASME, 135(7).

[15] Ditlevsen, O., and Madsen, H. O., 1996, Structural Reliability Methods, Wiley New York.

[16] Zou, T., Mourelatos, Z. P., Mahadevan, S., and Tu, J., 2008, "An Indicator Response Surface Method for Simulation-Based Reliability Analysis," Journal of Mechanical Design, 130(7), pp. 071401-071401.

[17] Sacks, J., Welch, W. J., Toby, J. M., and Wynn, H. P., 1989, "Design and Analysis of Computer Experiments," Statistical Science, 4(4), pp. 409-423.

[18] Lophaven, S. N., Nielsen, H. B., and Sondergaard, J., 2002, "Dace-a Matlab Kriging Toolbox, Version 2.0," Technical University of Denmark.

[19] Jones, D. R., Schonlau, M., and Welch, W. J., 1998, "Efficient Global Optimization of Expensive Black-Box Functions," Journal of Global Optimization, 13(4), pp. 455-492.

[20] Zhu, Z., and Du, X., 2015, "Extreme Value Metamodeling for System Reliability with Time-Dependent Functions," Proceedings of ASME 2015 Design Engineering Technical Conference, Paper DETC2015-46162, Boston, Massachusetts.

[21] Deng, J., Gu, D., Li, X., and Yue, Z. Q., 2005, "Structural Reliability Analysis for Implicit Performance Functions Using Artificial Neural Network," Structural Safety, 27(1), pp. 25-48.

[22] Song, H., Choi, K. K., Lee, I., Zhao, L., and Lamb, D., 2013, "Adaptive Virtual Support Vector Machine for Reliability Analysis of High-Dimensional Problems," Structural and Multidisciplinary Optimization, 47(4), pp. 479-491.

[23] Blatman, G., and Sudret, B., 2010, "An Adaptive Algorithm to Build up Sparse Polynomial Chaos Expansions for Stochastic Finite Element Analysis," Probabilistic Engineering Mechanics, 25(2), pp. 183-197.

[24] Huang, X., Chen, J., and Zhu, H., 2016, "Assessing Small Failure Probabilities by Ak–Ss: An Active Learning Method Combining Kriging and Subset Simulation," Structural Safety, 59, pp. 86-95.

[25] Bourinet, J.-M., Deheeger, F., and Lemaire, M., 2011, "Assessing Small Failure Probabilities by Combined Subset Simulation and Support Vector Machines," Structural Safety, 33(6), pp. 343-353.

[26] Kersaudy, P., Sudret, B., Varsier, N., Picon, O., and Wiart, J., 2015, "A New Surrogate Modeling Technique Combining Kriging and Polynomial Chaos Expansions–Application to Uncertainty Analysis in Computational Dosimetry," Journal of Computational Physics, 286, pp. 103-117.

[27] Schöbi, R., Sudret, B., and Marelli, S., 2016, "Rare Event Estimation Using Polynomial-Chaos Kriging," ASCE-ASME Journal of Risk and Uncertainty in Engineering Systems, Part A: Civil Engineering, p. D4016002.

[28] Dubourg, V., Sudret, B., and Bourinet, J.-M., 2011, "Reliability-Based Design Optimization Using Kriging Surrogates and Subset Simulation," Structural and Multidisciplinary Optimization, 44(5), pp. 673-690.

[29] Kleijnen, J. P. C., 2009, "Kriging Metamodeling in Simulation: A Review," European Journal of Operational Research, 192(3), pp. 707-716.

[30] Viana, F. A. C., Simpson, T. W., Balabanov, V., and Toropov, V., 2014, "Metamodeling in Multidisciplinary Design Optimization: How Far Have We Really Come?," AIAA Journal, 52(4), pp. 670-690.

[31] Razavi, S., Tolson, B. A., and Burn, D. H., 2012, "Review of Surrogate Modeling in Water Resources," Water Resources Research, 48(7), p. W07401.

[32] Cadini, F., Santos, F., and Zio, E., 2014, "An Improved Adaptive Kriging-Based Importance Technique for Sampling Multiple Failure Regions of Low Probability," Reliability Engineering & System Safety, 131, pp. 109-117.

[33] Dubourg, V., Sudret, B., and Deheeger, F., 2013, "Metamodel-Based Importance Sampling for Structural Reliability Analysis," Probabilistic Engineering Mechanics, 33, pp. 47-57.

[34] Dubourg, V., Deheeger, F., and Sudret, B., 2011, "Metamodel-Based Importance Sampling for the Simulation of Rare Events," Applications of Statistics and Probability in Civil Engineering, 26, p. 192.

[35] Balesdent, M., Morio, J., and Marzat, J., 2013, "Kriging-Based Adaptive Importance Sampling Algorithms for Rare Event Estimation," Structural Safety, 44, pp. 1-10.

[36] Wang, Z., and Wang, P., 2015, "A Double-Loop Adaptive Sampling Approach for Sensitivity-Free Dynamic Reliability Analysis," Reliability Engineering & System Safety, 142, pp. 346-356.

[37] Hu, Z., and Mahadevan, S., 2016, "A Single-Loop Kriging Surrogate Modeling for Time-Dependent Reliability Analysis," Journal of Mechanical Design, 138(6), p. 061406.

[38] Echard, B., Gayton, N., and Lemaire, M., 2011, "Ak-Mcs: An Active Learning Reliability Method Combining Kriging and Monte Carlo Simulation," Structural Safety, 33(2), pp. 145-154.

[39] Bichon, B., Eldred, M., Swiler, L., Mahadevan, S., and McFarland, J., 2007, "Multimodal Reliability Assessment for Complex Engineering Applications Using Efficient Global Optimization," AIAA Paper No. AIAA-2007-1946.

[40] Bichon, B. J., McFarland, J. M., and Mahadevan, S., 2011, "Efficient Surrogate Models for Reliability Analysis of Systems with Multiple Failure Modes," Reliability Engineering and System Safety, 96(10), pp. 1386-1395.

[41] Fauriat, W., and Gayton, N., 2014, "Ak-Sys: An Adaptation of the Ak-Mcs Method for System Reliability," Reliability Engineering and System Safety, 123, pp. 137-144.

[42] Viana, F. A. C., Venter, G., and Balabanov, V., 2010, "An Algorithm for Fast Optimal Latin Hypercube Design of Experiments," International Journal for Numerical Methods in Engineering, 82(2), pp. 135-156.

[43] Huang, S., Mahadevan, S., and Rebba, R., 2007, "Collocation-Based Stochastic Finite Element Analysis for Random Field Problems," Probabilistic Engineering Mechanics, 22(2), pp. 194-205.

[44] Zhang, J., and Du, X., 2011, "Time-Dependent Reliability Analysis for Function Generator Mechanisms," Journal of Mechanical Design, 133(3), p. 031005.

[45] Hu, Z., and Mahadevan, S., 2015, "Time-Dependent System Reliability Analysis Using Random Field Discretization," Journal of Mechanical Design, 137(10), p. 101404.

SECTION

2. CONCLUSIONS

The performance of an engineering system varies over time when time, or stochastic processes, or both are involved in the system performance functions. To estimate the reliability of time-dependent systems, time-dependent reliability methods need to be employed. As many decisions, like product warranty and maintenance strategies, are made based on the system reliability, it is essential for engineers to be able to accurately estimate reliability of time-dependent systems.

Current methods for time-dependent system reliability analysis can be generally classified into three groups, uncrossing rate methods, extreme value methods, and sampling-based methods. Upcrossing rate methods are based on the Rice's formula and assume that all upcrossing events arrive independently. This assumption simplifies the process of calculating reliability, but it also brings errors into reliability analysis, especially for problems with low failure thresholds or having strong correlations between responses. Although some methods have been developed to relax the independent assumption, the accuracy of upcrossing rate methods will still not be satisfactory for some problems as long as the independent assumption is not removed completely. Extreme value methods use the extreme responses to estimate system reliability, and accurate reliability analysis is obtained by accurate distributions of extreme responses. However, the distributions of extreme values are difficult to get, and the need of global optimization makes extreme values methods computational expensive. Sampling methods can get accurate reliability analysis results when large samples are draw, but the direct use of sampling methods for systems with high reliability over a long time period could

be extremely expensive. Building surrogate models for performance functions and use the surrogate models to substitute original performance functions in reliability analysis is a promising approach.

In this dissertation, a new reliability method is proposed for multidisciplinary systems with stationary stochastic processes. The proposed method is based on the First and Second Order Reliability Methods (FORM and SORM) and the Multidisciplinary Analysis (MDA) is incorporated while approximating performance functions. To deal with the challenge of strong couplings between multiple subsystems, the proposed method uses linking variables as constraints in the process of searching for Most Probable Point (MPP). This not only guarantees the consistency of multidisciplinary systems, but also ensures high efficiency. The method has been successfully applied to a compound cylinders system, and the results show that the proposed method has much better accuracy than upcrossing rate method.

Independent Kriging methods neglect the dependencies between Kriging predictions and focus on the accuracy of surrogate models instead of the accuracy of reliability estimate itself. A dependent Kriging method is developed in this dissertation and demonstrates that the efficiency of independent Kriging methods can be further improved by accounting for the dependencies. A new formula of calculating the probability of failure is derived which uses both means and standard deviations of Kriging predictions at all Monte Carlo samples. A new learning function is also derived. For a new training point, the learning function considers not only the contribution of the point to the error of reliability estimate but also those of the dependencies from all the other points. Then the dependent Kriging method is extended to systems, three widely

used benchmark examples from literature demonstrate that the proposed method outperforms independent Kriging methods in accuracy, efficiency, and robustness.

A new surrogate modeling method for time-dependent systems is also developed in the dissertation. Current time-dependent system reliability methods require a double-loop procedure: the inner loop searches for the extreme response at new training points, and the outer loop builds surrogate models for extreme responses. The new method building surrogate models of performance functions directly instead of building surrogate models for the extreme responses of performance functions. This overcomes the difficulty of obtaining extreme values distributions and avoids the errors that may be introduced. And the new method improves efficiency by removing the time-consuming global optimization needed in the inner loop of double-loop procedure. The new method is applicable to general time-dependent systems with random variables, time, and stochastic processes in performance functions. Four examples show the effectiveness of the new method.

BIBLIOGRAPHY

[1] Hu, Z., and Du, X., 2012, "Reliability Analysis for Hydrokinetic Turbine Blades," Renewable Energy, 48, pp. 251-262.

[2] Rice, S. O., 1944, "Mathematical Analysis of Random Noise," Bell System Technical Journal, 23(3), pp. 282-332.

[3] Rice, S. O., 1945, "Mathematical Analysis of Random Noise," Bell System Technical Journal, The, 24(1), pp. 46-156.

[4] Hu, Z., and Du, X., 2013, "Time-Dependent Reliability Analysis with Joint Upcrossing Rates," Structural and Multidisciplinary Optimization, 48(5), pp. 893-907.

[5] Hu, Z., Zhu, Z., and Du, X., 2015, "Time-Dependent Reliability Analysis for Bivariate Responses," Proceedings of ASME 2015 International Mechanical Engineering Conference & Exposition, Paper IMECE2015-53441, Houston, Texas.

[6] Viana, F. A. C., Simpson, T. W., Balabanov, V., and Toropov, V., 2014, "Metamodeling in Multidisciplinary Design Optimization: How Far Have We Really Come?," AIAA Journal, 52(4), pp. 670-690.

[7] Simpson, T. W., Peplinski, J. D., Koch, P. N., and Allen, J. K., 2001, "Metamodels for Computer-Based Engineering Design: Survey and Recommendations," Engineering with Computers, 17(2), pp. 129-150.

[8] Swiler, L. P., and West, N. J., "Importance Sampling: Promises and Limitations," Proc. Proceedings of the 12th AIAA Non-Deterministic Approaches Conference.

[9] Morio, J., Pastel, R., and Gland, F. L., 2010, "An Overview of Importance Splitting for Rare Event Simulation," European Journal of Physics, 31(5), pp. 1295-1303.

[10] Dubourg, V., Sudret, B., and Deheeger, F., 2013, "Metamodel-Based Importance Sampling for Structural Reliability Analysis," Probabilistic Engineering Mechanics, 33, pp. 47-57.

[11] Balesdent, M., Morio, J., and Marzat, J., 2013, "Kriging-Based Adaptive Importance Sampling Algorithms for Rare Event Estimation," Structural Safety, 44, pp. 1-10.

[12] Sacks, J., Welch, W. J., Toby, J. M., and Wynn, H. P., 1989, "Design and Analysis of Computer Experiments," Statistical Science, 4(4), pp. 409-423.

[13] Lophaven, S. N., Nielsen, H. B., and Sondergaard, J., 2002, "Dace-a Matlab Kriging Toolbox, Version 2.0," Technical University of Denmark.

[14] Zhu, Z., and Du, X., 2015, "Extreme Value Metamodeling for System Reliability with Time-Dependent Functions," Proceedings of ASME 2015 Design Engineering Technical Conference, Paper DETC2015-46162, Boston, Massachusetts.

[15] Zhu, Z., Hu, Z., and Du, X., 2015, "Reliability Analysis for Multidisciplinary Systems Involving Stationary Stochastic Processes," Proceedings of ASME 2015 Design Engineering Technical Conference, Paper DETC2015-46168, Boston, Massachusetts.

[16] Wang, Z., and Wang, P., 2012, "A Nested Extreme Response Surface Approach for Time-Dependent Reliability-Based Design Optimization," Journal of Mechanical Design, Transactions of the ASME, 134(12).

[17] Hu, Z., and Du, X., 2015, "Mixed Efficient Global Optimization for Time-Dependent Reliability Analysis," Journal of Mechanical Design, 137(5), pp. 051401-051409.

[18] Zhu, Z., and Du, X., 2016, "Reliability Analysis with Monte Carlo Simulation and Dependent Kriging Predictions," Journal of Mechanical Design, 138(12), p. 121403.

[19] Zhu, Z., and Du, X., 2016, "A System Reliability Method with Dependent Kriging Predictions," Proceedings of ASME 2016 Design Engineering Technical Conference, Paper DETC2016-59030, Charlotte, North Carolina.

[20] Hu, Z., and Mahadevan, S., 2016, "A Single-Loop Kriging Surrogate Modeling for Time-Dependent Reliability Analysis," Journal of Mechanical Design, 138(6), p. 061406.

[21] Zhu, Z., and Du, X., 2016, "A Kriging Method for Time-Dependent System Reliability Analysis," Reliability Engineering & System Safety (under review).

[22] Bichon, B. J., McFarland, J. M., and Mahadevan, S., 2011, "Efficient Surrogate Models for Reliability Analysis of Systems with Multiple Failure Modes," Reliability Engineering and System Safety, 96(10), pp. 1386-1395.

[23] Fauriat, W., and Gayton, N., 2014, "Ak-Sys: An Adaptation of the Ak-Mcs Method for System Reliability," Reliability Engineering and System Safety, 123, pp. 137-144.

VITA

Zhifu Zhu was born in Liuyang, Hunan, the People's Republic of China. He received his Bachelor of Science degree in Mechanical Engineering in 2010 from Chongqing University, Chongqing, China. Then he continued his education in Chongqing University and received his Master of Science degree in Mechanical Engineering in 2012. Zhifu Zhu started pursuing the degree of Doctor of Philosophy in the Department of Mechanical and Aerospace Engineering at Missouri University of Science and Technology in January 2013. He worked with Dr. Xiaoping Du in the areas of time-dependent system reliability analysis and probabilistic engineering design. In December 2016, he received his Doctor of Philosophy in Mechanical Engineering from Missouri University of Science and Technology, Rolla, Missouri.